

# A spatial approach to edge effect modelling for plantation forestry

by

André Wise

*Thesis presented in fulfilment of the requirements for the degree of  
Master of Science in Forestry at the Faculty AgriSciences at Stellenbosch University*



Supervisor: Prof Thomas Seifert  
Co-supervisor: Dr Stefan Seifert

December 2013

## **Declaration**

By submitting this thesis electronically, I declare that the entirety of the work contained therein is my own, original work, that I am the sole author thereof (save to the extent explicitly otherwise stated), that reproduction and publication thereof by Stellenbosch University will not infringe any third party rights and that I have not previously in its entirety or in part submitted it for obtaining any qualification.

December 2013

Copyright © 2013 Stellenbosch University  
All rights reserved.

## Acknowledgements

My warmest thanks are extended to my supervisor Prof Thomas Seifert for his support and insightful contributions throughout this study. I am also grateful to my co-supervisor Dr Stefan Seifert for his contribution to the study and to my education.

My appreciation is also extended to Anton Kunneke for the provision of remote sensed data and for the technical help in data collection. Thank you also to Mark Februarie for his help with the fieldwork and practical arrangements. I would also like to thank the first year class of 2012, for the help with the data collection. Cape Pine allowed us to collect data from their plantations and I would like to thank them too.

Particular thanks are due to Peter Wise and Johnny Wise for the late night discussions and their contributions of patient engineering rationality. Also thanks to Cori Ham for his enlightening contributions in various aspects of my studies.

I would like to thank all the contributors to the *R* project, the QGIS project and to online forums and help sites who are actively contributing of their time and freely sharing their knowledge and experience in order to make open source technological solutions a viable reality. This group of people have contributed greatly to this study and to my technical education in general

I am grateful to my friends and family who patiently supported and encouraged me throughout the study. My appreciation is also extended to my colleagues at the Department of Forestry and Wood Science who made the experience a most enriching one.

This study was financed by the National Research Foundation (NRF) within the scope of the Green Landscapes Project in the GCSSR call. I am grateful for the opportunity, which was presented me as a result of this funding. However, any opinion, findings and conclusions or recommendations expressed in this material are those of the author and the NRF does not accept any liability in regard thereto.

## Abstract

One of the major objectives in plantation forestry is to achieve a high level of homogeneity of distribution and dimension of trees within the stand. Precise planting geometries, intensive silviculture and genetic selection are used to achieve this homogeneity. However, a natural variability is still introduced by micro-site conditions and disturbances. A substantial source of variation is caused by edge effects of neighbouring stands or other land use forms. The edge effect causes trees at the stand edge to develop differently from trees in the interior of the stand.

The overarching objective of this study is to simulate the edge effect based on average stand interior variables as typically received from an enumeration and spatial information on the current and historic stand neighbourhood. With re-introducing this natural variance as well as its spatial pattern, we expect to derive improved planning information.

A major aim is thus separating the effect of the edge interaction from the other factors contributing to stand variance and quantifying the result in terms of stand output. A methodology is introduced for quantifying interaction at stand edges between a given stand and its neighbouring stands over its lifetime. Transferring the edge interaction value from the edges to all the trees within the stand is then done by applying inverse distance weighting interpolation from the edges to the tree position within the stand. Once an edge interaction value has been calculated for each point, the extent of the edge effect is quantified. The spatial extent of the edge effect is derived empirically from an existing fully spatially mapped stand by means of breakpoint regression. The expected variance as a result of edge influence is then quantified by producing a set of models, which can reproduce the effect of the edge interaction on tree height, diameter and volume.

The edge effect is treated as a dynamic interaction for which the temporal aspect needs to be considered, because the current spatial structure of a stand is influenced by its current neighbourhood, but also by the historic development of the neighbourhood in relation to the stand in question. Each stand therefore undergoes an edge effect which is completely unique to that stand, within a given time period. For this reason the presented methodology is a spatial-temporal one, aimed at providing a way in which growth and yield forest modelling can be augmented by the inclusion of the edge effect in a practical way.

To explicitly quantify edge effects, the natural variance had to be separated into a component explained by edge effect and a second component introduced by other factors such as micro site conditions and disturbance. The second component is treated as an unexplained residual variance. In order to provide a realistic simulation of a stand output at a finer, tree level, this second stand variance needs nonetheless to be quantified. The variance attributable to factors other than the edge effect is mimicked by generating a random number by means of a parameterised stochastic process based on the variance of the inner stand region, which is beyond the reach of the edge effect. In this way, a realistic spatial pattern of a plantation forest stand, taking into account the edge effect and combining it with the natural stand variance is achieved.

This study, within the field of plantation forest management, aspires to land use optimization both in terms of productive capacity estimation and for the provision of information for effective land use management planning. It makes use of open source software resources namely the *R* framework and QGIS and explores aerial stereophotogrammetry as an option for data collection.

## Opsomming

Een van die hoofdoelwitte in plantasie bosbou praktyk is hoë vlakke van homogeniteit met betrekking tot die verspreiding en die dimensies van die bome in die plantasie opstand. Simetriese aanplantings, intensiewe bosboupraktyk en genetiese seleksie word gebruik om hierdie homogeniteit te verkry. Natuurlike verskille word egter nog steeds gevind as gevolg van groeiplek mikro toestande en ander versteurings in die opstand. Een van die hoofbronne van hierdie variasie is die randeffekte van buurplantasies en ander gebruike van grond. Hierdie randeffekte veroorsaak dat bome aan die rand van die opstand anders ontwikkel as die bome binne in die opstand.

Die oorhoofse doelwit met hierdie navorsing is om die randeffekte te simuleer. Hierdie randeffekte is gegrond op die gemiddelde binneopstand boom veranderlikes soos afgelei uit die opmeting en uit ruimtelike inligting oor die huidige en geskiedkundige toestande in die omgewing. As hierdie natuurlike variasies asook die ruimtelike patrone weer in berekening gebring word, verwag ons om beter beplanningsinligting te bekom.

'n Belangrike doelwit tydens hierdie navorsing is dus om die effek van die rand-interaksie te skei van die effek van ander faktore wat bydra tot variasies binne-in die opstand en om die resultaat in terme van plantasie produksie te kwantifiseer. 'n Metodiek word voorgestel vir die kwantifisering van die interaksie op die rande tussen die opstand en die buuropstande tydens die leeftyd van die opstand. Die oorplasing van die rand interaksie waarde van die rand af na al die bome in die plantasie word dan gedoen deur om geweegde inverse afstand interpolasie vanaf die rand tot by die ligging van die boom, toe te pas. As die rand interaksie waarde vir elke punt bereken is, kan die omvang van die randeffek gekwantifiseer word. Die ruimtelike omvang van die rand effek is, met die gebruik van breekpunt regressie, empiries afgelei van 'n bestaande ten volle karteerde plantasie. Die verwagte variasie as gevolg van die randeffek word dan met die gebruik van 'n stel modelle gekwantifiseer, wat dan die effek van die rand interaksie op boomhoogte, deursnit en volume kan weergee.

Die randeffek word as 'n dinamiese interaksie beskou waarvan die tydspek in ag geneem moet word, want die huidige ruimtelike struktuur van die plantasie word beïnvloed deur die huidige omgewing asook deur die historiese ontwikkeling van die omgewing met betrekking tot die opstand onder bespreking. Elke opstand ondergaan 'n randeffek wat uniek is aan daardie plantasie op die gegewe tydstip. Die doelwit is om 'n wyse te vind waarvolgens groei-en-opbrengs plantasie modellering deur die insluiting van randeffek op 'n praktiese wyse, aangevul kan word. Om hierdie rede is die aanbevole metodiek ruimtelik-tydelik en gerig daarop om 'n wyse te vind waarvolgens groei-en-opbrengs modellering deur die insluiting van die randeffek, op 'n praktiese wyse aangevul kan word.

Om randeffek eksplisiet te kwantifiseer, moes die natuurlike afwyking gedeel word in die komponent wat die gevolg is van die randeffek, en 'n tweede komponent wat die gevolg is van ander faktore soos mikroligging toestande en versteurings. Die tweede komponent word behandel as 'n onverklaarde oorblywende afwyking. Hierdie tweede plantasie afwyking moet nogtans kwantifiseer word om sodoende 'n realistiese simulatie van plantasie opbrengs op 'n fyner boom vlak te verkry. Die afwyking wat toegeskryf kan word aan faktore buiten die randeffek, word nageboots deur om 'n lukrake nommer (wat gebaseer word op die afwyking van die binne-plantasie gebied wat buite die strekwydte van die randeffek is) deur middel van 'n geparameteriseerde stogastiese proses te genereer. Sodoende word 'n realistiese ruimtelike patroon van 'n plantasie opstand verkry, wat die randeffek in ag neem en dit kombineer met die natuurlike plantasie afwyking.

## Table of Contents

<b>Table of figures.....</b>	<b>viii</b>
<b>Table of tables.....</b>	<b>xiii</b>
<b>Table of equations.....</b>	<b>xiv</b>
<b>Chapter 1. Introduction.....</b>	<b>1</b>
1.1 Problem statement .....	1
1.2 Aim and objectives of the study .....	1
1.3 Structure of this document .....	2
<b>Chapter 2. Literature review .....</b>	<b>4</b>
2.1 Edges, edge effect and edge interaction .....	4
2.1.1 Edge zones.....	4
2.1.2 Edge effect and edge influence .....	5
2.1.3 Edge effect in plantation forestry.....	6
2.2 Remote sensing of plantations.....	7
2.2.1 Photogrammetry .....	7
2.2.2 Digital elevation, surface and height models .....	8
2.2.3 Remote sensing using LiDAR .....	9
2.3 Spatial modelling of DBH as a function of height .....	10
2.4 Regularity, or evenness of stand structure .....	10
<b>Chapter 3. Analysis and quantification of edge effects .....</b>	<b>13</b>
3.1 Terrestrial data collection .....	14
3.2 Data preparation .....	16
3.2.1 Spatial data manipulation in the <i>R</i> environment.....	17
3.3 Introducing a regularity index for diameter-height modelling.....	17
3.3.1 Delaunay triangulation edge effect .....	17
3.3.2 Testing the contribution of the evenness index to the DBH-height relationship.....	18
3.4 Quantifying interaction at the stand edge .....	19
3.4.1 Neighbour Interaction .....	20
3.4.2 Accumulated Interaction .....	21
3.4.3 The dynamics of Accumulated Interaction units .....	22
3.4.4 Calculating Accumulated Interaction for the edges of stand E3b .....	24
3.5 Identifying the extent of the edge effect by segmented regression .....	27
3.5.1 Segmented regression of stand E3b data .....	27
3.6 Separating inner and outer regions.....	29
3.7 Spatially interpolating AI values from the edges into the stand .....	29

3.7.1	An inverse distance weighting approach.....	30
3.7.2	The inverse distance weighting process for stand E3b.....	31
3.8	Taking spaces between edges into account .....	32
3.9	Model fitting of stand data.....	34
3.9.1	DBH as a function of AI and local density .....	34
3.9.2	Volume as a function of AI and local density .....	34
3.9.3	Height as a function of AI .....	34
3.10	Taking the cardinal direction of the edge into account when calculating AI .....	35
<b>Chapter 4.</b>	<b>Model application on an independent dataset .....</b>	<b>37</b>
4.1	Remote data collection .....	38
4.1.1	Simulation dataset: Compartment G36.....	39
4.2	Data preparation .....	41
4.2.1	Identifying tree position and height from the DSM using the <i>R</i> Package.....	41
4.3	AI calculation at stand edges.....	47
4.4	Generating a regular points grid .....	47
4.5	Separation of inner and edge regions .....	47
4.6	Interpolation of AI into the stand.....	50
4.7	Calculation of local tree density .....	50
4.8	Prediction of stand variables.....	52
4.9	Generating random values based on natural stand variance.....	52
4.10	Combining distributions to predict expected stand output .....	53
4.11	Comparing the edge region with the inner region .....	56
<b>Chapter 5.</b>	<b>Discussion and conclusions .....</b>	<b>58</b>
5.1	Quantifying edge interaction .....	58
5.1.1	Permanent sample plot data .....	58
5.1.2	Including aspect in edge interaction calculation .....	59
5.2	Transferring edge interaction into the stand .....	59
5.3	Identifying the spatial extent of the edge effect .....	59
5.3.1	Including aspect in edge effect extent calculation .....	60
5.4	A methodology for taking spaces between stands into account. ....	60
5.5	Modelling the edge effect .....	61
5.5.1	Taking stand age into account.....	61
5.6	Simulating the edge effect and natural stand variance.....	62
5.6.1	Using local maxima to extract tree positions .....	62
5.6.2	Correcting CHM data .....	63

5.6.3	Adjusting the models to different stand conditions.....	63
5.6.4	Generating natural variance distributions.....	64
5.6.5	Combining variances .....	64
5.7	Quantifying evenness.....	64
5.8	Using the <i>R</i> framework for spatial data analysis .....	65
5.9	Taking relief into account.....	65
5.10	Achieving the overall aim of the study and continuing this work .....	65
<b>References .....</b>		<b>67</b>
<b>Appendix A. Additional results.....</b>		<b>I</b>
5.11	DBH simulation results .....	I
5.12	Height simulation results.....	III



## Table of figures

Figure 2.1. (a) Magnitude and (b) distance of edge influence (EI) for different categories of response variables. Means (bars) of the mean absolute value per study were calculated for each category of response variables. Maximum absolute values (lines) are for individual values (i.e., not averaged by study). (Harper <i>et al.</i> 2005: 774).....	5
Figure 2.2. A demonstration of a CHM and a DEM of the underlying ground level. A DSM is the combination of these two. (P. Wężyk, 2013) .....	9
Figure 2.3. Overview of the three major characteristics of forest structure and the groups of variables by which forest structure is assessed. (Pommerening 2002).....	11
Figure 2.4. Points with varying levels of regularity generated by (Dryden <i>et al.</i> 1999). The parameter controls the amount of regularity in the model – smaller $\tau$ producing more regular patterns.....	12
Figure 3.1. Flow chart indicating the steps for the edge effect quantification process. ....	13
Figure 3.2. The study region in Western Cape Province of South Africa, with terrestrial data collected from the study stand (in orange) at the bottom of the image and the remotely sensed data collected for the stand on the upper right of the image. (Base map provided by Google Maps 2013, in QGIS) .....	14
Figure 3.3. An aerial view of compartment E3b, taken 12 November 2012. ....	15
Figure 3.4. A screenshot of shapefile preparation in QGIS. ....	16
Figure 3.5. An illustration of Delaunay triangulation, demonstrating the problem at the edge of the stand where improbably long lines are generated at the edges of the stand. ....	18
Figure 3.6. Delaunay triangulation after edge correction, where all lines linking “neighbouring trees” with a length greater than 3 times the mean line length had been removed.....	18
Figure 3.7. Visualisation of the proposed evenness index, with smaller circles representing a lower coefficient of variation for distances to neighbouring trees and thus a higher degree of evenness.....	19
Figure 3.8. An example of the calculation of NI on an edge where the given stand <i>c</i> starts at age zero and the neighbouring stand <i>n</i> at age 12. The broken line indicates the NI value for a given point in time plotted on the interaction axis. ....	21
Figure 3.9. Accumulated Interaction for an edge of stand <i>c</i> if the neighbouring stand <i>n</i> is 12 years of age when stand <i>c</i> was planted and rotation length is 30 years. AI and NI are plotted on the interaction axis.....	22
Figure 3.10. Accumulated Interaction for an edge of stand <i>c</i> if the neighbouring stand is 3 years of age when stand <i>c</i> was planted and rotation length is 30 years. AI and NI are plotted on the interaction axis.....	23

Figure 3.11. Accumulated Interaction for an edge of stand c if the neighbouring stand is 28 years of age when stand c was planted and rotation length is 30 years. AI and NI are plotted on the interaction axis.....	24
Figure 3.12. The result of the process of quantifying edge interaction for E3b. The edge of E3b is marked in graduated blue for negative AI values moving to lighter green for positive, higher AI values. The neighbouring stands with E3b are coloured according to their relative ages, with a lighter colour indicating a lower age.....	25
Figure 3.13. This figure illustrates the process of calculating AI values. In the first stage, the algorithm looks inward at the stand in question to identify which segments interact with neighbouring stands (steps a, b and c) and in the second stage the algorithm looks outward from each interacting segment to the neighbouring stands to identify which of these neighbouring stands interact at that segment (steps d, e and f). The level of interaction is calculated based on an interaction index by the difference in height over time. 26	26
Figure 3.14. Stand E3b with graduated blue colours indicating the distance from the edge and circle size indicating relative DBH for each tree.....	28
Figure 3.15. Piecewise linear regression, indicating the relationship between the distance from the edge of the stand and DBHs of the respective trees. The vertical dashed line indicates the breakpoint at 14.88m from the edge, the red sloping dashed line indicates the linear regression line and the grey curve indicates Loess fitting of the data. ....	29
Figure 3.16. Representation of interpolated AI values for stand E3b with inner region AI values set to 0. 31	31
Figure 3.17. An illustration of height as a function of AI, indicating the positive linear relationship. ...	32
Figure 3.18. The local density calculation of trees in stand E3b, taking a 15m radius into account for each tree.....	33
Figure 3.19. A scatterplot indicating the relationship between the local tree density (within 15m of the tree) and DBH for all trees in the outer region of stand E3b. The red curve represents a generalized additive smoothing function applied using the gamLine smoother in the scatterplot function. The blue line represents a linear fit of the data.....	33
Figure 3.20. Calculation of the bearing of the stand edge with the results of the interpolation of those values to the points within the stand. Bearing is given in degrees. ....	35
Figure 3.21. A scatterplot indicating the relationship between the bearing in degrees and DBH for all trees in the outer region of stand E3b. The red curve represents a generalized additive smoothing function applied using the gamLine smoother in the scatterplot function that allows a flexible nonparametric regression model fit. The blue represents a linear fit of the data.....	36
Figure 4.1. A flow chart indicating the steps for the edge effect model application process. ....	38

Figure 4.2. Digital surface model of G plantation, overlaid on Google satellite layer in QGIS. The compartment to be simulated is outlined by the dashed line. The location of this plantation is shown in Figure 3.2. ....	39
Figure 4.3. An image of the aerial view of stand G36, taken on November 12, 2012.....	40
Figure 4.4. A three dimensional rendering of a digital surface model of the G plantation, generated in R using the <i>rgl</i> package (Adler & Murdoch 2013).....	40
Figure 4.5. Representation of the approximate size of the moving window (1ha) used in the raster normalisation process in order to adjust a pixel by the neighbourhood mean (within the moving window).....	42
Figure 4.6. An illustration of the slope error problem, where, in the original CHM on the left, the lower left of the region has unrealistically lower elevations when compared to the upper region of the CHM. In the normalised image on the right, the result of the moving window process is shown. A more homogenous elevation distribution is achieved, keeping local interactions intact by using a moving window of approximately 1ha. ....	43
Figure 4.7. A graphical comparison of the CHM data before and after normalisation, showing a bar graph on the left with the original CHM data distribution in red bars and the normalised CHM data on the right. As expected, the distribution shifts upward in general, also removing both upper and lower extreme values. The resultant boxplot (on the right) presents a slightly narrower distribution for the normalised raster as opposed to the original. ....	43
Figure 4.8. A demonstration of the problem created by a slope-biased CHM is shown in this figure. When removing the understory of the raster, within the slope-affected CHM there was excessive removal in the lower left region of the canopy (left) while almost all the understory remained in the upper region. In the normalised raster, a more homogenous removal of understory was possible (right).....	44
Figure 4.9. The result of the CHM shifting process is shown in this figure. The image on the right is the raster before the ground level is moved to zero and the raster on the right is the result when the lowest raster value is zero (see raster legends). ....	45
Figure 4.10. A three-dimensional representation of the output from the local maxima identification process, visualising the left-hand side raster shown in Figure 4.11.....	46
Figure 4.11. The result of local maxima extraction with the local maxima process output on the left and the identification of individual treetops on the right.....	46
Figure 4.12. The result of the process of calculating Accumulated Interaction for the edges of stand G36. The edges of G36 are marked from blues for lower AI values moving to lighter greens for higher AI values. The neighbouring stands of G36 are coloured according to their relative ages, with a lighter colour indicating a lower age. ....	47

Figure 4.13. A representation of the separation between the inner and the edge region. The size and positions of the sample plots are also indicated by the circular dashed lines. ....	49
Figure 4.14. A comparison between the complete dataset of inner region tree data and the sampled data from trees falling within the sample plot areas. The red bars also represent the spread of data which will be used in simulation in order to generate random values for each tree in order to simulate natural stand variance.....	49
Figure 4.15. A visual comparison between the distribution of the AI values for stand E3b (the model calibration dataset) and stand G36 (the simulation stand). The spread of AI values of stand G36 is wider and more positive than that of stand E3b.....	50
Figure 4.16. A figure demonstrating virtual tree positions with the points indicating interpolated AI values in graduated colouring from 0 to 14.3. ....	51
Figure 4.17. The local density calculation of tree positions in stand G36, taking a 15m radius into account for each tree. ....	51
Figure 4.18. A comparison between the volume predicted for the edge region of stand G36 without simulation of the natural variance shown by the red bars, and the distribution of the volumes as calculated from data extracted from the CHM (blue bars).....	52
Figure 4.19. A comparison between the random values generated for volume of the complete stand G36 (blue bars) and the distribution of the volumes as extracted from the sample plots (red bars). The random values were generated based on the distribution of the sample plot volumes. ....	53
Figure 4.20. A comparison between the distributions of the predicted edge tree volumes (red bars) and the edge tree volumes as calculated from data extracted from the CHM for the complete stand (blue bars). ....	55
Figure 4.21. A comparison between the distributions of the predicted volumes for all the trees within the complete stand (red bars) and the stand volumes as calculated from data extracted from the CHM for the complete stand (blue bars). ....	55
Figure 4.22. A spatial representation of the simulated stand G36. The colour and size graduated circles represent the simulated DBH per point where blue is a smaller and green a higher DBH as well as DBH increasing with increasing circle size. ....	56
Figure 4.23. A comparison between the simulated heights for the outer region of the stand (red bars), with the inner region of the stand (blue bars). ....	57
Figure 5.1. A simplistic, exaggerated representation of a stand with an edge effect of varying extent, depending on the cardinal direction of the edge. The solid region represents the inner region of the stand, beyond the extent of the edge effect, while the striped region represents the area affected by the edge.....	60
Figure 5.2. A visualisation of the effect that age could possibly have on the relationship between AI and height for a <i>Pinus radiata</i> stand on a site index of $SI_{20}=25$ . ....	62

- Figure A.1. A comparison between the DBH predicted for the edge region of stand G36 (red bars) and the distribution of the volumes as calculated from data extracted from the CHM (blue bars). .....I
- Figure A.2. A comparison between the random values generated for DBH of the complete stand G36 (blue bars) and the distribution of the DBHs as extracted from the sample plots (red bars). The random values were generated based on the distribution of the sample plot DBHs. ....I
- Figure A.3. A comparison between the distributions of the predicted edge DBHs (red bars) and the edge tree DBHs as calculated from data extracted from the CHM (blue bars). .....II
- Figure A.4. A comparison between the distributions of the predicted DBHs for the complete stand (red bars) and the stand DBHs as calculated from data extracted from the CHM (blue bars). II
- Figure A.5. . A comparison between the height predicted for the edge region of stand G36 (red bars) and the distribution of the heights as calculated from data extracted from the CHM (blue bars). .....III
- Figure A.6. A comparison between the random values generated for height of the complete stand G36 (blue bars), and the the distribution of the heights as extracted from the sample plots (red bars). The random values were generated based on the distribution of the sample plot DBHs. ....III
- Figure A.7. A comparison between the distributions of the predicted edge heights (red bars) and the edge tree heights as calculated from data extracted from the CHM (blue bars). .....IV
- Figure A.8. A comparison between the distributions of the predicted heights for the complete stand (red bars) and the stand heights as calculated from data extracted from the CHM (blue bars). .....IV

## Table of tables

Table 1.1. Table of abbreviations used throughout the document.....	3
Table 3.1. ANOVA table comparing the models of height as a function of DBH, with and without the inclusion of the evenness index. The AIC values for both models are also included....	19
Table 3.2. A summary of the NI scale, with the type of interaction taking place at the upper, middle and lower extremes of the scale, and a visual representation of the interaction between the two stands n and c. ....	20
Table 4.1. Table of values calculated from the sample plots within the inner stand region.....	48

## Table of equations

Equation 1. Neighbour Interaction (NI) calculation .....	20
Equation 2. Calculation of Accumulated Interaction (AI) .....	22
Equation 3. Equation for inverse distance weighting interpolation .....	31
Equation 4. Model of DBH as a function of AI and local density .....	34
Equation 5. Model of volume as a function of AI and local density .....	34
Equation 6. Model of height as a function of AI and local density .....	34
Equation 7. Equation for calculating new centre pixel value during raster normalisation .....	42
Equation 8. Equation for combining predicted tree variable with random variable.....	54

## Chapter 1. Introduction

### 1.1 Problem statement

A key concept in land use management is sustainability modelling, which implies planning and managing in such a way as to utilize a resource so as to maximise benefit and minimise loss. For effective, sustainable management of a resource to transpire, it is necessary to be able to quantify the resource and to predict how it will develop in future. In plantation forestry, inventory is used as a starting point in order to acquire this information.

Inventory alone is not sufficient for sustainability modelling. It only provides a snapshot of the current situation. Also, inventory data are point data, which do not provide information regarding spatial patterns within the plantation. These data need to be spatialised in order to utilise the information fully. Spatial models are thus required to incorporate the spatial features and patterns which present themselves within a forest plantation. The prediction and projections of what the forest will become in future is done by means of growth models, different from spatial models. Although various decision support tools are available for the application of growth models, there is a gap in the incorporation of spatial modelling within current decision support systems used in South African plantation forestry (Seifert *et al.* 2010).

Stand edge effects have been identified as one of the possible factors responsible for bias in plantation inventory (Ducey *et al.* 2004 and others as shown in Gregoire 2012). Edge effect is defined as the change in ecological traits within a transition zone at the boundary between two homogeneous patches (Cadenasso *et al.* 1997). This interaction with stand surroundings takes place at the edge of the stand, within a transition zone of a certain extent and magnitude (Ewers & Didham 2006). In many plantation inventories, edge effects are ignored (T. Seifert, personal communication, August 2012). Frequently, inventory manuals prescribe that enumeration should start 30m away from every edge, thus introducing a bias. If the variance in tree size as caused by the edge effect for any given stand in terms of interaction with its surroundings can be quantified in a universally applicable model, better estimation of the stand tree variables would be possible, even based on inventory information that excludes the edge effect.

During this study, a spatial modelling approach is developed and tested, where the effect of the edge on the stand is quantified as a function of stand neighbour interaction. The natural variance of the stand is then also reintroduced. Bias introduced into inventory by edge effect is thus removed and conformity can be achieved as to the approach when dealing with edges in forest inventory.

### 1.2 Aim and objectives of the study

The aim of the study is to provide a methodology for quantifying the variance in tree size within a stand which is attributable to the interaction between the stand and its neighbour, and applying this quantification within a standardised inventory system in order to deliver improved information as to the composition of a stand.

Variance within a stand should be separated into two components, namely a component explained by edge effect and a second component introduced by other factors such as micro site conditions



and disturbance. These two components then need to be combined in a final estimate of stand composition.

Five objectives contribute to achieving the main aim of the study, namely:

1. Providing a methodology for quantifying interaction at stand edges between trees of a given stand and trees of a neighbouring stand over the lifetime of the stand.
2. Transferring the edge interaction value from the edges to all the affected trees within the stand in a coherent way.
3. Identifying the spatial extent of the edge effect into the stand.
4. Providing a methodology for taking spaces between stands into account.
5. Modelling the expected variance caused by the edge and thus explaining the relationship between the edge interaction and tree variables, taking the spaces between compartments into account.
6. Simulating the edge effect and combining it with the natural stand variance in order to predict stand output by taking the edge influence into account.

This study therefore seeks to create models for the effect of the forest neighbour on the tree variables for those trees within the edge zone in terms of diameter, height and volume. It also investigates the application of relatively cost-effective remotely-sensed data as input data in combination with manually collected ground proofing data. It is implemented within a modelling and simulation framework built in *R* (*R* Core Team 2013) in such way that the framework could be applied to future projects with different input data in order to generate different models or to combine with data generated during this study in a cumulative fashion. Open source software was chosen in order to allow ease of access to the framework for future use and development.

An additional aspect of this study is to define the position of a given tree within the stand in relation to its neighbouring trees and the effect that this relative position has on its diameter and height. An evenness index is introduced which quantifies this relative position of a tree in terms of regularity. It is then tested in order to ascertain whether there is any link between the evenness index of a tree and its diameter at breast height (DBH) or height and if there is, to potentially include it in modelling DBH from heights or vice versa.

Achieving these objectives should then aid in the optimisation of the stand resource utilization by providing information to better assist in:

1. Predicting production, potential product mix
2. Improving planning at all levels
3. Inventory optimization
4. Harvesting optimization
5. Valuation
6. Minimizing loss and maximize benefit

### 1.3 Structure of this document

The structure of this document varies slightly from the customary structure since the focus of this study was clearly on the development of a novel methodology. A study of previous work and relevant subject areas regarding key topics of the study was carried out and is presented in Chapter 2. In

Chapter 3, the analysis and quantification of the edge effect for a given stand is presented instead of the customary methodology chapter. An application of the edge effect quantification on an independent dataset with relevant outputs are presented in Chapter 4, where a different compartment for which remotely sensed data were collected, is simulated, based on the analysis and modelling carried out in Chapter 3. . Both Chapters 3 and 4 contain the methodology and the results of their individual processes. In the final discussion chapter, the efficacy of the spatial edge effect modelling and simulation methodology as presented in Chapters 3 and 4 are discussed by reconciling the outcomes presented in those chapters with the objectives of the framework as laid out in Chapter 1.

A table with abbreviations used throughout this document is provided below.

**Table 1.1.** Abbreviations used throughout the document.

<b>AI</b>	Accumulated Interaction at a given edge
<b>c</b>	Compartment in question
<b>CHM</b>	Canopy height model (A subtraction of DEM from DSM)
<b>DBH</b>	Diameter at breast height
<b>DEM</b>	Digital elevation model (of the bare ground)
<b>DSM</b>	Digital surface model (Including anything on the ground)
<b>GIS</b>	Geographic information systems
<b>IDW</b>	Inverse distance weighting
<b>n</b>	Neighbouring compartment
<b>NI</b>	Instantaneous Neighbour Interaction
<b>PSP</b>	Permanent sample plot

## Chapter 2. Literature review

Within this chapter, some topics central to the context of the spatial modelling of edge effects are investigated in terms of previous work and background. These topics include:

1. Edges, edge effect and edge interaction (Section 2.1)
2. Remote sensing of plantations (Section 2.2)
3. Spatial modelling of DBH as a function of height (Section 2.3)
4. Regularity, or evenness of stand structure (Section 2.4)

### 2.1 Edges, edge effect and edge interaction

In order to model the edge effect, it is necessary to have a consistent definition for what and where the edge is. In one study, it was noted that “a clear definition of edge in functional terms has proven elusive” (Cadenasso *et al.* 1997: 774). Various definitions are discussed where the edge of a stand is defined as the alteration of conditions by the presence of a boundary between a forest and a non-forest area.

In another study the forest edge is defined as the “plane defining the boundary that separates the stand from open sector or from other stands” (Cancino 2005: 160) and the area unaffected by the edge effect as the interior. For the remainder of this document, this non-edge, or interior of a plantation forest stand will be termed “stand interior”

For the purposes of this study, the edge is demarcated as that point where the tree canopy ends, in other words, the dripline of the canopy, defined by Cadenasso *et al.* (1997) as “the outer reach of edge canopy tree branches and often outside of the sidewall” (p. 775). This definition is selected because remotely sensed data are used when defining the compartment edge. In aerial photographs and in canopy height models, the outer reaches of the canopy are easily and consistently identifiable and this provides a clear boundary between what is plantation and what is not.

In their work on creating a framework for the study of ecological boundaries, Cadenasso *et al.* (2003) explain that a landscape can be divided into two kinds of structures, namely patches and boundaries. Patches are described as those “volumes which can be positionally, structurally, or functionally distinguished from adjacent volumes at a given scale” (p. 751). Boundaries mark the limits between neighbouring patches.

#### 2.1.1 Edge zones

Edge zones are defined in a study by Cadenasso *et al.* (1997) as a “volume of space over which an environmental transition occurs” and a “heterogeneous region bounded by two relatively homogeneous, and often contrasting, environments” (p. 775). This definition was simplified in a study by Porensky (2011) where it was defined as a “zone within a given landscape where ecological traits (e.g. land cover, soil properties or tree density) undergo large changes over a relatively short distance” (p. 923). It is clear, therefore that some kind of change takes place at the interface between two patches, at the boundary, but that these changes take place over a distance. This area

between two patches within which a boundary falls can therefore be classified as the edge zone. The change then, within an edge zone, is the edge effect.

### 2.1.2 Edge effect and edge influence

This edge effect is defined by Cadenasso *et al.* (1997) as the “alteration of environmental conditions by the presence of a boundary between a forest and a non-forest area” They further explain that “the edge effect describes the magnitude of change in a factor whereas the edge zone describes the region within which this change takes place” (p. 775).

In a synopsis regarding the edge influence on forest structure and composition, Harper *et al.* (2005), preferred the term “edge interaction” above edge effect to describe “the effect of processes (both abiotic and biotic) at the edge that result in a detectable difference in composition, structure, or function near the edge, as compared with the ecosystem on either side of the edge” (Harper *et al.* 2005: 773). They summarise the studies regarding edge influence done in the past and the various variables measured, classified by region and forest type with the general trend as established at the edge as compared to the interior of the forest patch. The study summarises the percentage by which a given parameter differs at the edge as compared to the interior region of the forest (Figure 2.1). Of interest is the influence of edge on growth rate, which was found to have on average approximately a 50% difference at the edge as opposed to the interior, with a maximum absolute value of approximately 70%. In some studies the influence of edge on growth rate was found to be positive whereas in others it was found to be negative.

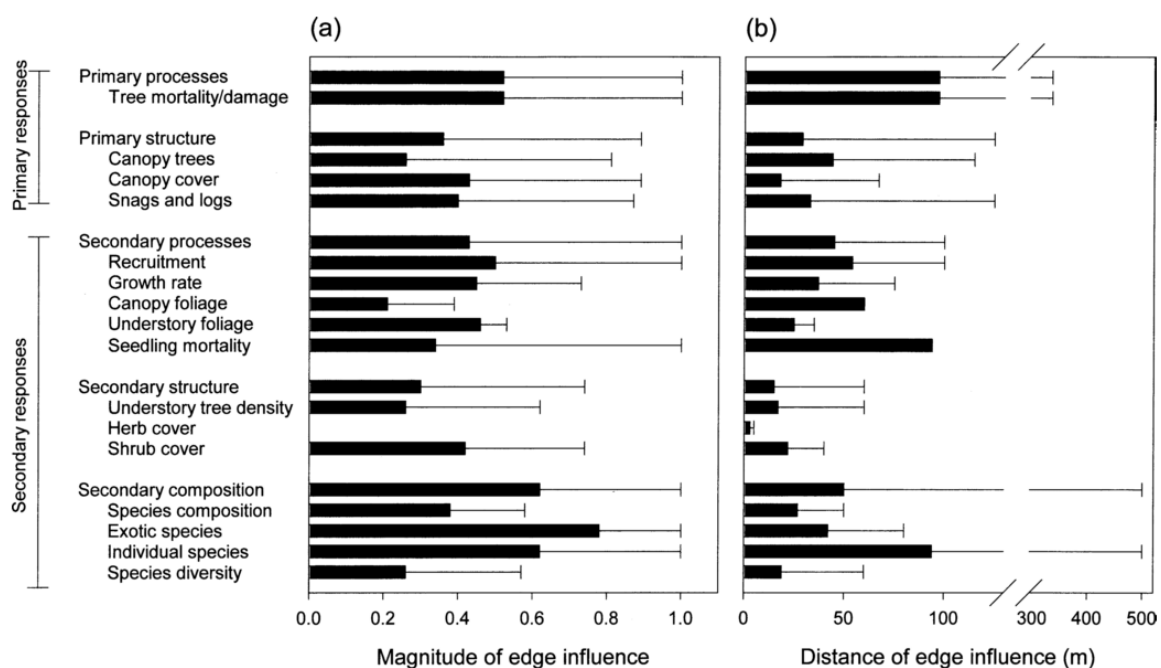


**Figure 2.1.** (a) Magnitude and (b) distance of edge influence (EI) for different categories of response variables. Means (bars) of the mean absolute value per study were calculated for each category of response variables. Maximum absolute values (lines) are for individual values (i.e., not averaged by study). (Harper *et al.* 2005: 774)

The distance which the edge effect reached into the stand was also summarised for the different categories of response variables as well as for the different regions and forest types as mean values from the different studies. The distance for which the edge influences the growth rate was found to be on average 40m from the edge with a maximum absolute value of approximately 80m. Their study

indicates that the edge influence has been studied on a wide range of interactions that are expected to be of some ecological significance.

Some studies which have considered the influence of edge on various interactions include, to name but a few:

- The additive effect of nearby edges (Porensky 2011; Malcolm 1994)
- The effect of aspect (Hylander 2005; Tuller 1973)
- The effect on the light environment (Dignan & Bren 2003)
- The effect on biodiversity (Pryke & Samways 2012)
- The effect on faunal interaction (Donovan *et al.* 1997; Porensky 2011)
- A combination of factors (Cadenasso *et al.* 2003; Huggard & Vyse 2002)

However, given that the focus in the current study is on the effect of the edge on the variation of growth within a plantation stand, more attention was given to work within the context of plantation forestry.

### 2.1.3 Edge effect in plantation forestry

The work of Cancino (2005) provided interesting insights into the study of edge effects in plantation forestry. In his study, he presented six different models, predicting DBH, total height, crown height, and basal area as a function of edge effect. He considered two different compartment ages, namely old and young stands as well as aspect of the edge. These models were parameterised using measurements from data collected from two adjacent *Pinus radiata* stands in Chile and the various models discussed and assumptions made regarding the edge effect under these conditions. In a later study (Sandoval & Cancino 2008), a competition index was incorporated into these edge models in order to take into account competition within the stand. The inclusion of this index was found to significantly reduce the residual variation in the modelling. The concept of taking additional stand structural indices into account when creating the edge model was motivated by this finding.

Additional traditional studies have been carried out on plantation forests of *Pinus radiata* where the effect of edge on tree growth was investigated. These include studies by:

- Berg (1973), who investigated the effect of gap size on edge tree development and found that a larger opening size resulted in a logarithmically larger DBH. Edge trees on a site with the same site index were found to have significantly larger DBHs than inner-stand trees. The effect of age on the difference was found to become clear only after canopy closure, exhibiting a difference of 15cm on average productivity sites at age 30.
- Van Laar (1978), where the change in DBH over the outer six rows of *Pinus radiata* stands was investigated. He found a significant effect of edge on the first three rows adjacent to the edge in terms of increased DBH.
- Minko & Hepworth (1990) investigated the effect of increasing circular gap radius on the height, diameter, form, and branch size of *Pinus radiata*. It was found that trees adjacent to larger gaps had larger DBHs and larger volumes but that height did not change significantly moving outwards from the gap centre. It was also suggested that improved lateral light penetration into the crown promotes a lower slenderness ratio.
- Hansen *et al.* (1993), who studied the change in both height and DBH of *Pseudotsuga menziesii* up to a distance of 120m from the edge also taking tree density into account. It was

found that both diameter and height were significantly depressed at distances of 20m from the stand edge.

- Ackerman *et al.* (2013), where irregular inner stand structure was used to mimic edges inside the stand by gap formation in *Pinus patula*.

Harper *et al.* (2005) explain that “the magnitude and distance of edge influence are a direct function of the contrast in structure and composition between adjacent communities on either side of the edge” (p.768). In the aforementioned studies, the characteristics of the two environments on either side of the edge zone in are described qualitatively. It would be beneficial to quantify the edge on a continuous scale, where the neighbouring land use and the proximity of that land use to the stand edge in some way quantifies the degree to which the edge was generally competition stressed on the one end of the scale or competition free on the other.

This study focuses specifically on plantation forestry and builds on these findings and methods by providing a framework that generates and fits edge models based on manual and remotely sensed input data for any possible plantation forestry circumstance or edge interaction, using a proposed method for quantifying the influences at the edge.

## 2.2 Remote sensing of plantations

Data requirements of this study are of such a scale that manual tree measurement will not suffice in order to provide tree height and tree position data encompassing a wide enough range of edge situations. The data is of a spatial nature and requires the measurement of a large number of trees, including their position, which is a time-consuming and costly exercise if carried out terrestrially. It is therefore proposed that data be collected from remote sensing sources in order to provide a larger dataset to analyse.

Campbell and Randolph (2011) define remote sensing as “The science of deriving information about an object from measurements made at a distance from the object, without actually coming into contact with it.” (p. 6) The process of forest inventory, where data is collected in the field by physically measuring different parameters of individual trees and stands is seen as “a field where improved technologies such as remote sensing in conjunction with Geographical Information Systems (GIS) may be used to reduce costs and improve upon inventory estimates” (Roberts *et al.* 2007: 184). In their study regarding the application of remote sensing to the collection of forest inventory data by remote sensing, Gong *et al.* (1999) propose the term ecometrics as an “interdisciplinary field defined as the science and technology of obtaining reliable ecological measurements over large landscapes” (p. 9).

### 2.2.1 Photogrammetry

Photogrammetry is defined by the American Society of Photogrammetry and Remote Sensing as “the art, science and technology of obtaining reliable information about physical objects and the environment through processes of recording, measuring and interpreting photographic images and patterns of recorded radiant electromagnetic energy and other phenomena”. (Wolf & DeWitt 2000:1). Gong *et al.* (1999) consider the use of digital photogrammetry as “a computerized technique that automates the measurement and mapping process of traditional photogrammetry” (p. 10).

In their overview of the application of remote sensing for forest inventory, Kätsch & Kunneke (2006), state that “the compilation of data on growing stock is one of the most costly aspects in forest management” (p. 43) and they propose that modern technologies based on photogrammetry and aerial photography can be used to obtain the majority of the required inventory data. The use of aerial photography for forest inventory makes practical sense because aerial photographs are available for many plantation areas, having been commissioned by forestry companies.

### 2.2.2 Digital elevation, surface and height models

Stereopsis is defined as the “ability to perceive depth and relief by stereoscopic vision” (Oxford English Dictionary Online, 2013). This ability is used to quantify tree height and has been discussed various times since at least 1936 when Andrews (1936) presented the parallax method to extract tree heights from aerial photographs. The classic parallax method is carried out by calculating the difference between the tip of the canopy and the base of trees on stereopairs of aerial photographs by means of photogrammetric measurement (St-Onge *et al.* 2008). Since that time, manual plotting of spatial data and paper prints have been replaced in most cases with digital formats of the data (Miller *et al.* 2000). Miller *et al.* (2000) explain that a number of advantages came with the digitisation of spatial and photogrammetric data including the possibility of carrying out repeated analyses with a higher level of accuracy by utilising new techniques offered by Geographic Information Systems (GIS). Obtaining photogrammetric depth measurements in a digital format is thus referred to as digital stereophotogrammetry.

For the purposes of this study, the variable of interest is the height of the tree above the ground i.e. the elevation of the tree, as well as the position of that tree. Digital stereophotogrammetry is used for the extraction of tree canopy surfaces from aerial photos. A tree canopy elevation surface (digital surface model or DSM) is produced and subtracted from a surface representing the elevation of the underlying ground (digital elevation model or DEM). By computing the difference between these two surfaces, a canopy height model (CHM) can be created that accurately reflects the spatial variations of the height of the canopy surface (St-Onge *et al.* 2008). An example of such surfaces is shown in Figure 2.2. Tree heights and positions can be extracted from such a CHM.

Extracting data from CHMs can, however, prove challenging since some inherent problems in using stereophotogrammetry include:

- Identifying the tree base or correctly identifying the ground level (St-Onge *et al.* 2004)
- Tree diameters cannot be directly measured from aerial photographs but have to be estimated in an alternative way (Kätsch & Kunneke 2006)
- Identifying the exact tree position (Pitkänen 2001)



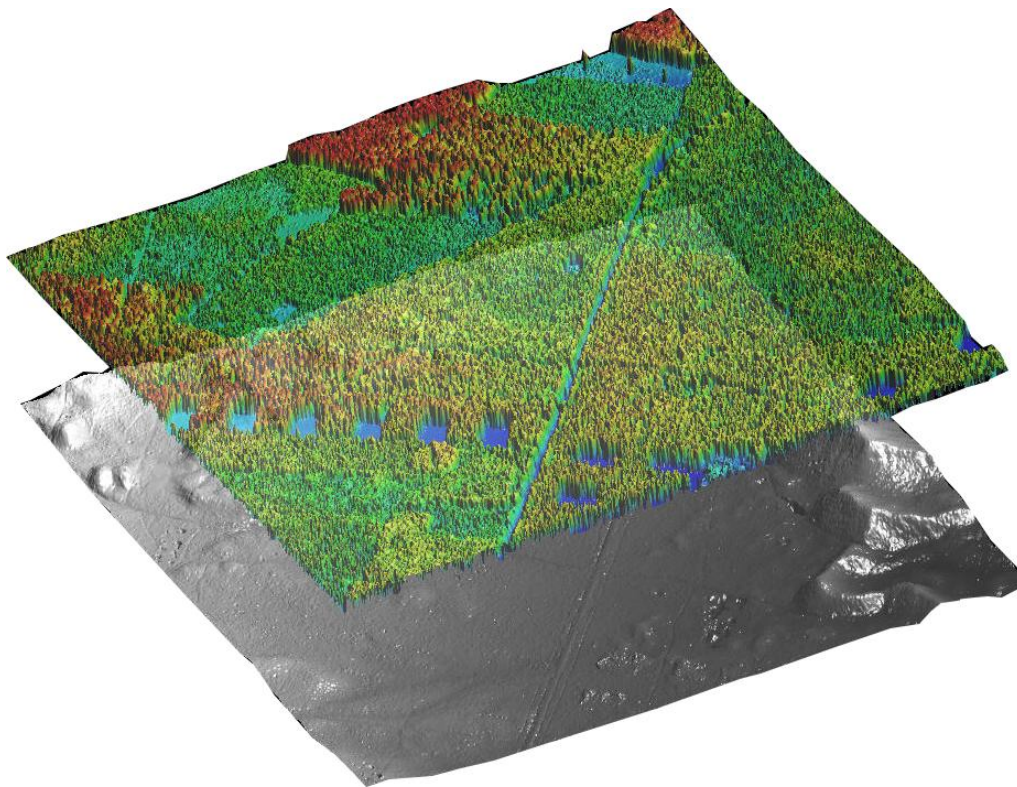


**Figure 2.2.** A demonstration of a CHM and a DEM of the underlying ground level. A DSM is the combination of these two. (P. Wężyk, 2013) <sup>1</sup>

### 2.2.3 Remote sensing using LiDAR

Another remote sensing technology that has been receiving a lot of attention in the forest industry as a “rapid and efficient tool for forest inventories” (Leeuwen & Nieuwenhuis, 2010, p. 749) is Light Detection and Ranging (LiDAR). This form of remote sensing is similar to radar in that it “exploits electromagnetism for the detection and ranging of spatial objects, and it is similar to optical forms of remote sensing in the sense that it uses optics for the refraction of these electromagnetic waves” (Leeuwen & Nieuwenhuis, 2010, p. 749). Measuring and ranging of objects is done by calculating the time that passes between the emission and reflection of pulses. A collimated beam of laser light is used which “gives the advantage of having an energy-efficient means of ranging relatively small objects and discerning a finer spatial detail than radar allows for” (Leeuwen & Nieuwenhuis, 2010, p. 750). Objects are measured in three-dimensional space using a LiDAR sensor in combination with global positioning systems (GPS) and inertial navigation systems (INS). Used in this way, LiDAR provides for different platform types such as ground-based, airborne or spaceborne platforms which “allow for a variety of information to be acquired with relative ease, whether large scale, small scale, stand level, or at the level of the individual trees, with each platform type suited to specific forest inventory information needs” (Leeuwen & Nieuwenhuis, 2010). LiDAR therefore is highly adequate remote sensing technology for the measuring of forest attributes. It is however a technology that is not available for use in this study and was not applied.

<sup>1</sup> Numerical model of land cover and terrain model aircraft registered laser scanner, District Chojna. [ONLINE]. Available at: [http://www.ibles.pl/struktura/zaklady\\_naukowe/zuml/grafika/DSM\\_DTM.jpg](http://www.ibles.pl/struktura/zaklady_naukowe/zuml/grafika/DSM_DTM.jpg) [Accessed 09 September 13].)



### 2.3 Spatial modelling of DBH as a function of height

A substantial amount of work has been done in quantifying the relationship between tree DBH and height. Generally, the focus appears to be on modelling the height from the DBH as the DBH is cheaper and faster to measure from the ground. However, the approach of using remotely sensed tree heights necessitates the inverse relation to be used when modelling the DBH as a function of the tree height.

Traditionally, the relationship between height and DBH is determined for the compartment as a whole, using standard statistical regression procedures (Howard 2012). The simplest would be to use manually measured DBH-height pairs and generate a model that best fits the relationship and repeat this exercise for each study area in question. However, the possibility of including spatial tree and stand attributes in the model, which could modify DBH-height relations, warrants further investigation.

Various ways of including spatial variables into the height-diameter relationship were tested at various levels, starting from a countrywide positioning to within-stand competition.

In a study to model individual tree height–diameter relationships for Scots pine, it was found that a single height–diameter function without further predictor variables is not able to correctly describe all the possible relationships that may be found within a given forest (Schmidt *et al.* 2010). They interpolated the effect of the geographic coordinates of various sites across Estonia on the DBH-height relationship. A similar study was earlier done in Spain by Nanos *et al.* (2004) where they attempted to derive a method for spatially predicting the DBH-height relationship by means of a Kriging interpolation across a region in central Spain. On a slightly smaller spatial scale, a region was classified into ecologically homogeneous areas by Huang *et al.* (2000), where different diameter-height models were defined for these different ecoregions.

Moving the spatial perspective from the spatial position of the stand on a regional scale to the position and interactions of the tree within the stand, Zhang *et al.* (1997) studied the effect of thinning on the relationship between DBH and height for *Pinus taeda*. In this study it was found that tree height by diameter class significantly decreased as thinning intensity increases since thinning effects on diameter growth are relatively greater than on tree height growth (Zhang *et al.* 1997). Various other spatial structural indices have been developed, which could potentially be used to quantify more accurately the relationship between DBH and height (Aguirre *et al.* 2003; Pommerening 2002; Evans & Clark 1954). Pommerening (2002) reports that the diversity of tree dimensions involves the spatial arrangement of, for example, diameters or heights. However, the inclusion of evenness into height-DBH or DBH-height models does not seem to have received sufficient attention.

### 2.4 Regularity, or evenness of stand structure

As stated by Evans and Clark (1954), “the pattern of distribution of a population of plants or of animals is a fundamental characteristic of that population.” In a study by Gadown *et al.* (2012), the authors state that “forest structure usually refers to the way in which the attributes of trees are distributed within a forest ecosystem” (Gadow *et al.* 2012, p.30). It was found that tree growth and the interactions between trees depend, to a large degree, on the structure of the forest (Gadow *et al.* 2012). In order to be able to simulate the growth of a tree, stand or forest, it is therefore

necessary to take into account the structure of the forest. According to Pommerening (2002), the quantification of forest structure as mean values or empirical distribution has been done by statisticians since the 1970s. He explained how forest structure can be quantified in a number of ways, but can generally be grouped into distance dependent and distance independent measures at the stand level as shown in Figure 2.3 below.

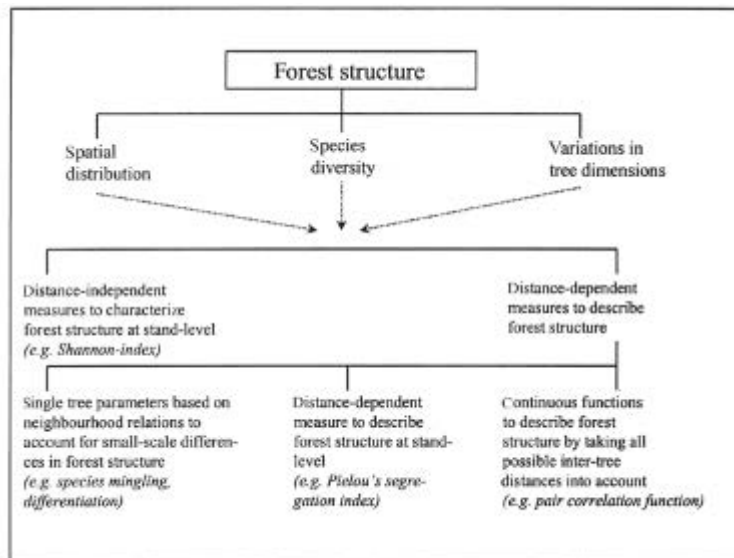


**Figure 2.3.** Overview of the three major characteristics of forest structure and the groups of variables by which forest structure is assessed. (Pommerening 2002)

The spatial nature of the current study, in conjunction with computing capacity available for the execution of complex algorithms, as well as the availability of fairly large datasets of remotely sensed spatial plantation data allows for the investigation of distance dependent forest structural measures. An index of interest is the evenness or regularity of the stand. In a recent study by Ackerman *et al.* (2013), regularity of a pine plantation stand is defined as trees growing in a situation with spatially symmetric competition. It was found that local stand density variations affect DBH. The question of the effect of evenness on height growth was not discussed. However, hypothesising that DBH is affected by local density variations but height is not, it could prove significant to use tree regularity as an additional explanatory variable when modelling DBH as a function of height or *vice versa*. Also, considering that the edge might not have the same effect on height as it has on DBH, it would be advantageous to be able to include an additional spatial variable when modelling the relationship between these two variables so as to better model the relationship between DBH and height especially for edge trees.

In their study of the quantification of the non-randomness in spatial patterns, Evans & Clark (1954) produced a measure using nearest neighbour measures which they defined as “the ratio of the observed mean distance” between all trees in a stand of interest “to the expected mean distance” (for a randomly distributed population) “as the measure of departure from randomness” (Evans & Clark 1954, p.447). This measure is denoted R. They further explain that a randomly distributed population would result in an R value of 1 and that a population in which all points are equidistant from one another (a perfectly even, hexagonal pattern), the R value would be 2.1491. Combining this train of thought with the work by Ackerman *et al.* (2013), this evenly distributed, equidistant, hexagonal spatial arrangement should result in improved space-use efficiency and crown growth proportionality. Thus the deviation of a stand from a hexagonal pattern might be a relevant measure.

A feasible approach to quantify spatial evenness is provided by Delaunay triangulation (Delaunay 1934). In a study applied to human muscle cells, Dryden *et al.* (1999) were able to use the coefficient of the area of Delaunay triangulation to quantify regularity of a spatial point pattern. They proceeded to produce a model that could simulate the pattern of a given regularity as shown in Figure 2.4. Using the outputs from the model they then tested the validity of various test statistics to describe the regularity. They propose using the coefficient of variation of the squared sizes of the Delaunay triangles to describe regularity of a point pattern.

An optimal, hexagonal arrangement can be visualised by considering a Delaunay triangulation of a perfectly even, regular stand. All triangles would be equilateral. Analysing any arrangement of trees in a forest by carrying out a Delaunay tessellation not only provides the distance to the nearest neighbour but a distance to all neighbouring trees for any given tree. The variation in the lengths of all the lines related to a single tree should provide an indication of the extent to which that tree differs from the ideal situation of equidistant Delaunay lines. Thus, combining the distances, and calculating their variation from the mean distance, should provide a useful quantification of the forest structure, which could be linked to space use efficiency, DBH-height relationships, and tree growth.

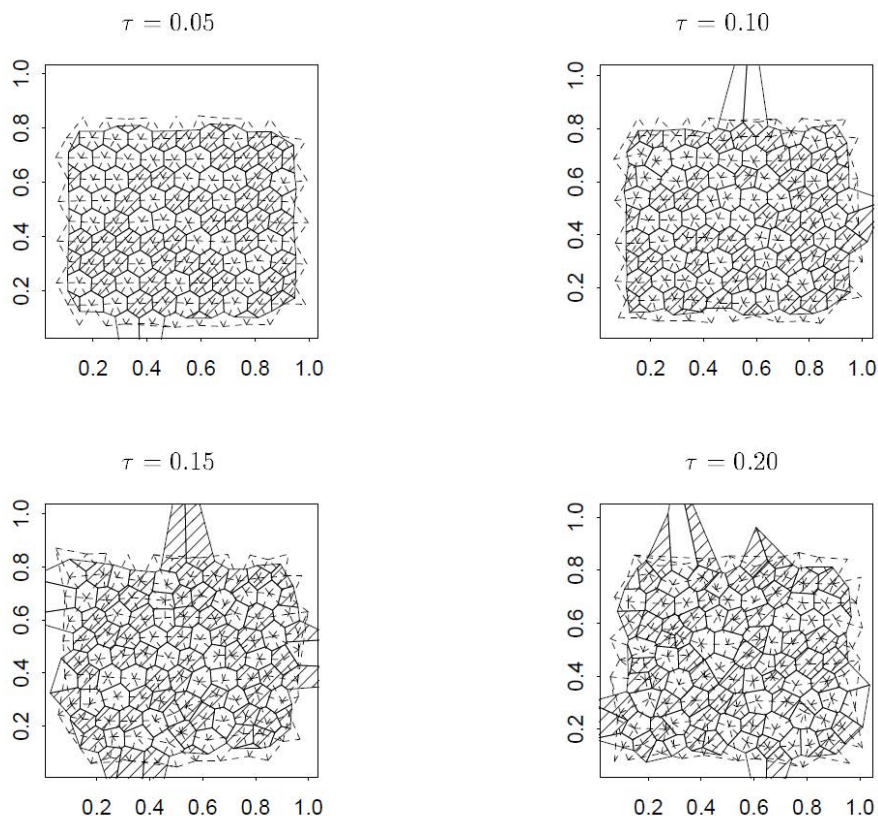


**Figure 2.4.** Points with varying levels of regularity generated by (Dryden *et al.* 1999). The parameter controls the amount of regularity in the model – smaller  $\tau$  producing more regular patterns.

### Chapter 3. Analysis and quantification of edge effects

This chapter will provide an overview on the applied process of achieving the first 5 objectives as laid out in Section 1.2, namely:

1. Providing a methodology for quantifying interaction at stand edges between trees of a given stand and trees of a neighbouring stand over the lifetime of the stand.
2. Transferring the edge interaction value from the edges to all the trees within the stand in a coherent way.
3. Identifying the spatial extent of the edge effect into the stand.
4. Providing a methodology for taking spaces between stands into account.
5. Modelling the expected variance caused by the edge and thus explaining the relationship between the edge interaction and tree variables, taking the spaces between compartments into account.

An evenness index will also be introduced as proposed, and tested for significance as an additional explanatory variable for modelling DBH as a function of height.

The inclusion of the cardinal direction of the edge in spatial edge effect modelling is considered and calculated but this is not included in the models because of insufficient data.

In Figure 3.1 below the steps of the process to be carried out in this chapter is illustrated and the respective chapter sections are numbered.

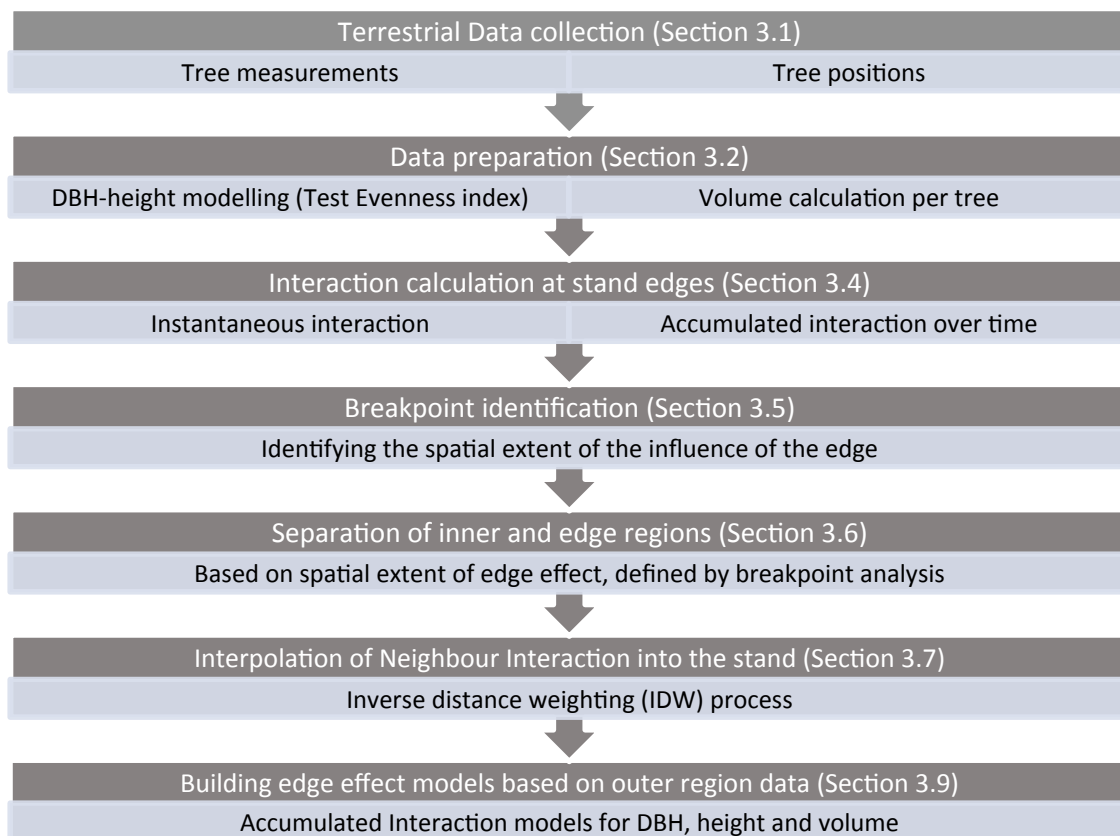


**Figure 3.1.** Flow chart indicating the steps for the edge effect quantification process.

In order to calculate edge effects, initially, the stand is quantified in terms of the edge interaction. Two edge interaction values are introduced to spatially quantify the interaction at the stand edge between neighbouring stands over time. An interpolation of these edge interaction values into the stand interior is carried out spatially using an inverse distance weighting (IDW) approach. It is assumed that the stand centre of a sufficiently sized stand is unaffected by the edge and a single, neutral interaction value is assigned to that region. The division between the affected and unaffected regions is estimated as the breakpoint calculated by means of segmented regression.

Modelling of a stand in terms of tree volume, DBH and height based on the edge interaction is carried out on a dataset of a fully terrestrially measured stand. Linear regression is applied to the data to produce the various models for these variables.

### 3.1 Terrestrial data collection

Data for the study were collected from Monterey Pine (*Pinus radiata*) plantations in the Grabouw district of the Western Cape Province of South Africa (Figure 3.2). Monterey Pine was selected because of the availability of results from previous studies carried out on the same species (Cancino 2005; Sandoval & Cancino 2008; Minko & Hepworth 1990; Berg 1973; Van Laar 1978). The plantations in the Grabouw district are also undergoing various concurrent studies and thus data and results were interchanged between the various researchers. The plantations are typical even-aged single species plantations grown on an approximately 29 year rotation primarily for pine saw-timber (Cape Pine 2013).

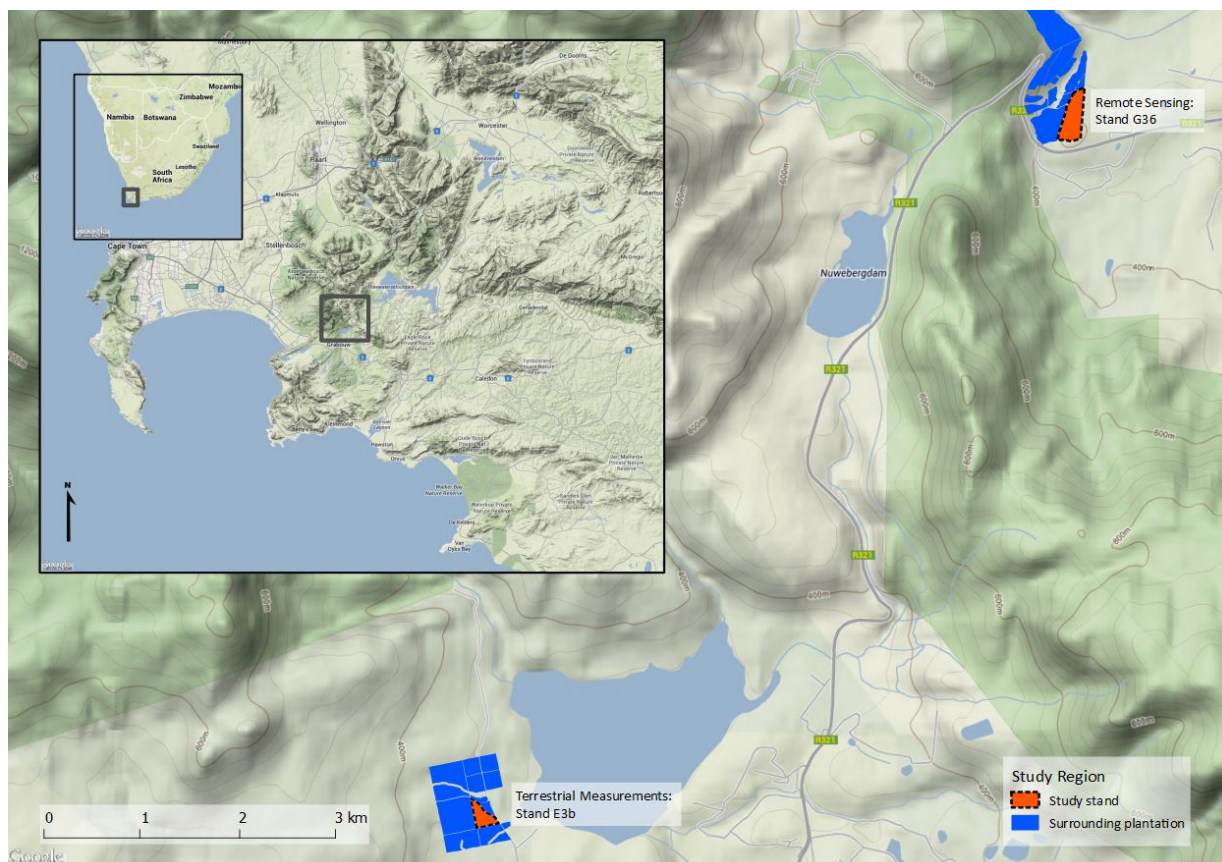


**Figure 3.2.** The study region in Western Cape Province of South Africa, with terrestrial data collected from the study stand (in orange) at the bottom of the image and the remotely sensed data collected for the stand on the upper right of the image. (Base map provided by Google Maps 2013, in QGIS)



A stand from compartment E3b (Figure 3.2 and Figure 3.3) was selected as the pilot stand for the majority of manual measurements. It was selected because of its variety of edge types (competition free edges, dominant edges, suppressed edges) and its size, which allows a large enough interior where it can safely be assumed that the edge effect is no longer significant. Stand E3b is a *Pinus radiata* stand of 2.84ha and 25 years of age. All edges of E3b are adjacent to forest roads. A perennial stream flows through the upper middle region of the stand which introduces an undesired variability into the inner stand region. Data were collected terrestrially in this stand to provide the dataset for the generation of the interaction models in terms of volume, diameter and height.

In stand E3b there are 1124 trees. All trees were tagged in field and their diameters at 1.3m were measured using diameter tapes as well as two height measurements using a hypsometer (Haglöf ultrasound based Vertex Mark IV) and crown base measurements for 314 of the same trees.

Tree positions for all the trees in the stand were determined using a Trimble Surveyors Total Station in conjunction with a Trimble GPS.

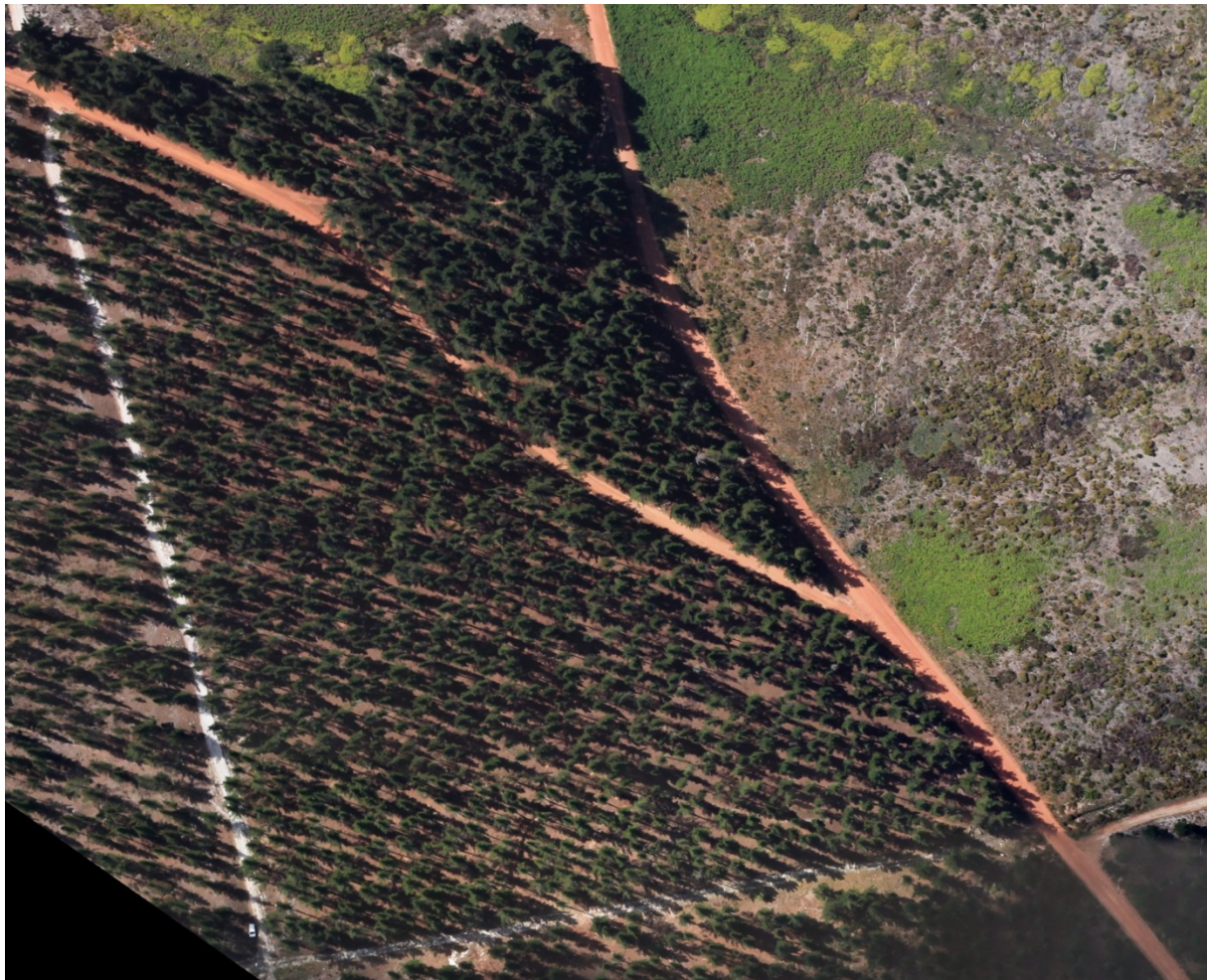


**Figure 3.3.** An aerial view of compartment E3b, taken 12 November 2012.

### 3.2 Data preparation

Various steps were carried out to extract and prepare the data collected in the process of achieving the four objectives as mentioned above. Three shapefiles were produced, namely:

1. A lines shapefile containing the line segments representing the dripline of the stand, as defined in Section 2.1. The outline of the stand is later split into various segments for the interaction at that segment to be calculated.
2. A points shapefile containing volume, diameter and height of all trees was prepared. The evenness index which describes regularity was also calculated for each tree.
3. A polygon shapefile containing polygons of the stand with all neighbouring stands and basic stand data.

In preparation for the data input, these shapefiles were prepared in QGIS version 1.8.0 (QGIS Development Team 2013) and later used as an input to R statistical environment (R Core Team 2013).

In order to produce the lines shapefile, the stand edge had to be delineated. As discussed in Section 2.1, for the purposes of this study the edge falls on the plantation dripline. These driplines were manually delineated in QGIS from the stand CHM, aerial photographs and satellite images.

The points shapefile was generated from the tree positions as measured using the Trimble Surveyors Total Station. The manually collected data were input to the shapefile. DBH values for all trees were input whereas the unmeasured heights were predicted based on the regression relationship between the measured diameters and heights.

The polygon shapefile was prepared by combining the dripline of stand E3b and the driplines of the neighbouring stand and converting these lines to polygons. Each stands age was then input to the shapefile as well as the rotation length and stand species for each stand. A screenshot of the shapefile preparation process is shown in Figure 3.4 below.

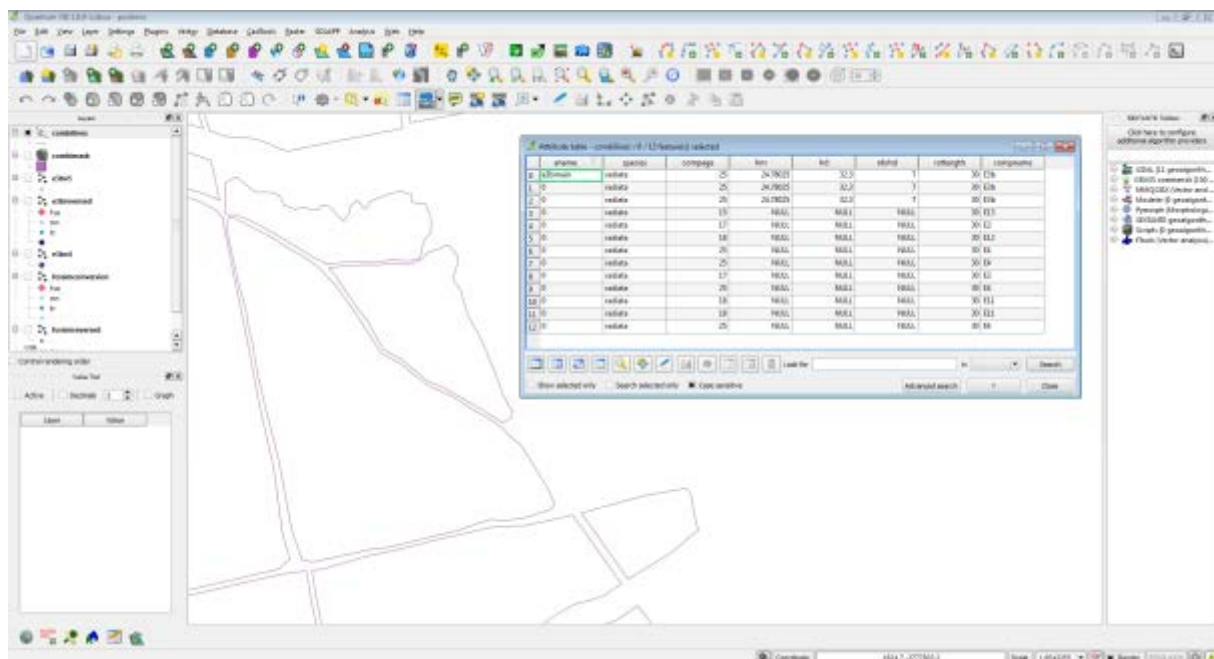


Figure 3.4. A screenshot of shapefile preparation in QGIS.

### 3.2.1 Spatial data manipulation in the *R* environment

Subsequent steps of the process took place within the statistical environment of *R* where the interaction calculation, modelling and simulation were carried out. Several further libraries were used in the process (spatstat, sp, shapefiles, maptools, plyr, rgdal, rgeos, raster, deldir, fields, rgl, car, scales, RColorBrewer, classInt, fields, gridExtra, gridBase, vcd, lattice, ggplot, geoconv).

## 3.3 Introducing a regularity index for diameter-height modelling

It was discussed in the literature review that trees with a higher regularity had a relatively greater DBH if they had the same growing space. It was hypothesised that regularity could play a role in the diameter-height relationship. It was also discussed how that a perfectly regular stand is one in which all points are equidistant from one another. Various indices can be extracted from the dataset to describe this regularity of a stand. It was decided that the coefficient of variation of all the distances between each tree and its neighbours would most clearly quantify the regularity of a tree position relative to its nearest neighbours. Neighbouring trees and their distance were defined by Delaunay triangulation. The coefficient of variation produces a value that is independent of unit and quantifies the extent to which the distances vary from the mean distance to neighbouring trees. In this way the concept of evenness should be captured fairly well.

Distances from each tree to its neighbours were extracted by applying the Delaunay algorithm from the deldir (Turner 2013) package in *R*, to the points pattern representing the trees. The evenness index was then calculated using the plyr (Wickham 2011) package, by combining the data for each tree and calculating the coefficient of variation of the distances to its neighbouring trees. The resultant index will subsequently be referred to as the evenness index.

### 3.3.1 Delaunay triangulation edge effect

One of the problems encountered when using Delaunay triangulation are the improbably long lines produced by edge trees when linking these with the nearest neighbouring tree, as shown in Figure 3.5. In the study of Dryden *et al.* (1997), the edge triangles were manually removed, however, in order to automate this procedure, in this study this problem was dealt with by removing all lines greater than three times the length of the average line, as demonstrated in Figure 3.6. This could however introduce some undesirable bias into the calculation of evenness. Another possibility would have been to exclude trees which fell within a given buffer of the stand edge as proposed by (Zenner & Hibbs 2000) and remove all lines that fall within the buffer. However, considering that edge trees are the focus of this study, excluding edge trees from the dataset was not deemed favourable.



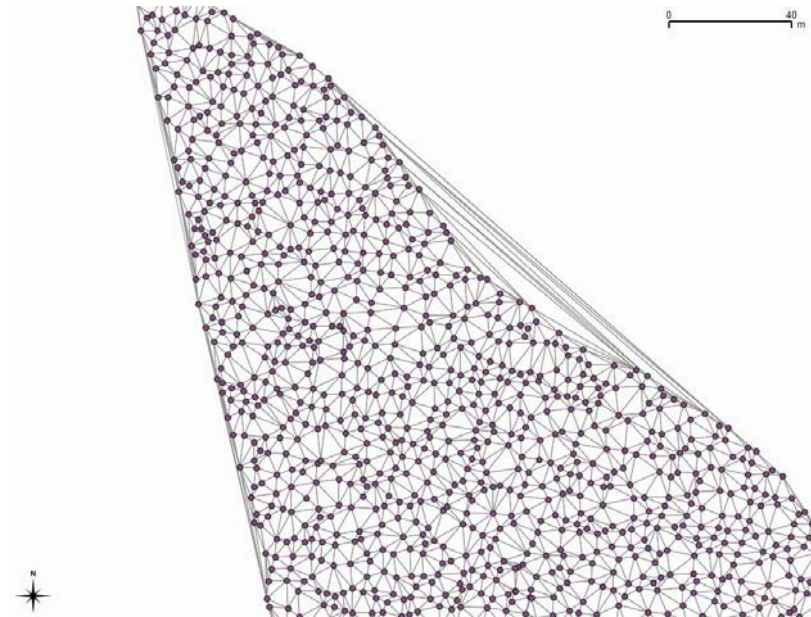


**Figure 3.5.** An illustration of Delaunay triangulation, demonstrating the problem at the edge of the stand where improbably long lines are generated at the edges of the stand.

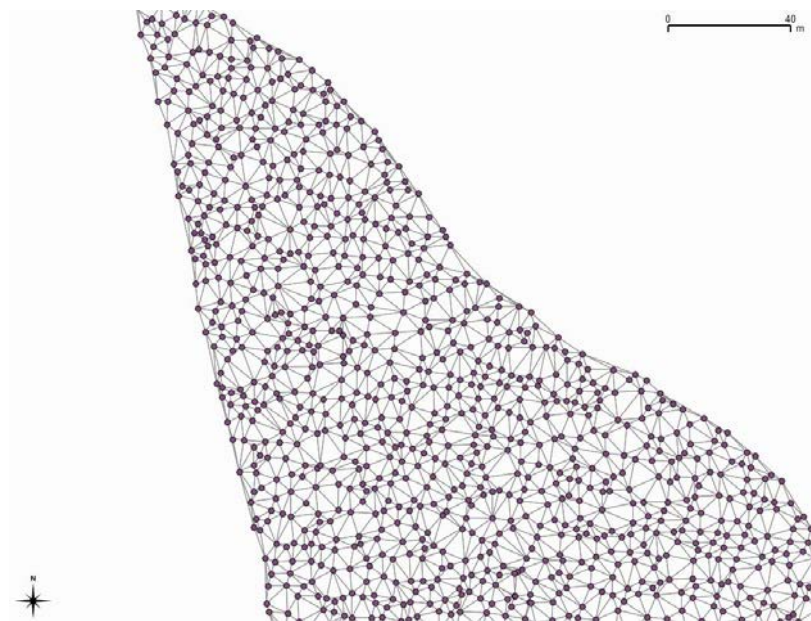


**Figure 3.6.** Delaunay triangulation after edge correction, where all lines linking “neighbouring trees” with a length greater than 3 times the mean line length had been removed.

### 3.3.2 Testing the contribution of the evenness index to the DBH-height relationship

An evenness index as described was calculated for the data of stand E3b with a representation of the output shown in Figure 3.7, where smaller circles represent trees with a higher degree of regularity. Two models of height as a function of DBH were compared, including and excluding the evenness index in the respective models. As shown in table Table 3.1, it was found that there was no significant difference between the two models (p-value of 0.9962) and it was concluded that including the index in the model did not contribute significantly. The index should, however, undergo future testing on other spatial tree datasets.

**Table 3.1.** ANOVA table comparing the models of height as a function of DBH, with and without the inclusion of the evenness index. The AIC values for both models are also included.

Independent variables	Res.Df	RSS	Df	Sum of Sq	F	Pr(>F)	AIC
DBH	234.00	954.38					1005.484
DBH + Evenness Index	233	954.38	1	9.5174e-05	0	0.9962	1007.484

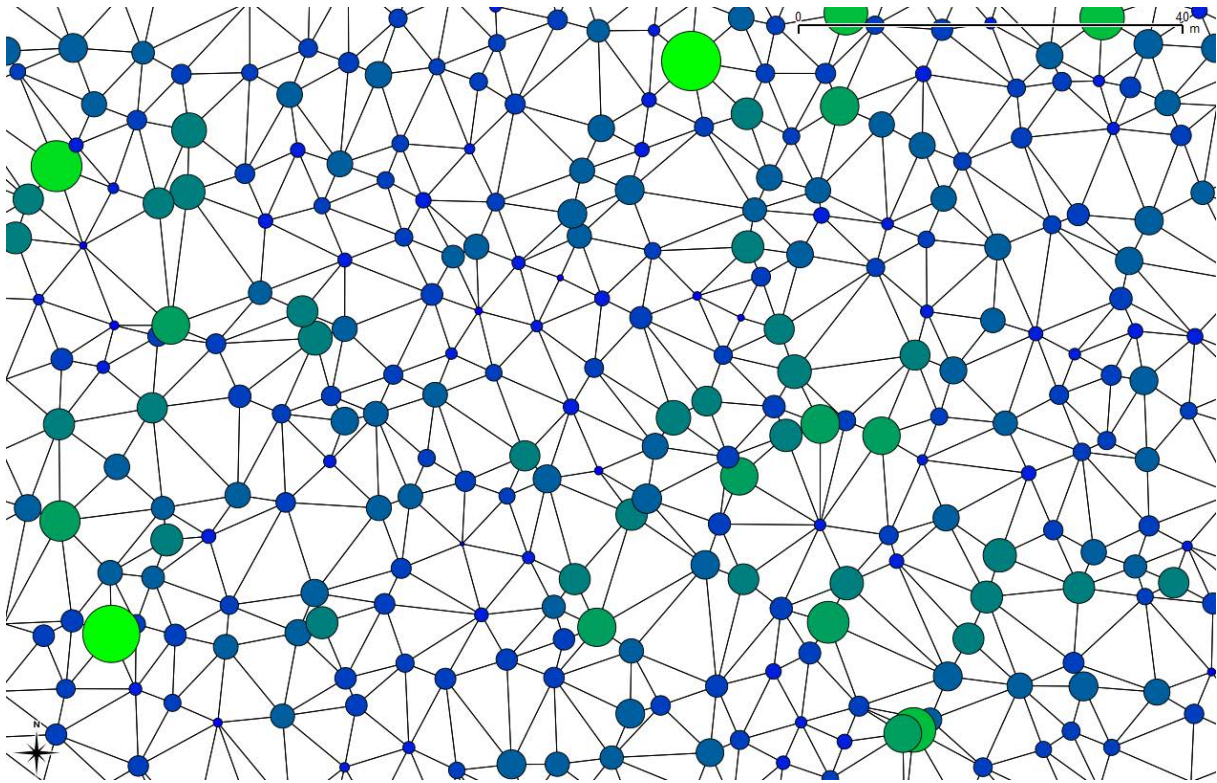


**Figure 3.7.** Visualisation of the proposed evenness index, with smaller circles representing a lower coefficient of variation for distances to neighbouring trees and thus a higher degree of evenness.

### 3.4 Quantifying interaction at the stand edge

In order to quantify edge interaction, the following question must be assessed: what was the effect of the neighbouring stand on the growth of a given stand throughout its lifetime?

This study undertakes to answer this question by evaluating the competitive relationship between a stand and its neighbouring stands throughout the lifetime of the given stand, at a given stand edge. It compares heights as extracted from a yield table for the given site and species under the assumption that competition and resource availability scale with tree height of the trees in the stand versus the trees of neighbouring stands. Two values quantifying this height relationship were introduced, namely:

1. **Neighbour Interaction (NI)**, which is an instantaneous interaction value quantifying the interaction between two stands at a given point in time.
2. **Accumulated Interaction (AI)**, which is the accumulation of Neighbour Interaction over a period of time at a given edge.

### 3.4.1 Neighbour Interaction

Neighbour Interaction (NI) was calculated as shown in Equation 1 below. The expected difference between the height of a given stand  $c$  and the height of its neighbouring stand  $n$  as a quotient of the maximum possible expected height was calculated for the given stand.  $h_{\max}$  is the maximum possible expected height to which the stand can possibly grow (height at rotation age) and is extracted from the yield table. The denominator  $h_{\max}$  is introduced to standardise the value and make it comparable across site classes.

$$NI = \frac{h_c - h_n}{h_{\max}} \quad (\text{Equation 1})$$

Where:

$NI$  = Neighbour interaction

$h_c$  = Height of given stand

$h_n$  = Height of neighbouring stand







$h_{\max}$  = Maximum possible expected height

As shown in Table 3.2 below, an NI value of 1 implies an interaction free edge, i.e. one with no neighbouring stand. Another scenario where  $NI=1$  could be where the height of the given stand  $h_c = h_{\max}$  and the height of the neighbouring stand  $h_n = 0$ .

An NI value of 0 implies an edge where the neighbouring stand is of the same age and therefore  $h_c = h_n$ .

When  $NI = -1$ , it implies that the neighbouring stand height  $h_n = h_{\max}$  and that  $h_c = 0$ , thus a complete dominance by the neighbouring stand on the given stand  $c$ . Other levels of interaction fit in somewhere between these values. In those cases where more than one neighbouring stand interacts on an edge, the mean interaction with all the neighbouring stands for that edge is calculated. A neighbouring stand is defined as one which falls within a buffer of width  $\approx h_{\max}$  of the edge of stand  $c$ .

**Table 3.2.** A summary of the NI scale, with the type of interaction taking place at the upper, middle and lower extremes of the scale, and a visual representation of the interaction between the two stands  $n$  and  $c$ .

<b>NI</b>	<b>Type of interaction at edge</b>	<b><math>c</math></b>	<b><math>n</math></b>
1	Interaction free; no neighbour or completely dominant ( $h_c = h_{\max}$ and $h_n = 0$ )		
0	Same age edges ( $h_c = h_n$ )		
-1	Complete dominance by neighbouring stand ( $h_n = h_{\max}$ and $h_c = 0$ )		

The hypothesis that accompanies the scaling of the NI values from -1 to 1 is that NI and tree productivity are positively correlated. Stand edges that are free of competition ( $NI \approx 1$ ) from neighbouring compartments should subsequently have more resources available to them and thus trees on these edges are able to produce more biomass. Those edges which are suppressed by neighbouring compartments at that point in time ( $NI \approx -1$ ) have less available resources and thus are expected to grow less. It is therefore hypothesised that growth decreases in proportion to the extent by which the neighbouring stand exerts dominance on that edge, quantified by difference in height.

Stand edges adjacent to a neighbouring stand of the same age are neither suppressed by, nor dominating, a neighbouring stand. Same age edges can be compared to trees at the centre of a large stand, beyond the extent of the edge effect. Such edges are quantified as a zero NI value on the scale, NI neutral. An example of the calculation of NI for a given edge interaction is shown in Figure 3.8 below. Current NI for any given time in the duration of the lifetime of the stand can be extracted from this graph.

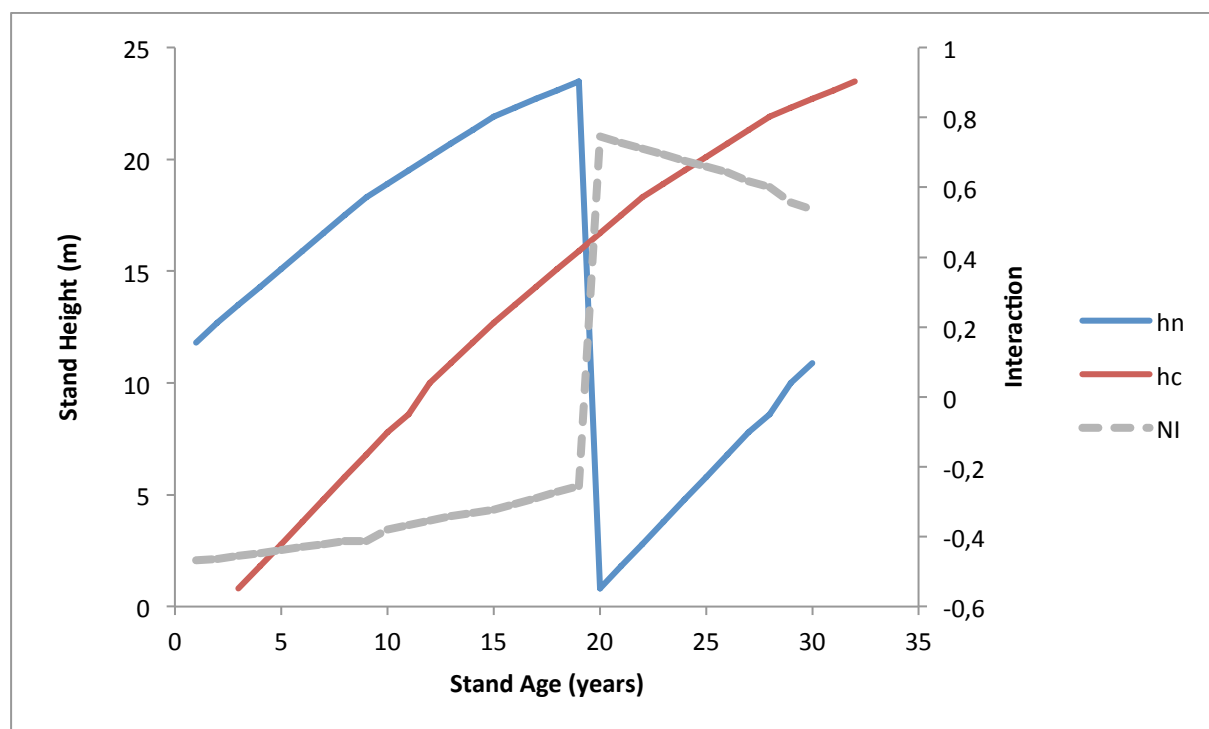


**Figure 3.8.** An example of the calculation of NI on an edge where the given stand *c* starts at age zero and the neighbouring stand *n* at age 12. The broken line indicates the NI value for a given point in time plotted on the interaction axis.

Rotation length in years  $I_r$  is also taken into account by the algorithm where the height of the neighbouring stand is set to zero at the year following  $I_r$ . When the neighbouring stand reaches rotation end as at stand age 20 in Figure 3.8, the predicted height of the neighbouring stand drops down to zero and resumes growth again. NI is therefore a dynamic value that changes during the lifetime of stand *c*, where at times the edge is under competition stress from a neighbouring stand but at some stage, when the neighbouring stand is harvested, this interaction is inverted and it becomes the dominant stand.

### 3.4.2 Accumulated Interaction

While Neighbour Interaction (NI) is an instantaneous value for interaction between two stands at a specific point in time, the Accumulated Interaction (AI) is the accumulation of these interactions over a given period of time. Stand *c*, at a given age, has been interacting with neighbouring stands for its complete lifetime, being suppressed or dominant by varying degrees for varying periods of time. Where the degree of dominance at a specific point in time is quantified by NI, the AI value

incorporates the temporal factor where the degree of dominance or suppression (quantified by NI) is weighted by the proportion of that time for which it was either dominant or suppressed.

Accumulated Interaction is calculated as the summation of the sum of the time-weighted dominant NI values with the sum of the time-weighted suppressed NI values (Equation 2). NI values representing dominance are weighted by the number of dominant years as a proportion of the total age of the stand. The same is done for the NI values representing suppression and for the number of suppressed years.

$$AI = \frac{age_d}{age_c} \sum_{i=1}^{age_d} NI_{d_i} + \frac{age_s}{age_c} \sum_{i=1}^{age_s} NI_{s_i} \quad (\text{Equation 2})$$

Where:

$AI$  = Accumulated Interaction

$age_d$  = Sum of years for which stand n was dominant

$age_c$  = Age of compartment

$NI_d$  = Sum of NI for dominant years (positive NI values as calculated in Equation 1)

$age_s$  = Sum of years for which stand n was suppressed

$NI_s$  = Sum of NI for suppressed years (positive NI values as calculated in Equation 1)

### 3.4.3 The dynamics of Accumulated Interaction units

An example of the calculation of AI is shown in Figure 3.9 below. This figure provides the same scenario as that in Figure 3.8 but includes the AI value represented by the dark solid line. For the purposes of this study, data for the prediction of heights was taken from the yield table in the South African Forest Handbook (Kotze *et al.* 2012) for *Pinus radiata* on a site index of  $SI_{20}=25$ .

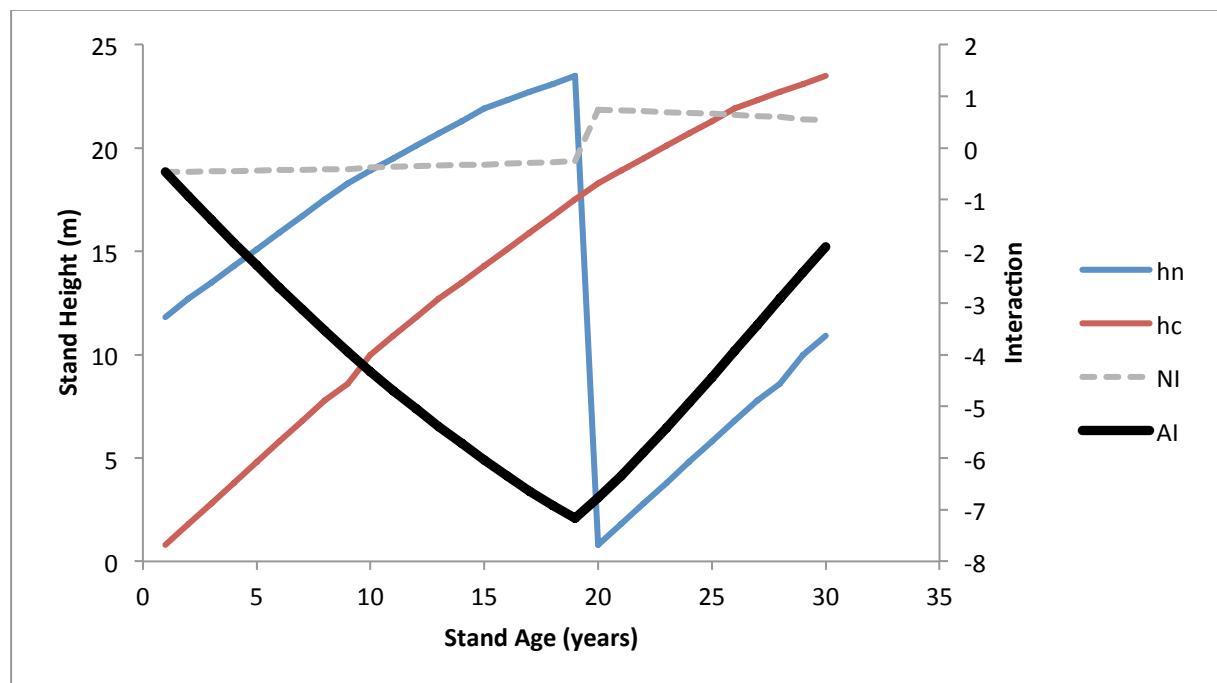


**Figure 3.9.** Accumulated Interaction for an edge of stand c if the neighbouring stand n is 12 years of age when stand c was planted and rotation length is 30 years. AI and NI are plotted on the interaction axis.



It is clear from the example that the accumulated negative NI values lead to a pronounced period of putatively negative impact on the edge trees of stand c, which is only reversed when the stand is relieved from the dominant competition stress of stand n in consequence of the clear felling of stand n. Accumulated Interaction can be regarded in terms of AI units, where one AI unit implies the accumulation of an NI of one over a period of one year, or an accumulation of an NI of 0.5 over a period of two years. AI goes beyond the scale of -1 and 1 and each value is edge specific. The maximum AI possible for a stand would be the AI at a given edge where only dominant NI values are accumulated, such as an edge with no neighbouring stand.

A further example demonstrating the dynamic of the AI value is given in Figure 3.10, where the neighbouring stand n is planted only three years before the given stand c, thus exerting dominance for almost the entire life of stand c. At age 29, the neighbouring stand n is harvested and stand c exerts dominance and begins to accumulate AI units. Figure 3.11 presents the opposite scenario, where stand c exerts dominance for the majority of its lifetime over stand n. In the first few years of its lifetime, stand c is suppressed after which it exerts dominance for the rest of its lifetime, accumulating a total of 2.175 AI units by rotation end.

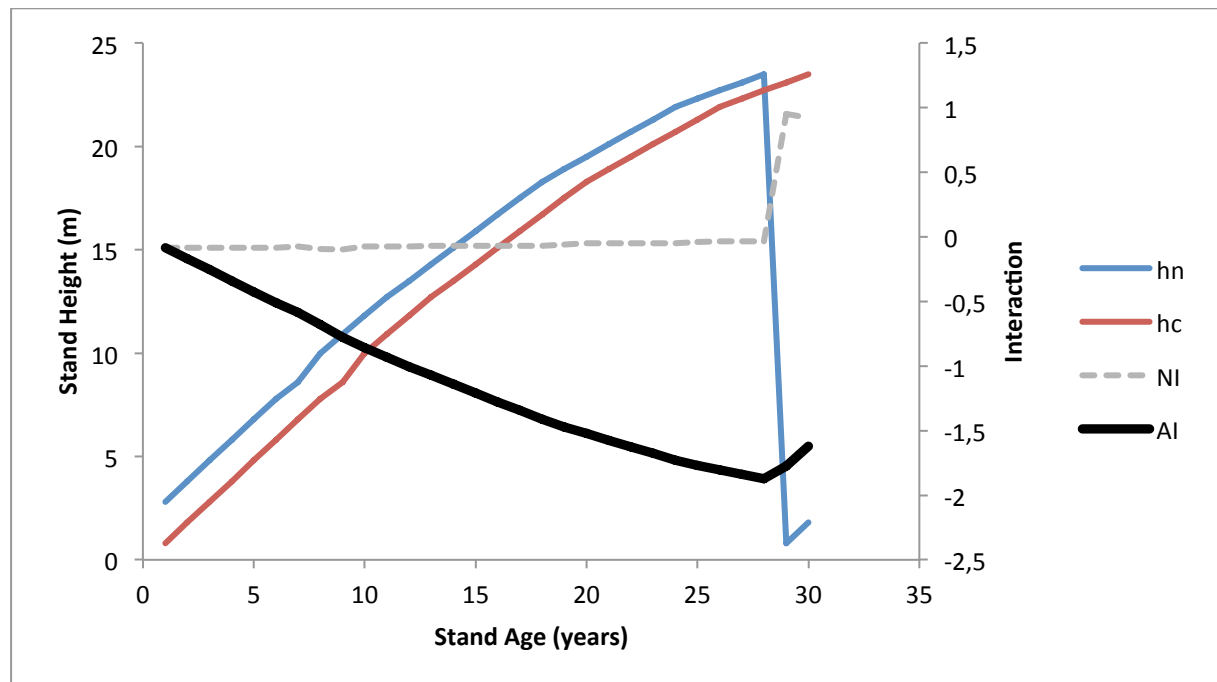


**Figure 3.10.** Accumulated Interaction for an edge of stand c if the neighbouring stand is 3 years of age when stand c was planted and rotation length is 30 years. AI and NI are plotted on the interaction axis.

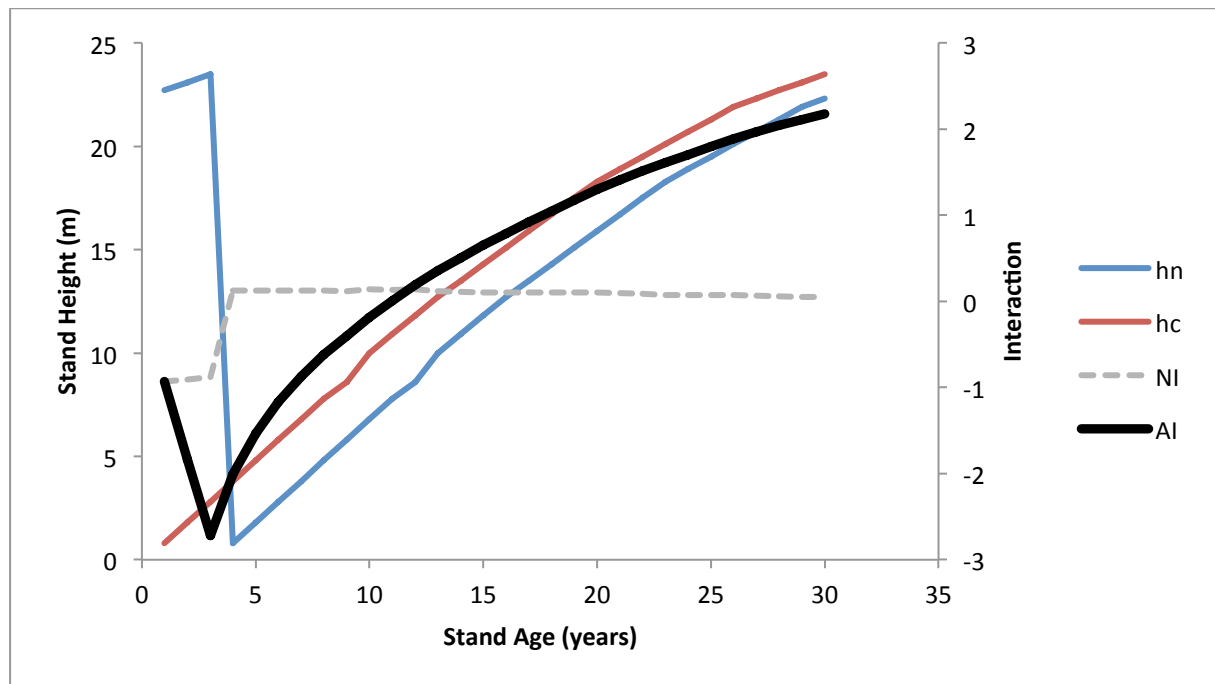


**Figure 3.11.** Accumulated Interaction for an edge of stand c if the neighbouring stand is 28 years of age when stand c was planted and rotation length is 30 years. AI and NI are plotted on the interaction axis.

#### 3.4.4 Calculating Accumulated Interaction for the edges of stand E3b

The algorithm for the calculation of the AI value was programmed fully in *R*. The algorithm works through the complete lines shapefile of stand E3b by identifying which edges of the stand of interest are subject to an interaction with neighbouring stands. It then quantifies the effect of this interaction in space and over time.

The spatial extent of this interaction zone is set to the maximum expected tree height in accordance with previous studies (Golser & Hasenauer 1997; Olson & Helms 1996), determined from the yield table and rounded to the nearest integer (30m). In spatial terms, this means that a buffer of 30m was generated around the given edge and was used to identify the neighbouring stands, which fall within the interaction zone of a stand edge. Comparing the expected height differences for each year of the duration of the lifetime of the stand then provides a quantification of the dynamic of the plantation forest system. In those cases where more than one neighbour has an effect on the edge segment, the AI was calculated for each neighbour individually and the mean AI value is linked to the edge segment.

##### 3.4.4.1 Identifying affected line segments and neighbouring stands which interact

Affected lines segments were identified in two steps in order to determine which neighbouring stands act on which edge segments. Firstly, all of the neighbouring stands are buffered at 30m. The outline of stand E3b was segmented at the areas where the buffer of any neighbouring stand intersected the outline of E3b. Essentially, this procedure was inward looking at the stand to assess which segments of the stand edge were affected by neighbouring stands. A segmented lines shapefile of E3b was produced for which each segment either fell within the interaction zone of one or more neighbouring stand *n*, or did not, in which case the segment was defined as an interaction

free edge. Identification of those segments of the outline affected by a neighbouring compartment are shown in steps a, b and c (Figure 3.13).

In the second step of identification, the affected segments of stand E3b itself are buffered, thus looking outwards from the stand in order to identify which of the neighbouring stands are responsible for the edge interaction, which can be one or more. These three steps are presented as steps d, e and f in Figure 3.13.

#### 3.4.4.2 Calculating AI for interacting edges

Accumulated Interaction for the interacting edges was then calculated using Equation 2 in an algorithm which iterates over the segments in the shapefile and calculates the AI units over the lifetime of the stand. Free edges, which did not undergo interaction with a neighbouring compartment, only accumulate dominant AI units. In order to calculate AI at these edges, all positive NI values were summed and weighted by one, as all the years in the lifetime of the stand were dominant years at that edge. In the case of E3b, AI values for free edges were calculated to be 18.6 and this value was assigned to the free edges.

Calculation of AI for the edges of stand E3b was carried out and an image of the output is shown in Figure 3.12. AI units for the edges of the stand ranged from -1.5 on the edges which were suppressed for more than half of their lifetime to 16.8 on the open edge. It was found that the majority of the sides had negative AI values. The stretch of the data therefore did not cover the complete range of AI values. There was a concentration of values between -1.5 and 0 with 16.8 at the other end of the range.

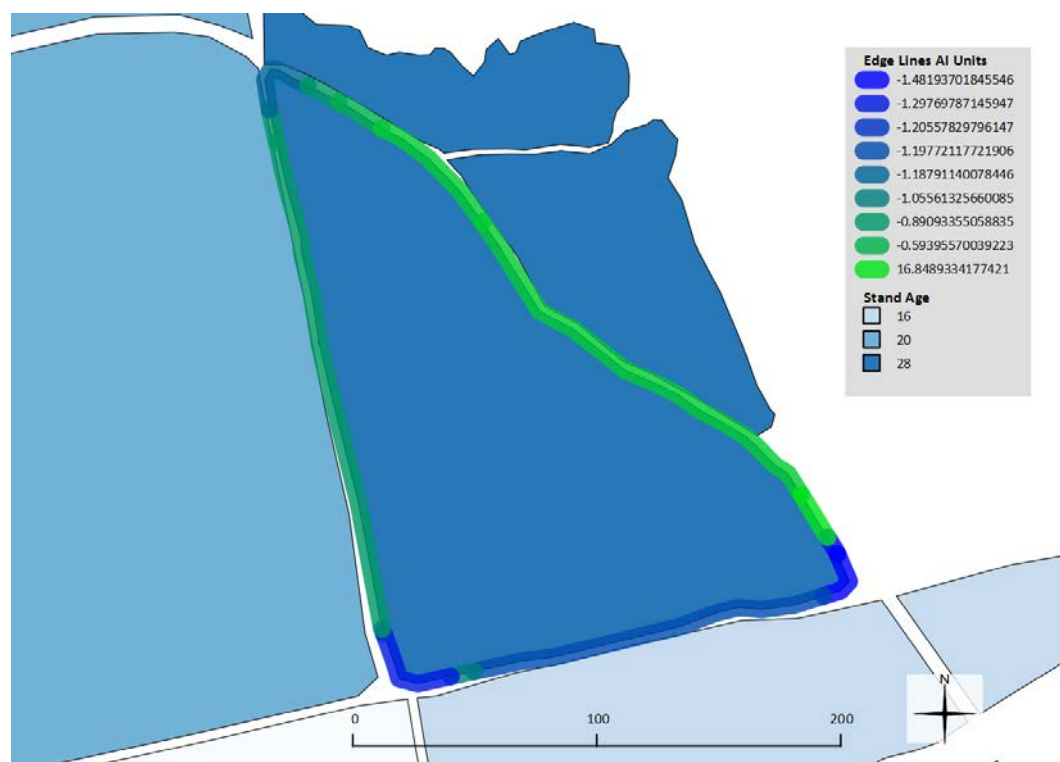


**Figure 3.12.** The result of the process of quantifying edge interaction for E3b. The edge of E3b is marked in graduated blue for negative AI values moving to lighter green for positive, higher AI values. The neighbouring stands with E3b are coloured according to their relative ages, with a lighter colour indicating a lower age.



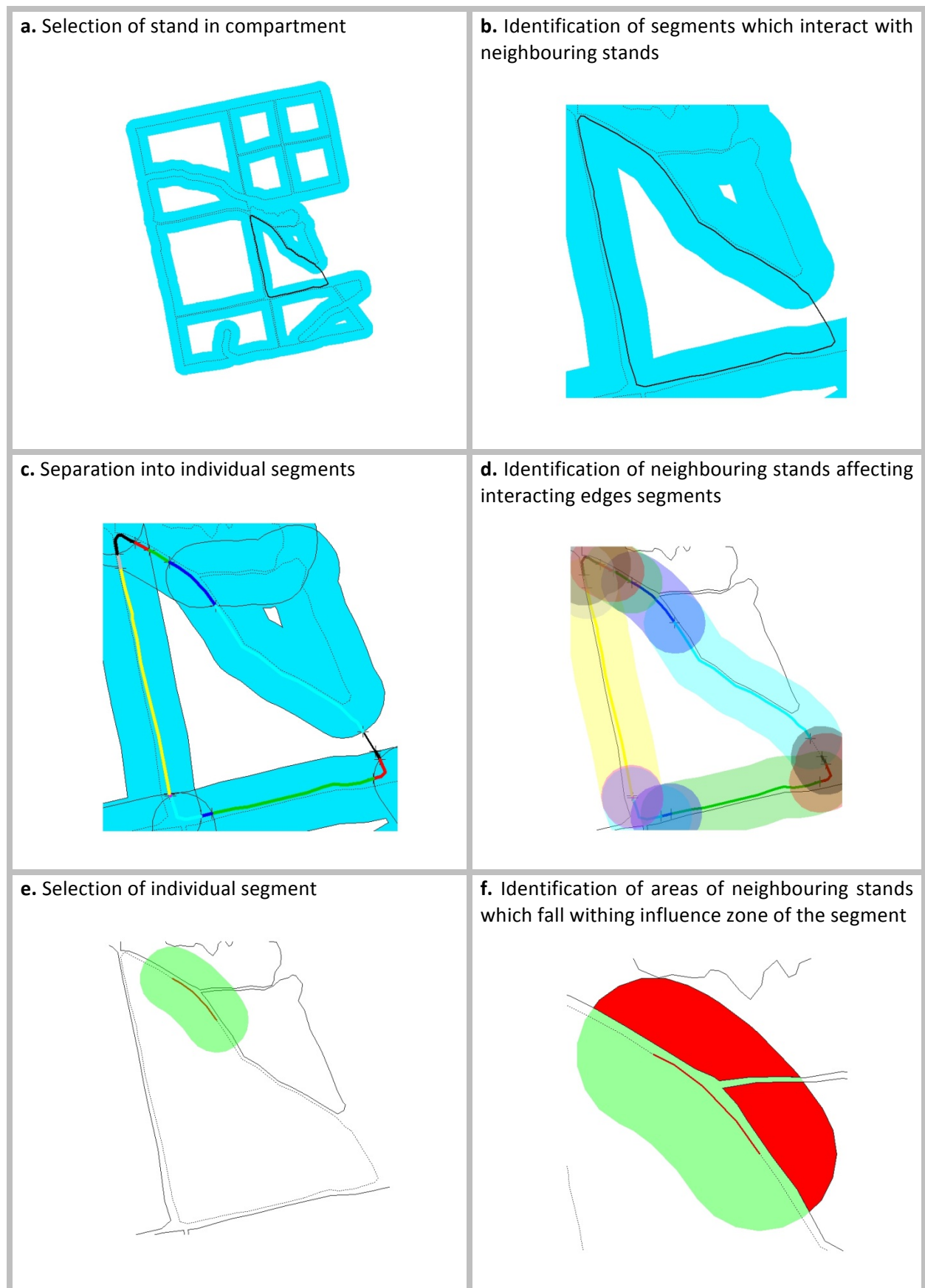


**Figure 3.13.** This figure illustrates the process of calculating AI values. In the first stage, the algorithm looks inward at the stand in question to identify which segments interact with neighbouring stands (steps a, b and c) and in the second stage the algorithm looks outward from each interacting segment to the neighbouring stands to identify which of these neighbouring stands interact at that segment (steps d, e and f). The level of interaction is calculated based on an interaction index by the difference in height over time.

### 3.5 Identifying the extent of the edge effect by segmented regression

As mentioned, the influence on tree growth as a result of the edge effect, takes place within a transition zone of a certain extent. Beyond the extent of that transition zone the edge effect is no longer of significance. It is therefore necessary to differentiate between that region of a stand affected by the edge and that region that is not. In his book dealing with point patterns, Diggle (2003) highlights the difficulty in identifying accurately the extent of the edge effect. He explains how that, if the extent is underestimated some residual effect remains of the edge within the unaffected area. If the extent is overestimated data are unnecessarily lost. It is therefore necessary to find a method of statistically identifying the extent of the edge effect. It was decided that the segmented regression approach would be used in this study in order to identify that point in the stand where the influence of the edge on tree growth is no longer of significance.

In his introduction of the “segmented” package for the *R* package, Muggeo (2008), described segmented or broken-line models as regression models where the relationships between the response and one or more explanatory variables are piecewise linear, in other words, relationships represented by two or more straight lines connected at unknown values. These values are usually referred as breakpoints, change points or even join points. He explains how segmented regression can be used to assess threshold value where the effect of the covariate changes.

In applying this method of generating segmented linear models for diameter as a function of distance to the edge, it should be possible to identify that position at a certain distance from the stand edge, where the edge effect is no longer significant. The point where the linear model representing the inner region of the stand meets with the model representing the edge region of the stand is the point that can be accepted to represent the extent of the edge effect.

This method was effectively tested and applied by Betts *et al.* (2007) to identify thresholds in the occurrence of bird species in order to quantify the exact suitable habitats for those species. It was also successfully applied by Ulm (1991) who used it within the *R* framework in an epidemiological study of the relationship between occupational dust exposure and chronic bronchitic reactions.

#### 3.5.1 Segmented regression of stand E3b data

The shortest distance between each tree and its nearest edge was calculated for all trees within the stand. Figure 3.14 below depicts a spatial representation of the DBH-distance relationship, where the size of each circle represents DBH of that tree, giving an indication of the relationship between distance from the edge and diameter and the shading of each circle is from dark to light with increase in distance.

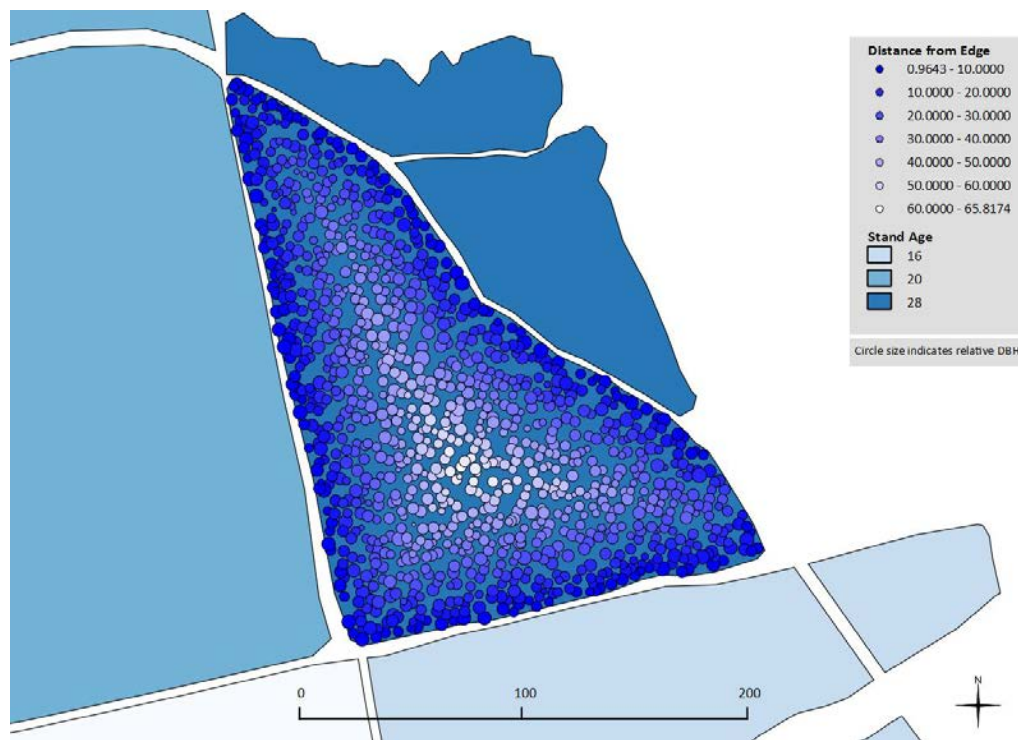


**Figure 3.14.** Stand E3b with graduated blue colours indicating the distance from the edge and circle size indicating relative DBH for each tree.

Diameter was modelled as a function of distance from the edge using the segmented regression function provided in the segmented package built by Muggeo (2008). The regression model output is shown in Figure 3.15 below, where the breakpoint between a regression line representing DBH in the edge region and a regression line for the inner region was found at 14.88m from the edge. During the process of this regression, a test was done to see whether more breakpoints exist and no others were found. Parameter statistics extracted from *R* directly are provided in the grey box below, where coefficients for the piecewise linear model are given. The intercept is at 39.56m in height at the edge of the stand and the coefficient of the section of the model representing the slope of the edge trees model is -0.284. At the breakpoint, the change in slope between the section of the model representing the edge trees and the section representing the inner region is 0.262, this indicating a real slope for this section of -0.02.

#### Model output with parameter statistics of the segmented regression for stand E3b

```
***Regression Model with Segmented Relationship(s)***

Call:
segmented.lm(obj = lm, seg.Z = ~dist, psi = 15, model = T)

Estimated Break-Point(s):
  Est. St.Err
14.880 2.897

t value for the gap-variable(s) V: 0

Meaningful coefficients of the linear terms:
      Estimate Std. Error t value Pr(>|t|)
(Intercept) 39.56043   0.62331  63.468 < 2e-16 ***
dist        -0.28436   0.07451  -3.816 0.000143 ***
U1.dist      0.26166   0.07705   3.396      NA
---
Signif. codes:  0 '***' 0.001 '**' 0.01 '*' 0.05 '.' 0.1 ' ' 1

Residual standard error: 6.183 on 1127 degrees of freedom
Multiple R-Squared: 0.05134, Adjusted R-squared: 0.04882
```

A value of 15m was therefore used in this study to indicate the spatial extent of the edge effect and separate the edge region from the inner, unaffected region of a stand. This distance also corresponded well with findings by Cancino (2005) where he found the edge effect to range somewhere between 5 and 30 metres from the edge. Differences in the extent are attributed to the cardinal direction of the edge.

### 3.6 Separating inner and outer regions

The inner stand was demarcated as the area of the stand beyond 15m from any edge. Compartment outlines were buffered into the stand by 15m and trees within the inner region of the stand, beyond the buffer were designated  $AI=0$ . A line was generated at the inner edge (15m in from the edge of the stand) of the buffer and the AI value for that line set to 0 in preparation for the interpolation process (Figure 3.16). This line was added to the lines segment shapefile and assigned an AI value of 0. All the trees that fell between this line and the edge of the compartment, i.e. within the region of edge influence, were designated as outer trees and the inner trees designated as such.

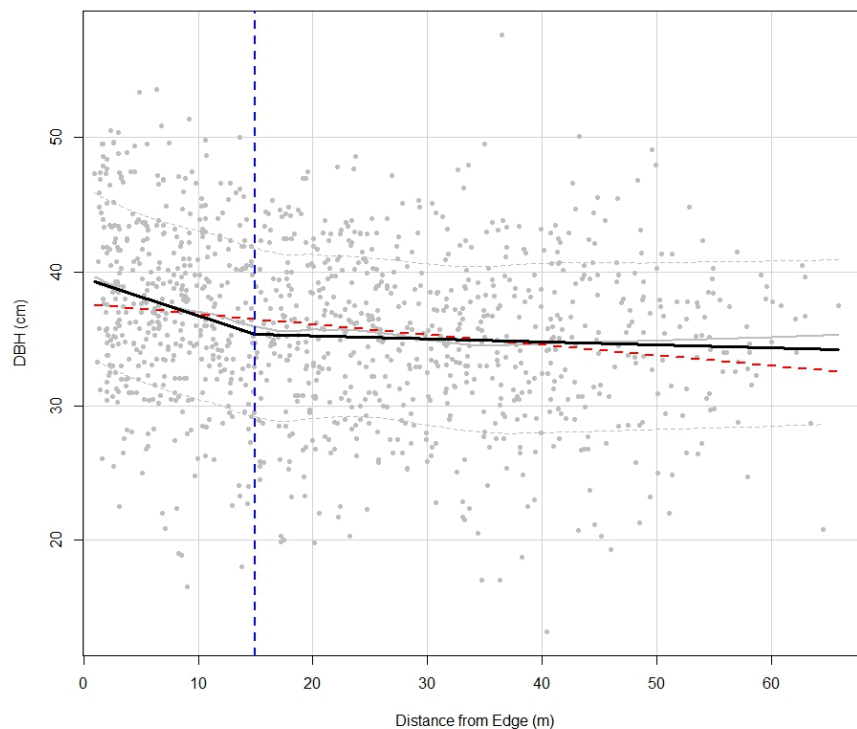


**Figure 3.15.** Piecewise linear regression, indicating the relationship between the distance from the edge of the stand and DBHs of the respective trees. The vertical dashed line indicates the breakpoint at 14.88m from the edge, the red sloping dashed line indicates the linear regression line and the grey curve indicates Loess fitting of the data.

### 3.7 Spatially interpolating AI values from the edges into the stand

Once all the edges of a stand had been quantified in terms of AI, these values needed to be transferred into the stand in accordance with the spatial position of each tree in relation to the stand edges.

In order to transfer data from the edges to any given position (or tree) within the compartment, one of two methods was applied in this study. The first is a direct link with the position of the tree with its nearest edge, where the characteristics of that edge are directly related to the position. This will result in discontinuities where the different points related to different edges meet. It is however a simple and direct way of linking a tree with an edge.

### 3.7.1 An inverse distance weighting approach

As a way of dealing with these discontinuities, some kind of spatial interpolation needs to take place between the edges and the points to effectively “smooth” out the quantification of the edges within the stand. An inverse distance weighting (IDW) approach has been selected for this purpose. Shepard (1968) describes IDW as producing a “surface based on a weighted average of the values at the data points, where the weighting was a function of the distances to those points” (Shepard 1968, p.518). For the application of passing data from the forest edge to a specific position in the forest, this means that each point is related to all of the different stand edges but that the relation is weighted according to the distance from that edge as an inverse function of the distance to all the other edges. The relationship therefore is one where a shorter distance has a higher weighting. Inverse distance weighting is an interpolation method proposed by Shepard (1968). He sought to find an interpolation function that would be “continuous and differentiable” and would meet the intuitive expectation of the phenomenon under investigation. The initial application by Shepard (1968) was an interpolation of four irregularly spaced data points in a mapping program in order to produce five levels of contours. Shepard suggests a quadratic distance exponent for purposes of general surface mapping and description. Since that initial application, IDW has been widely applied and studied. Lu and Wong (2008) refer to it in their study on a pattern modified IDW as one of the most frequently used deterministic models in spatial interpolation. Their study is one of many, which consider IDW and studies a variation on the original application such as Bartier & Keller (1996) and Joseph & Kang (2011).

Some advantages and disadvantages of IDW are discussed by Jacobs *et al.* (1986). They point out that some shortcomings are the limitation of IDW to extend beyond the range of the control points. This is not a problem in the case of this study because the transference of data points in the case of plantation stands is always towards the inside of the stand, i.e. within the range of the control points. It also weights highly similar control points equally with dissimilar control points and cannot supply analytical estimates of its error or confidence intervals on its predictions. They promote it as being “intuitively attractive” because it is “simple to understand and implement and is easy on computing time.” (Jacobs *et al.* 1986, p.582)

An inverse distance weighting approach was therefore applied in order to calculate an AI value for each tree, signified  $AI_p$ . As suggested by Shepard (1968), a distance exponent of 2 was used in the interpolation. Any given point within a stand with edges defined in terms of AI can therefore be quantified in terms of AI at that point. Calculation for the application of the inverse distance weighting as applied in this study for the calculation of  $AI_p$  for any given point within a compartment with  $e$  number of edges is laid out in equation 3 below, with  $d$  the distance between the point and edge  $e$  and the calculated AI for that edge:

$$AI_p = \frac{1}{\sum_{i=1}^e \frac{1}{d_i^2}} \left( \sum_{i=1}^e \frac{AI_e}{d_i^2} \right) \quad (\text{Equation 3})$$

Where:

$AI_p$  = Accumulated Interaction for a given point  $p$  in a stand

$AI_e$  = Accumulated Interaction for a given line segment

$e$  = A given line segment with attached  $AI_e$  value

$d$  = The shortest distance between point  $p$  and edge  $e$

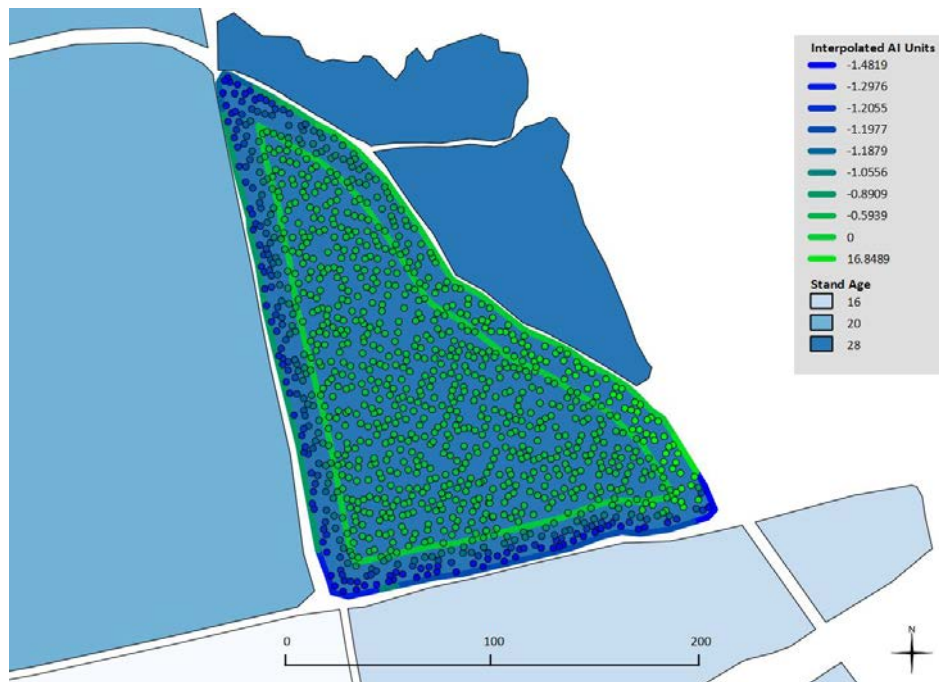


Figure 3.16. Representation of interpolated AI values for stand E3b with inner region AI values set to 0.

### 3.7.2 The inverse distance weighting process for stand E3b

Calculating an  $AI_p$  value for each tree in the stand was done by generating a table in the points shapefile with a distance and AI value for each different line segment of the stand outline. This table was then populated in a double for loop, each point was considered and all the different compartment edges for each point. The distance is the shortest distance to that edge and the AI value was directly extracted from that edge. Once the table was populated, the inverse distance weighting calculation was carried out as shown in Equation 3 for each point and an  $AI_p$  calculated for that point.

All trees in the inner region of the stand (beyond 15m from the edge) were assigned an  $AI_p$  of 0. Trees in the outer region of the stand tend towards the edge AI as they approach the edge with that AI value. As the tree position approaches the inner line of the stand for which the AI was set at 0 in a previous step of the process (Section 3.6), the  $AI_p$  tends towards 0. The outputs of this process for stand E3b is shown in Figure 3.16.



As mentioned, the data for stand E3b were concentrated in the range of -1.5 and 0 AI units with one edge at 16.8. Figure 3.17 below shows how the data for this stand were thinly spread for values above 0 because the stand was in such a situation that it had been historically suppressed for the majority of its lifetime along most of its edges. Interpolation of the data to each tree generated some spread in the data between these gaps but an ideal dataset would be more evenly spread in order to generate more accurate models.

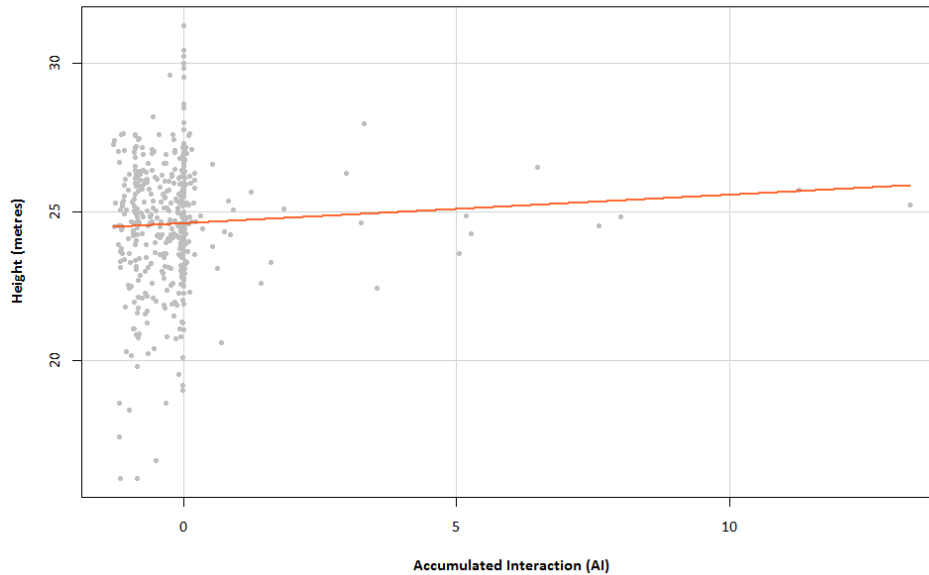


**Figure 3.17.** An illustration of height as a function of AI, indicating the positive linear relationship.

### 3.8 Taking spaces between edges into account

Accumulated interaction as explained up to this point does not take space between edges into account such as roads or firebreaks. It considers edges to be hard borders between stands with no gaps at the edges and homogenous tree spacing. To take the space between neighbouring stand edges into account, a tree density or neighbouring stand distance factor should be included into the edge effect model. A simple local tree density function was carried out using a circle with a radius of 15m for each tree and the stems per hectare calculated for each circle and thus for each tree. 15m was selected as the distance for the radius because it is the spatial extent of the edge effect. All trees less than 15m from the edge will have open area taken into account in the calculation of this density. The result of this process is shown in Figure 3.18 below. In the calculation of this function the space on all sides of the stand was considered to be at least 15m wide, thus no trees from the neighbouring compartments were considered. The subsequent plotting of the data clearly indicated a negative correlation between local density and DBH (Figure 3.19). Taking such a factor into account when generating the edge models provides a methodology in which allowance is made for open spaces between stands.

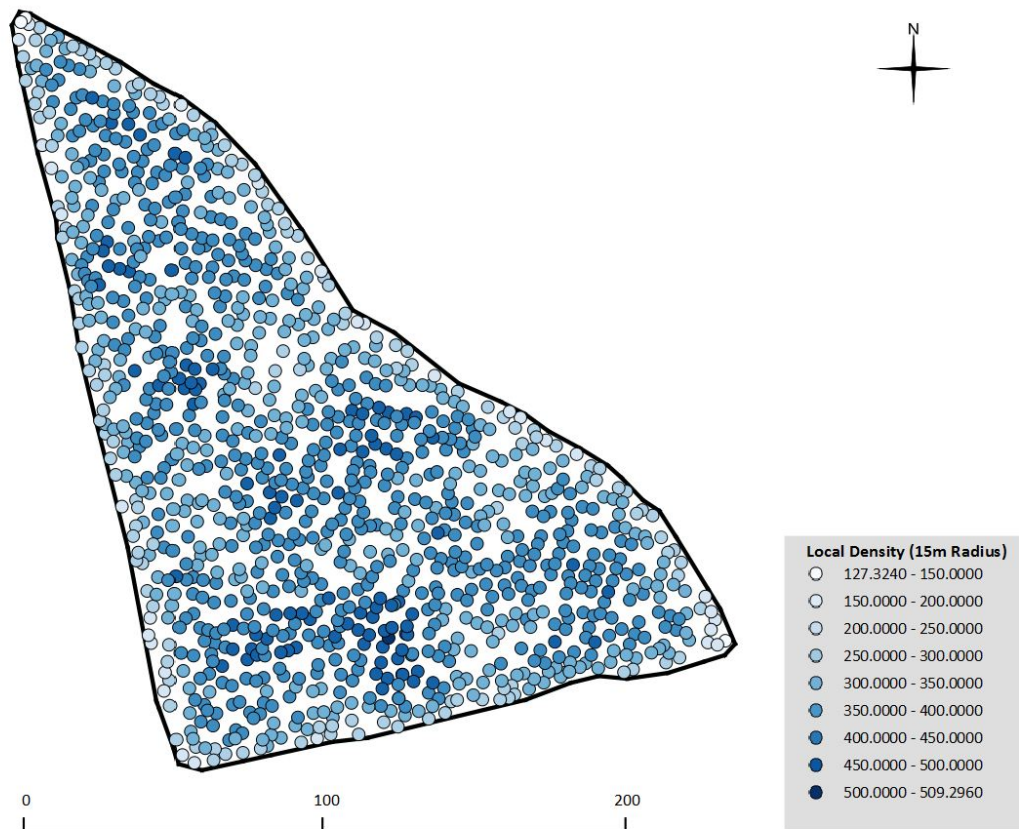


**Figure 3.18.** The local density calculation of trees in stand E3b, taking a 15m radius into account for each tree.

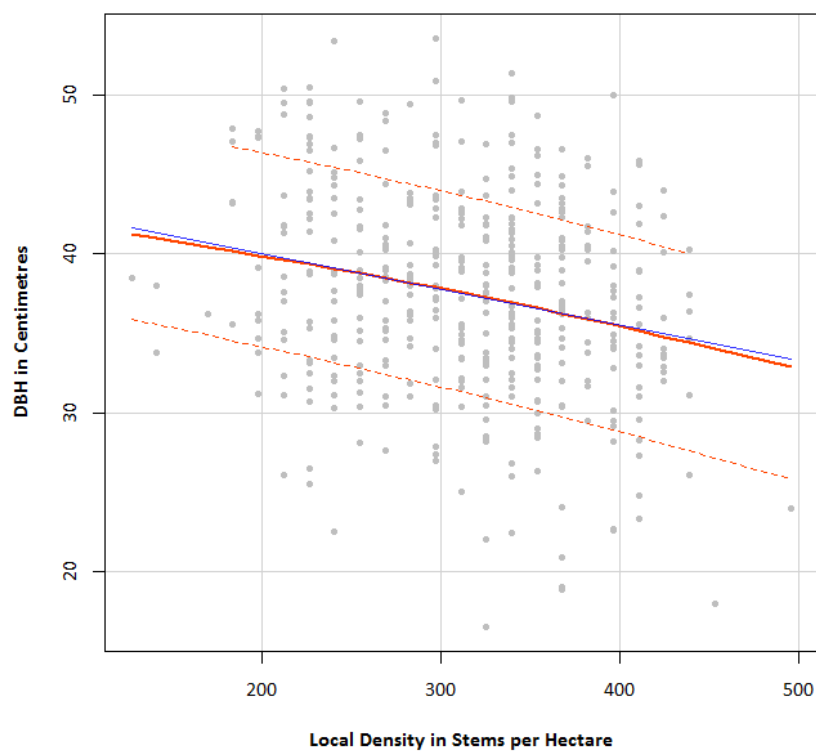


**Figure 3.19.** A scatterplot indicating the relationship between the local tree density (within 15m of the tree) and DBH for all trees in the outer region of stand E3b. The red curve represents a generalized additive smoothing function applied using the gamLine smoother in the scatterplot function. The blue line represents a linear fit of the data.



### 3.9 Model fitting of stand data

Modelling of the edge effect was carried out by building three separate models where AI and local density were the independent variables, with DBH, volume and height respectively as the dependent variables. In these models, the tree variables were thus modelled as a function of the interaction between neighbouring stands over time but also taking into account the space between stands.

A linear regression model was fitted to each of the three datasets based only on data from the trees falling within the edge influence zone of stand E3b. The three models are presented below.

#### 3.9.1 DBH as a function of AI and local density

$$DBH_p = 44.5607 - 0.109 (AI_p) - 0.0228(s_p) \quad (\text{Equation 4})$$

Where:

$DBH_p$  = Predicted diameter at breast height at a given point  $p$  within a given stand

$AI_p$  = Accumulated Interaction at given point  $p$

$s_p$  = Local density at given point  $p$

#### 3.9.2 Volume as a function of AI and local density

$$Volume_p = 1.3957 - 0.0026 (AI_p) - 0.0012 (s_p) \quad (\text{Equation 5})$$

Where:

$Volume_p$  = Predicted volume at a given point  $p$  within a given stand

$AI_p$  = Accumulated Interaction at given point  $p$

$s_p$  = Local density at given point  $p$

#### 3.9.3 Height as a function of AI

$$Height_p = 25.9731 + 0.1009 (AI_p) - 0.0043(s_p) \quad (\text{Equation 6})$$

Where:

$Height_p$  = Predicted height at a given point  $p$  within a given stand

$AI_p$  = Accumulated Interaction at given point  $p$

$s_p$  = Local density at given point  $p$

The models are now ready to be applied to a different stand with a similar age and structural characteristics as stand E3b. In chapter 4, this process and the results thereof are presented.

### 3.10 Taking the cardinal direction of the edge into account when calculating AI

It is clear from previous studies (Cancino 2005) that the direction which an edge faces has an effect on the magnitude and spatial extent of the edge effect. The calculation of AI at this stage does not consider the cardinal direction of the edge. However, this factor was not fully studied or applied during this study and is not included when applying the edge effect models in Chapter 4. However, a possible method by which the cardinal direction of the edge could be included within the spatial modelling of edges effects is shown below, where the AI is not altered directly, but the bearing is calculated for each tree, which can then be included in the models in a similar way as done for local density.

Quantifying the cardinal direction which an edge faces was done by running an algorithm<sup>2</sup> within QGIS, which calculates the bearing for an edge where, for example a directly north facing slope is at  $90^\circ$  and a south facing slope at  $270^\circ$ . The interpolation from the edges to the positions representing trees within the stand was carried out within *R* using the inverse distance weighting method as described in Section 3.7. The result of this process is shown in Figure 3.20. A scatterplot of the relationship between the DBH and the bearing is shown in Figure 3.21. From this figure, gaps in the data are clear and additional data are required in order to be able to model the relationship accurately.

Once a bearing has been calculated for each tree, this value can be included as an additional variable in the AI models.

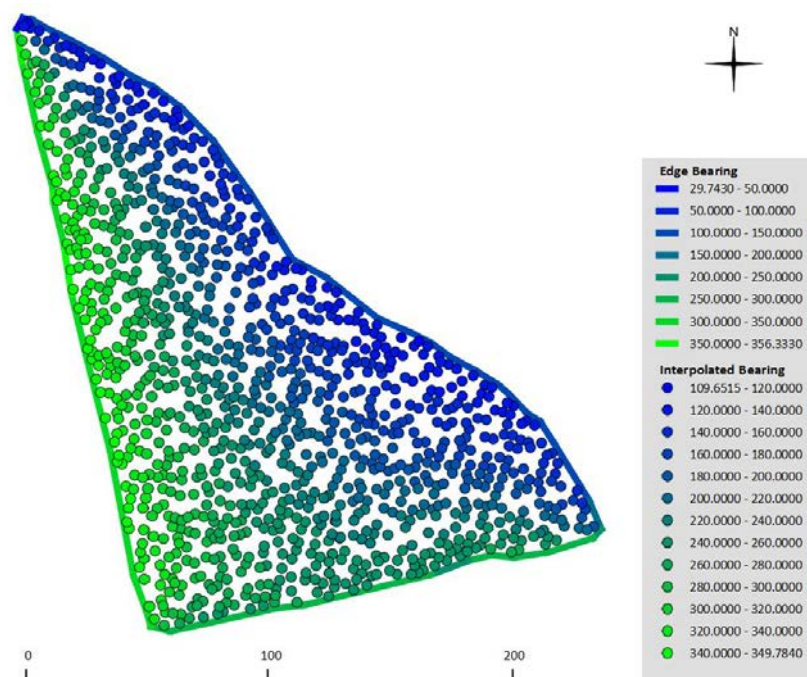


**Figure 3.20.** Calculation of the bearing of the stand edge with the results of the interpolation of those values to the points within the stand. Bearing is given in degrees.

Instructions and details for algorithm development were obtained from a forum discussion available online <http://gis.stackexchange.com/questions/24260/how-to-add-direction-and-distance-to-attribute-table>.<sup>2</sup>

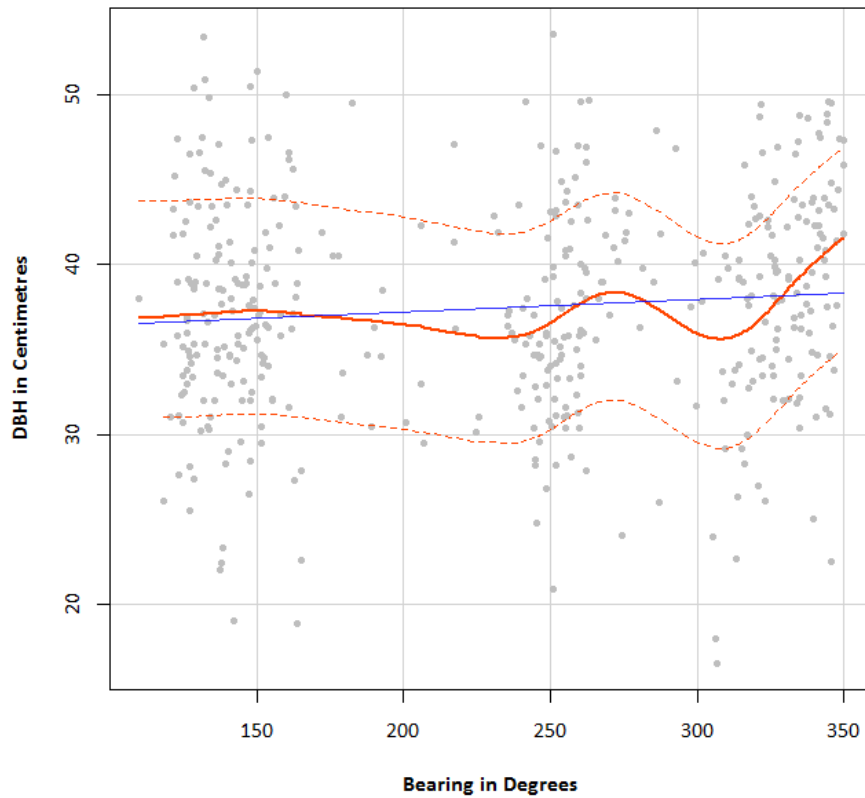


**Figure 3.21.** A scatterplot indicating the relationship between the bearing in degrees and DBH for all trees in the outer region of stand E3b. The red curve represents a generalized additive smoothing function applied using the gamLine smoother in the scatterplot function that allows a flexible nonparametric regression model fit. The blue represents a linear fit of the data.

## Chapter 4. Model application on an independent dataset

Within this chapter, the process followed in seeking to achieve the final objective as laid out in Chapter 1 is described, namely the simulation of a plantation forest stand taking into account the edge effect and natural stand variance in combination. It also presents the final results of the simulation. Some additional methodology, which was not presented in Chapter 3, is also introduced, thus separating the workflow of the analysis and model building as in Chapter 3 from the workflow of the application and simulation in this chapter.

An example of the application of the edge effect quantification based on remotely sensed data is described. The stand data were prepared in much the same way as the data for the terrestrially measured stand E3b. Certain basic stand data were extracted from the central region of the stand in order to adjust the models and their predictions to the reality of the stand.

Before the simulation, some stand data needed to be extracted, which would quantify the basic structure of the stand to be simulated. These data were obtained from a remotely sensed dataset. This data extraction procedure is presented in this chapter. Mean values as well as distributions for tree DBH, height and volume were extracted from a sample of the inner region.

Simulation of the stand was then carried out by initially calculating AI values for all edges. Hypothetical tree positions were generated within the stand at the same stand density as the remotely sensed dataset and AI values were interpolated to these tree positions by means of IDW. A separation was made between the inner and outer region of the stand based on the edge effect spatial extent threshold value as determined in Chapter 3. For each point representing a tree in the simulation stand, the predicted DBH, height and volume were calculated. These calculated values were then shifted according to the inner region mean values in order to fit the situation of the stand. An adjustment was made to the predicted output, based on a random number generated by mimicking the expected distribution at the inner region of the stand. The results were visualised in various ways for analysis. Figure 4.1 outlines broadly the steps followed in the application and simulation process.

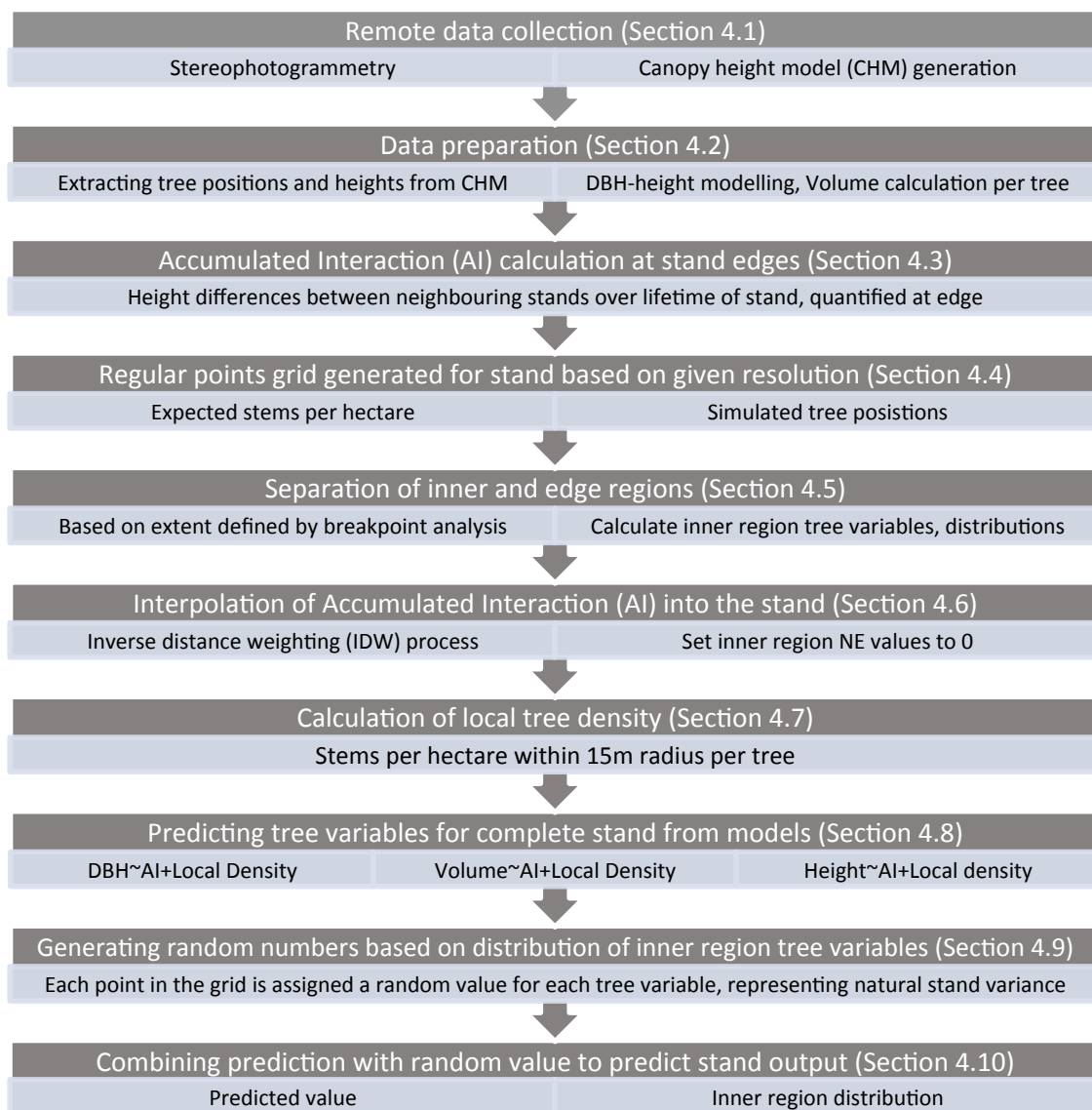


Figure 4.1. A flow chart indicating the steps for the edge effect model application process.

#### 4.1 Remote data collection

Canopy height models (CHMs) based on airborne stereo-photogrammetry were generated for the compartments around E3b (E plantation) as well as the G plantation, a plantation under the same management with similar characteristics as that of the E plantation (see Figure 4.2 and Figure 3.2). As explained in Chapter 2, a canopy height model of the forest is essentially a tree height surface, which can be used to identify individual tree heights by extracting the height at the point where the individual tree is positioned. Such a surface can be created by various means but, for the purposes of this study, stereophotogrammetry was used because of its cost advantage over other forms of collecting similar data, such as airborne LiDAR.

#### 4.1.1 Simulation dataset: Compartment G36

Verification of the models generated based on data from stand E3b was carried out on a stand in the G plantation, stand G36 (Figure 4.2). A stand with an area of approximately 6.4ha and an age of 20 years, G36 is 5 years younger than stand E3b but data for a suitable stand of exactly the same age were not available. This stand is also of a large enough area for the inner region to be beyond the reach of significant edge effects. 1327 tree positions were extracted for this stand from the dataset as well as their heights. Diameters for this dataset were modelled using the diameter-height model derived from the E3b dataset based on the height for each tree in G36. The evenness index was not applied in this simulation.

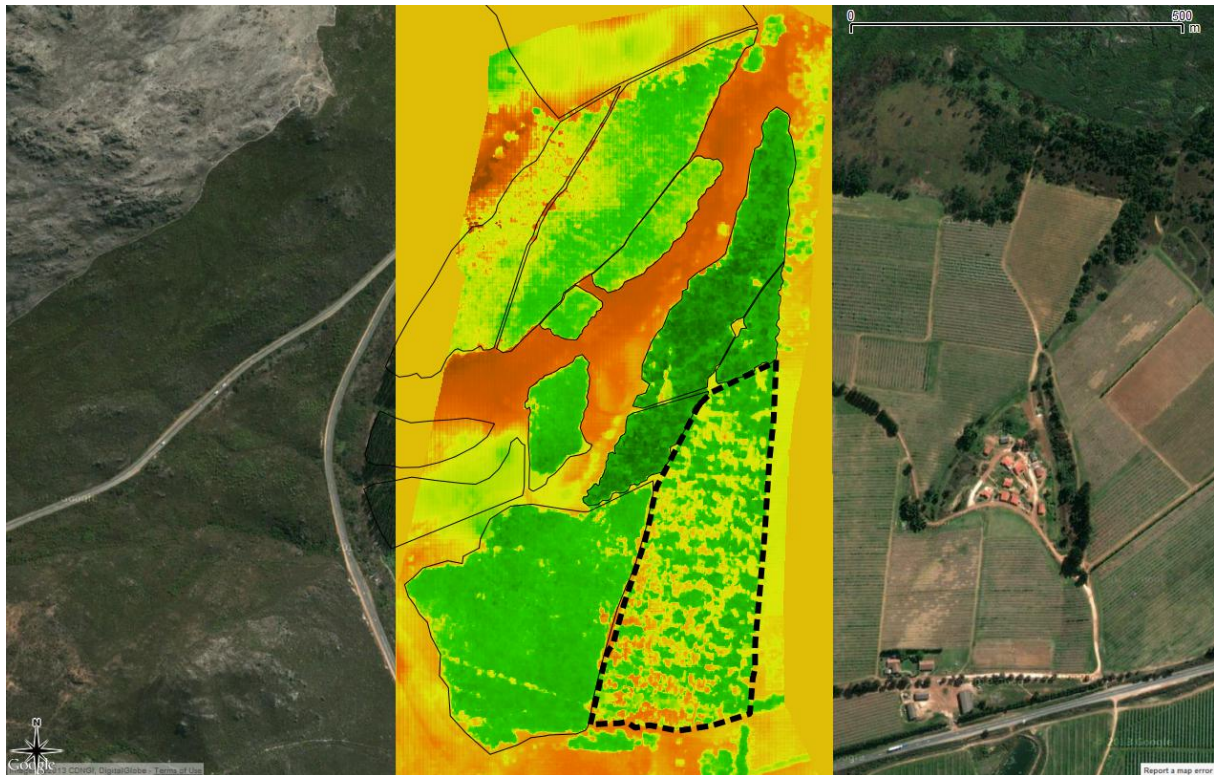


**Figure 4.2.** Digital surface model of G plantation, overlaid on Google satellite layer in QGIS. The compartment to be simulated is outlined by the dashed line. The location of this plantation is shown in Figure 3.2.

Subtraction of the digital elevation model (DEM) from a digital surface model (DSM), which contains elevations of both ground and objects on the ground, creates a tree height surface that can then be used to identify individual tree heights and possibly canopy projections. Extracting tree data is done by identifying the point where the individual tree is positioned and then extracting the elevation representing the tree height from the CHM at that point. The canopy projection can also be extracted if necessary. The DEM, as explained, depicts the elevation of the bare ground, and is generated by the interpolation of the heights of exposed areas of ground which can be identified by such in the data source.

The data from the aerial stereo photos were modelled using PCI Geomatica version 2012 ([www.pcigeomatics.com](http://www.pcigeomatics.com)) and CHMs were generated for both study plantations. These data were provided by Anton Kunneke of the Department of Forest and Wood Science at Stellenbosch University. The CHMs were generated at a scale of 1:600 (30 cm raster resolution) subtracted from a DEM of 1:10000 (5m raster resolution). A three dimensional representation of the G plantation is shown in Figure 4.4, with stand G36 in the lower right-hand side of the image.





**Figure 4.3.** An image of the aerial view of stand G36, taken on November 12, 2012.

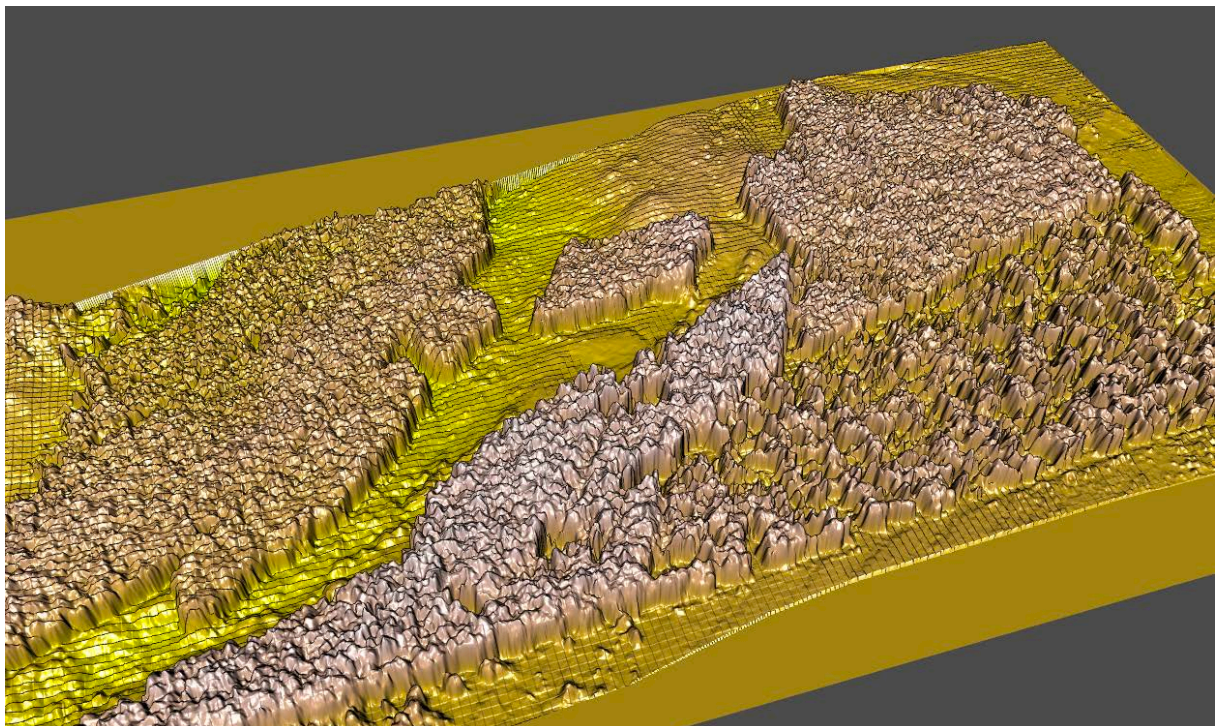


**Figure 4.4.** A three dimensional rendering of a digital surface model of the G plantation, generated in *R* using the *rgl* package (Adler & Murdoch 2013).



## 4.2 Data preparation

In order to prepare the data for the simulation process, tree positions were identified in the CHM and the heights at those points were extracted from the CHM. Local maxima identification as explained in section 4.2.1 was applied in order to extract these data.

A terrestrial transect for ground truthing and for the calculation of basic compartment parameters was carried out within stand G36 in order to verify or adjust the data collected by these means. It was not possible to pair the data from the terrestrial transect with the aerial data by matching individual trees.

The AI was calculated for the edges of compartment G36 in the AI calculation process as explained in Chapter 3.

### 4.2.1 Identifying tree position and height from the DSM using the R Package

Various methods were explored in order to automate the process of tree data extraction from the CHM. Greatest success was achieved when using local maxima detection within the R framework. Local maxima detection processes have been used various times with varying degrees of success in the past (for example Korpela *et al.* 2006; Pitkanen 2001).

Identification of treetop positions and the extraction of the heights at those points was carried out in R, making use chiefly of the *raster* package (Hijmans & Etten 2013) for data manipulation and the *rgl* package (Adler & Murdoch 2013) for visualisation. The CHM raster was masked by the stand outline as generated when delineating the dripline as shown in Figure 4.2. This was done to decrease processing time and also to increase accuracy by confining data manipulation to the area within the compartment only. Correction for slope bias as well as for a false ground level was necessary. Once the raster was adjusted and normalised, the process of tree data extraction from the CHM was carried out. Those regions of the CHM below the 30% quantile were removed from the dataset, thus excluding the majority of canopy undergrowth. A local maximum was calculated for each pixel in the CHM and data extracted for the position and height of the expected treetop position. A shapefile was generated containing these data.

#### 4.2.1.1 Normalising the raster for slope

As discussed, the CHM data for compartment G36 exhibited two problematic trends that were not apparent infield or from aerial photography. Towards the lower region of the stand, data were of an unrealistically low elevation (Figure 4.6). Also, values below zero were observed for some regions of the raster (Figure 4.9). Both of these problems were attributed to the subtraction process of the DEM from the DSM. Where an interpolated DEM is used, errors could be present when interpolation is not at a fine enough scale and an unrealistic slope could present itself, as in this case, showing a higher ground elevation at the lower part of the stand than the reality.

A clear illustration of the problem is demonstrated in Figure 4.8, during the operation of understory removal from the CHM. When removing the lower 30% quantile of the dataset, pixels are primarily removed from the lower left region of the CHM, whereas very few pixels are removed from the upper right region. This means that complete trees, not only understory are being removed in the lower region of the CHM whereas, in the upper right region, the understory, being exaggerated in height, remains largely intact. In order for the understory to be removed evenly throughout the

stand and in order to extract more accurate tree heights, a normalisation of this CHM proved necessary.

Correction was made for the discrepancies in local elevation by applying a moving window algorithm by means of the *focal* function from the *raster* package in *R* (Hijmans & Etten 2013). The mean value of the raster as a whole was calculated to be 8.822m. It was assumed that the error was spread evenly throughout the stand, overestimating at the high values and underestimating at the low values, at the stand level. A moving window of a 301x301 pixel size (90601 pixels), equal to just more than 1ha in size, was iterated over the stand. As the window iterated over the CHM, the centre pixel for that iteration was adjusted by the difference between the stand mean and the mean of the moving window as a whole at that position. The equation to calculate the normalised pixel value at the centre of the moving window is as follows:

$$p_n = p_o + (\bar{\sigma} - \bar{w}) \quad (\text{Equation 7})$$

Where:

$p_n$  = new pixel value for centre of moving window

$p_o$  = original pixel value

$\bar{\sigma}$  = mean stand pixel value

$\bar{w}$  = mean value for moving window

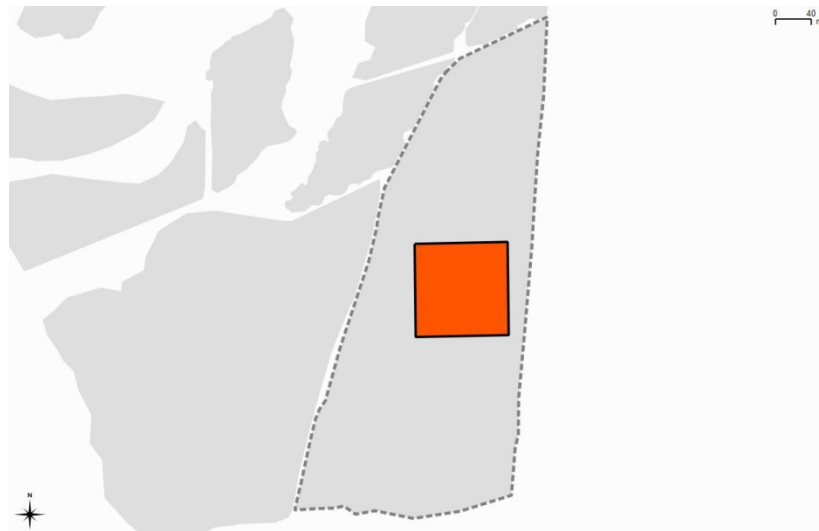


**Figure 4.5.** Representation of the approximate size of the moving window (1ha) used in the raster normalisation process in order to adjust a pixel by the neighbourhood mean (within the moving window).

A large window as this should keep local interactions in the tree data constant but adjust correct tree data at the stand level. The window was large enough for the distribution to remain similar as in the original raster as shown in Figure 4.7 below.

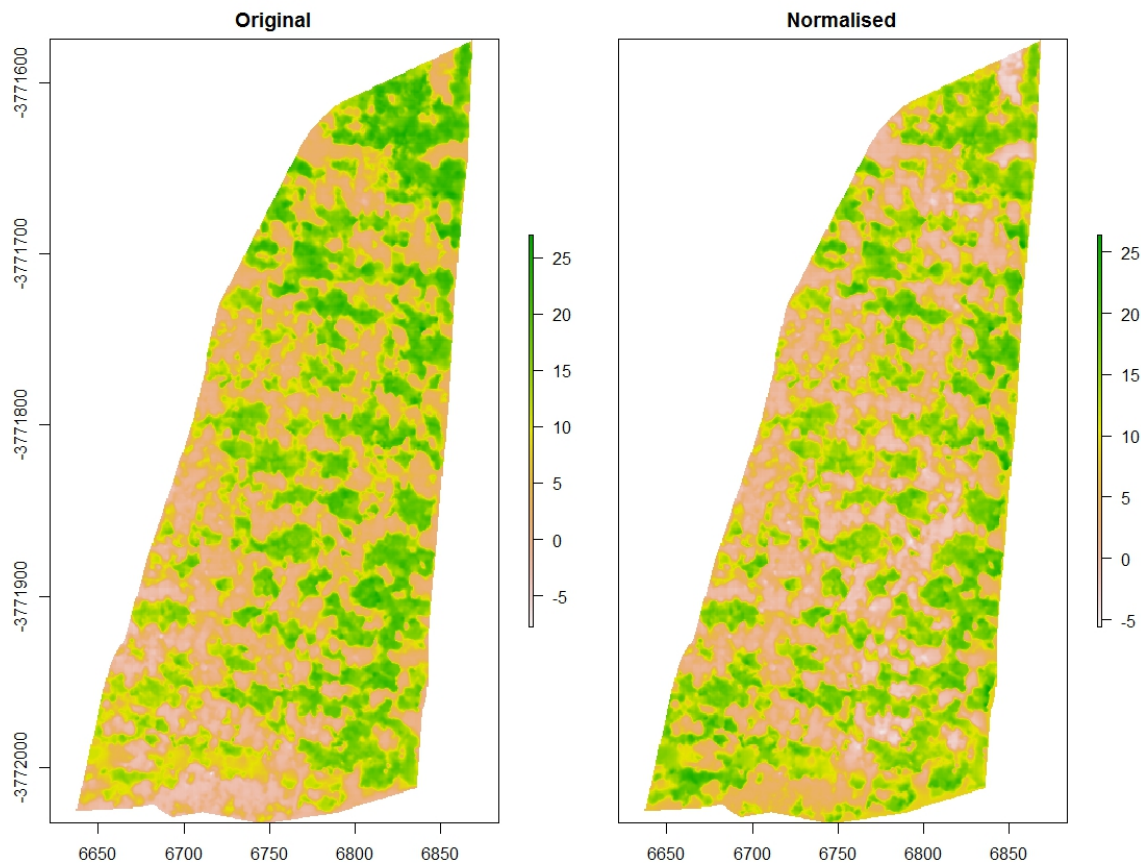


**Figure 4.6.** An illustration of the slope error problem, where, in the original CHM on the left, the lower left of the region has unrealistically lower elevations when compared to the upper region of the CHM. In the normalised image on the right, the result of the moving window process is shown. A more homogenous elevation distribution is achieved, keeping local interactions intact by using a moving window of approximately 1ha.

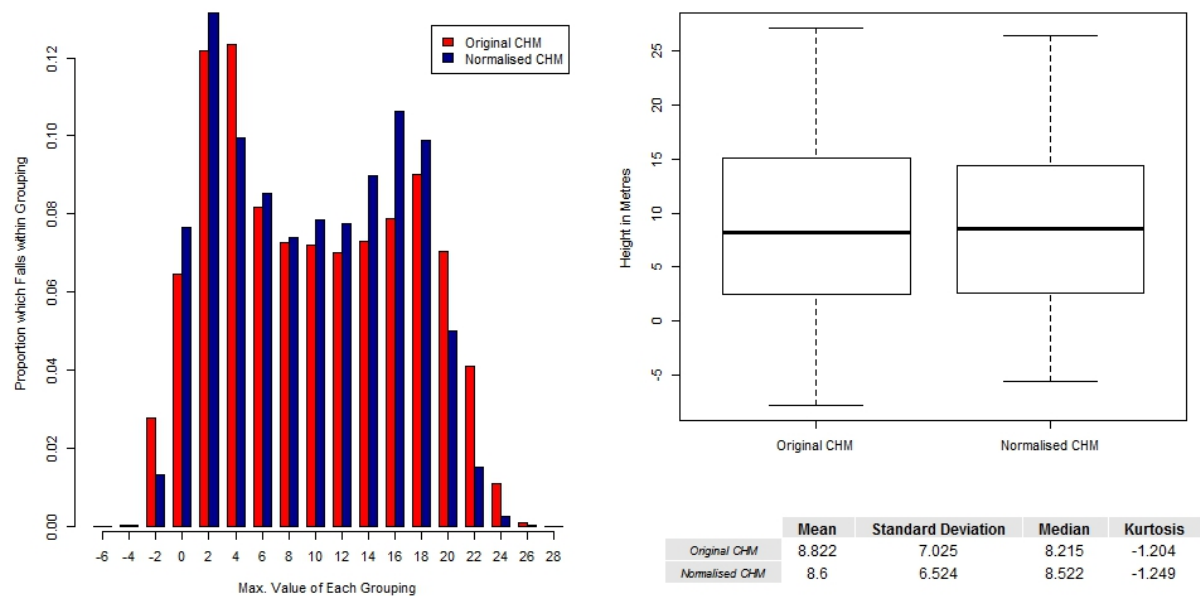


**Figure 4.7.** A graphical comparison of the CHM data before and after normalisation, showing a bar graph on the left with the original CHM data distribution in red bars and the normalised CHM data on the right. As expected, the distribution shifts upward in general, also removing both upper and lower extreme values. The resultant boxplot (on the right) presents a slightly narrower distribution for the normalised raster as opposed to the original.

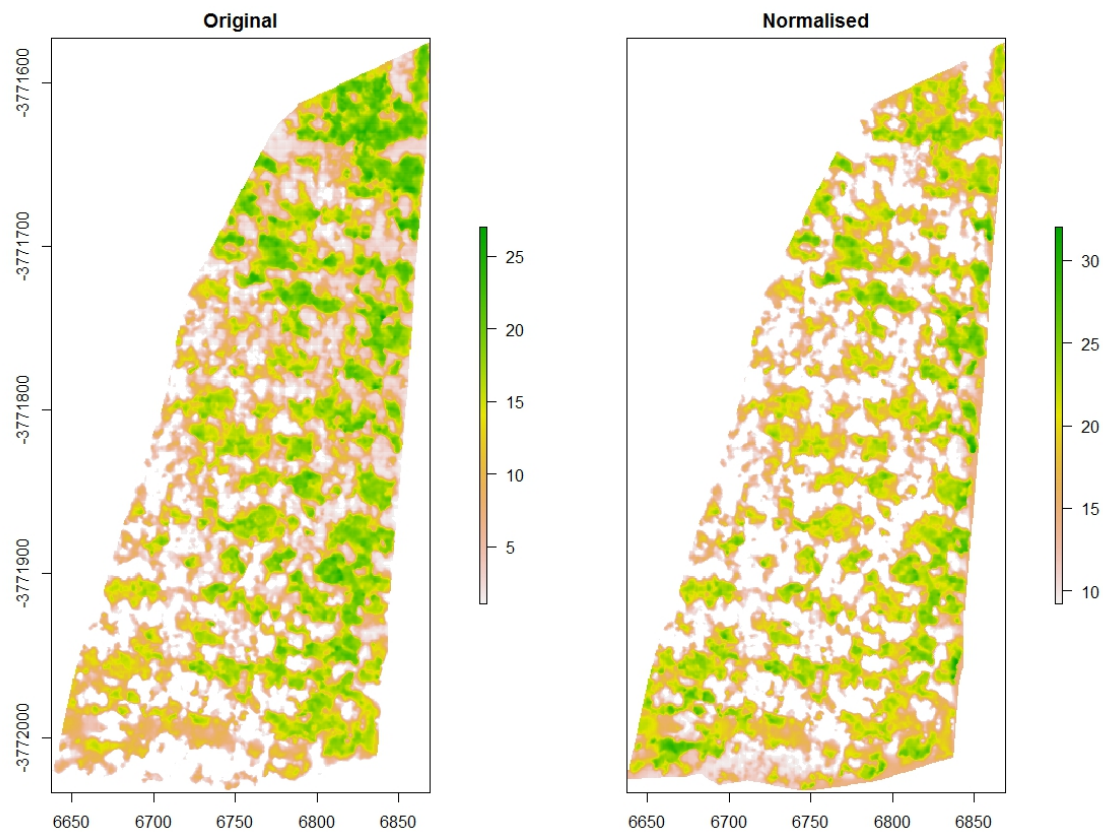


**Figure 4.8.** A demonstration of the problem created by a slope-biased CHM is shown in this figure. When removing the understory of the raster, within the slope-affected CHM there was excessive removal in the lower left region of the canopy (left) while almost all the understory remained in the upper region. In the normalised raster, a more homogenous removal of understory was possible (right).

#### 4.2.1.2 Zeroing the raster at ground level

As a result of using a lower resolution, interpolated DEM, error is introduced into the data when subtracting the DEM from the DSM. This error is manifest in the CHM when the ground level of the DEM is not at the same ground level as the DSM, thus generating a CHM that has as its ground level, an elevation that is more, or less, than zero. In order to correct for this error, the masked raster was zeroed at its lowest value, representing the ground. The minimum value in the CHM was subtracted from each pixel in the CHM, thus zeroing the lowest point at zero and moving the complete raster up or down depending on whether the lowest point was negative or positive.

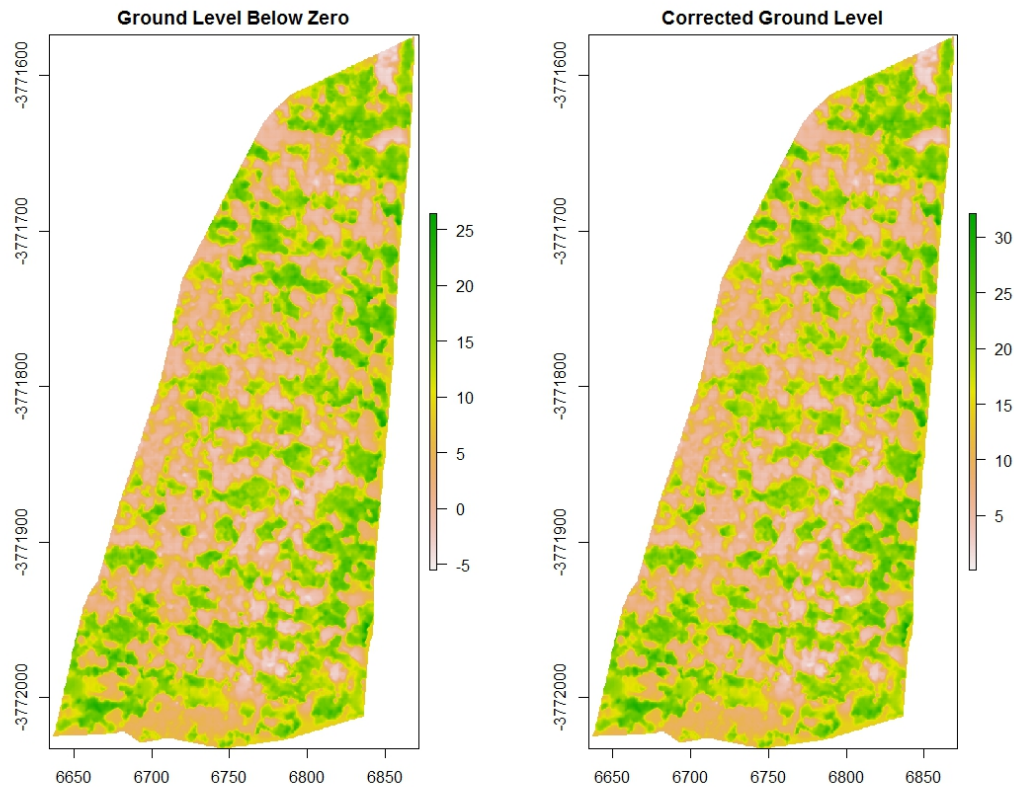


**Figure 4.9.** The result of the CHM shifting process is shown in this figure. The image on the left is the raster before the ground level is moved to zero and the raster on the right is the result when the lowest raster value is zero (see raster legends).

#### 4.2.1.3 Extraction of tree positions from the raster

Extraction of tree positions from the rasters was done also by using the focal function from the raster package in *R*. By iterating a weighted moving window of 9x9 pixels, roughly representing a circle over the masked raster, the centre value was assigned the maximum value of all the cells in its neighbourhood. The matrix for the weighting of the moving window is shown below.

```
0,0,0,1,1,1,0,0,0,
0,0,1,1,1,1,1,0,0,
0,1,1,1,1,1,1,1,0,
1,1,1,1,1,1,1,1,1,
1,1,1,1,1,1,1,1,1,
1,1,1,1,1,1,1,1,1,
0,1,1,1,1,1,1,1,0,
0,0,1,1,1,1,1,0,0,
0,0,0,1,1,1,0,0,0,
```

The original masked raster and the local maxima raster were overlaid and the points where these two rasters coincided, having the same value, were then identified as treetops in the process as illustrated in Figure 4.10 and Figure 4.11. The height values of these treetop pixels were then extracted and a points shapefile produced with the positions of the trees as well as their heights.



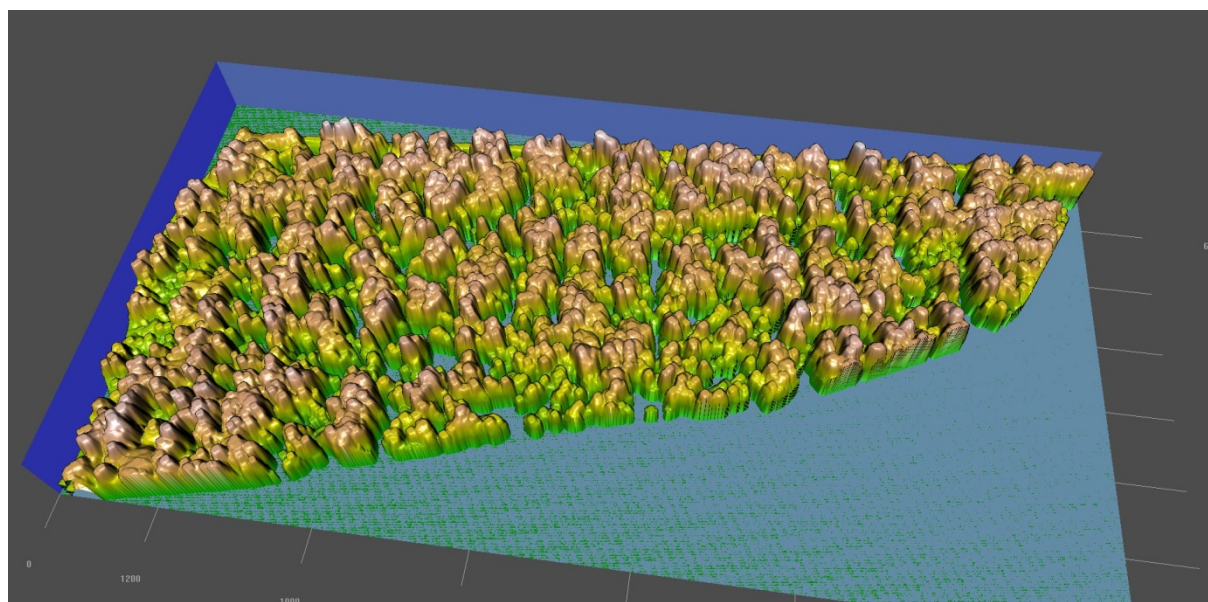


**Figure 4.10.** A three-dimensional representation of the output from the local maxima identification process, visualising the left-hand side raster shown in Figure 4.11.

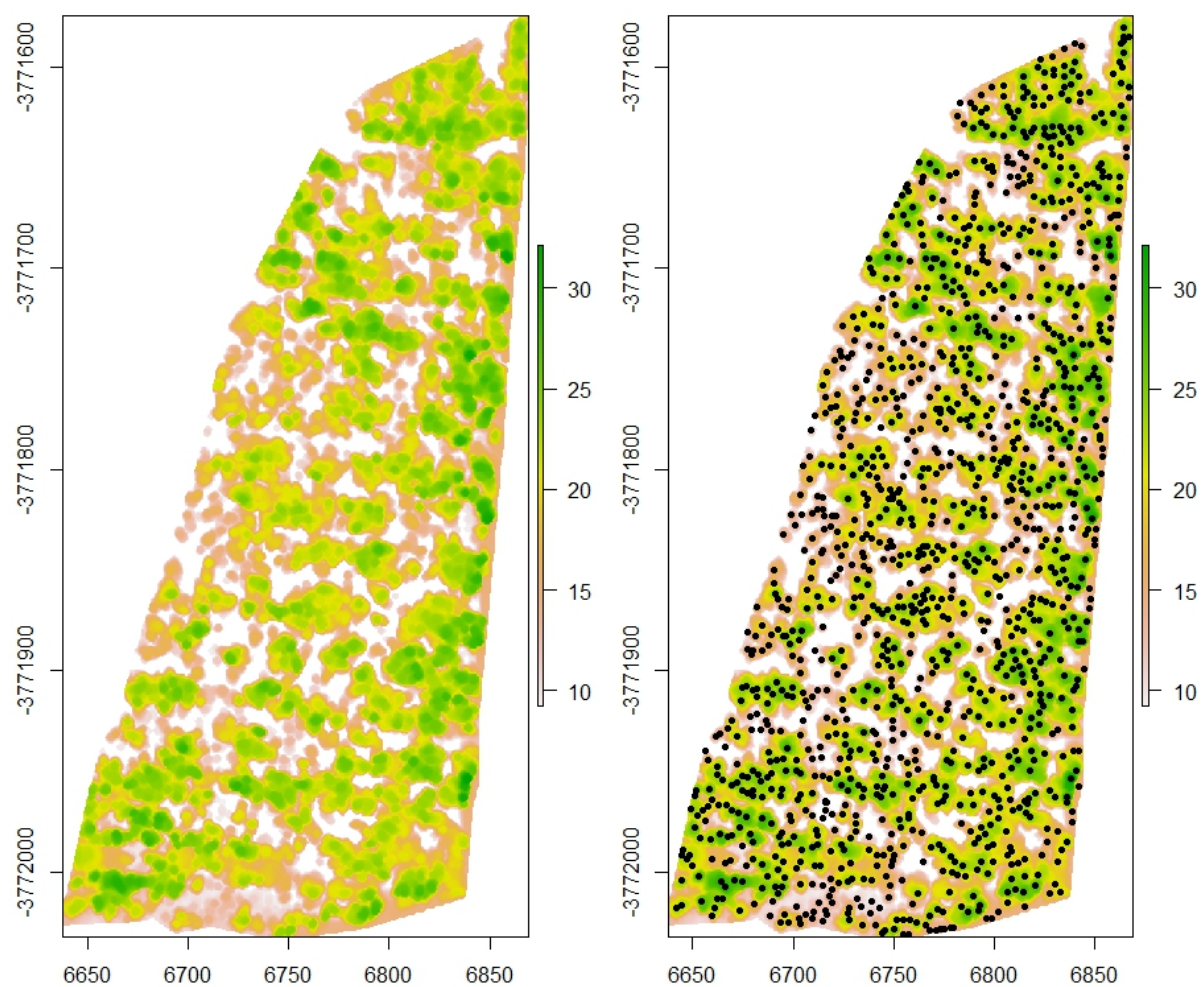


**Figure 4.11.** The result of local maxima extraction with the local maxima process output on the left and the identification of individual tree tops on the right.

### 4.3 AI calculation at stand edges

Accumulated Interaction for all edges of compartment G36 was calculated according to the process as explained in Section 3.4.1. The results of this process are shown in Figure 4.12. AI values for stand G36 vary from those of the terrestrially measured stand E3b in that they are all greater than zero, with three AI values at the edges: 2.025, 5.381 and 14.347. These values do not correspond very well with the data of stand E3b where the majority of values were negative and not very widely spread. A comparison of the two distributions after interpolation into the stand is shown in Figure 4.15. However, with the collection of more data in future comprising a wider spread of AI values, the models will improve in accuracy.

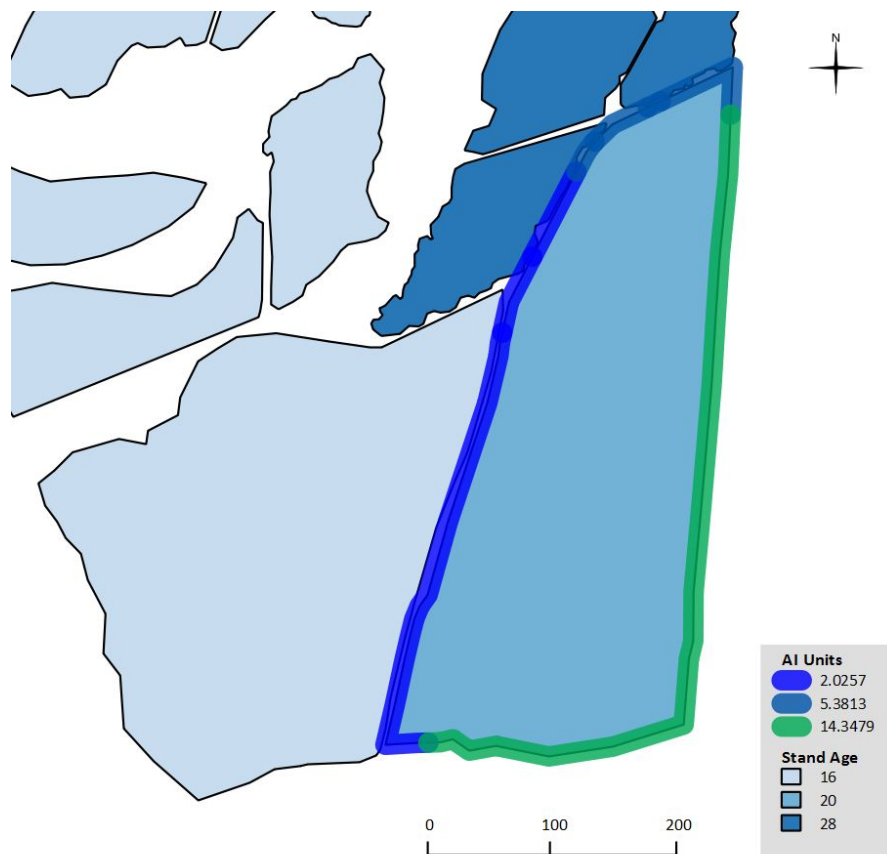


**Figure 4.12.** The result of the process of calculating Accumulated Interaction for the edges of stand G36. The edges of G36 are marked from blues for lower AI values moving to lighter greens for higher AI values. The neighbouring stands of G36 are coloured according to their relative ages, with a lighter colour indicating a lower age.

### 4.4 Generating a regular points grid

A points grid was generated based on the outline shapefile of G36. Each point in the grid represents a hypothetical tree or a cell in a raster. When simulating a stand, the tree positions are unknown and could be simulated in order to mimic a given density or mean evenness index, but for the purposes of this study it was decided to simply apply the simulation to a regular points grid.

### 4.5 Separation of inner and edge regions

Separating the edge region from the outer region of the stand was carried out at the threshold of 15m from the edge, as identified by means of breakpoint regression described in Section 3.5. DBH was predicted based on the relationship between DBH and height from the terrestrially measured data. From these data, a minimum ten percent sample was taken from the inner region by



generating circular sample plots of 20m radius spread evenly throughout the stand. Six plots with an area of approximately 1256m<sup>2</sup> each were generated, representing approximately 11.7% of the total stand area. Mean height, mean DBH, mean volume and stems per hectare were extracted from these plots, as shown in Table 4.1. The distributions of the tree data for each of these variables were also extracted. These values were then applied in the simulation process.

**Table 4.1.** Table of values calculated from the sample plots within the inner stand region.

Variable	Value calculated for sample plots
Mean Height	21.70
Mean DBH	24.98
Mean Volume	0.46
Stems per Hectare	206

The layout of the plots within the stand is presented in Figure 4.13, as well as a summarized comparison between the height data as extracted from the sample plot and the complete dataset of all the trees extracted from the inner region of the stand in Figure 4.14. By inspection, it seems clear that the samples are a good representation of the complete dataset. These data also show the distribution for the heights within the inner region of the stand. This distribution will be used at a later stage when generating random numbers to mimic the inner stand variance which this distribution represents.

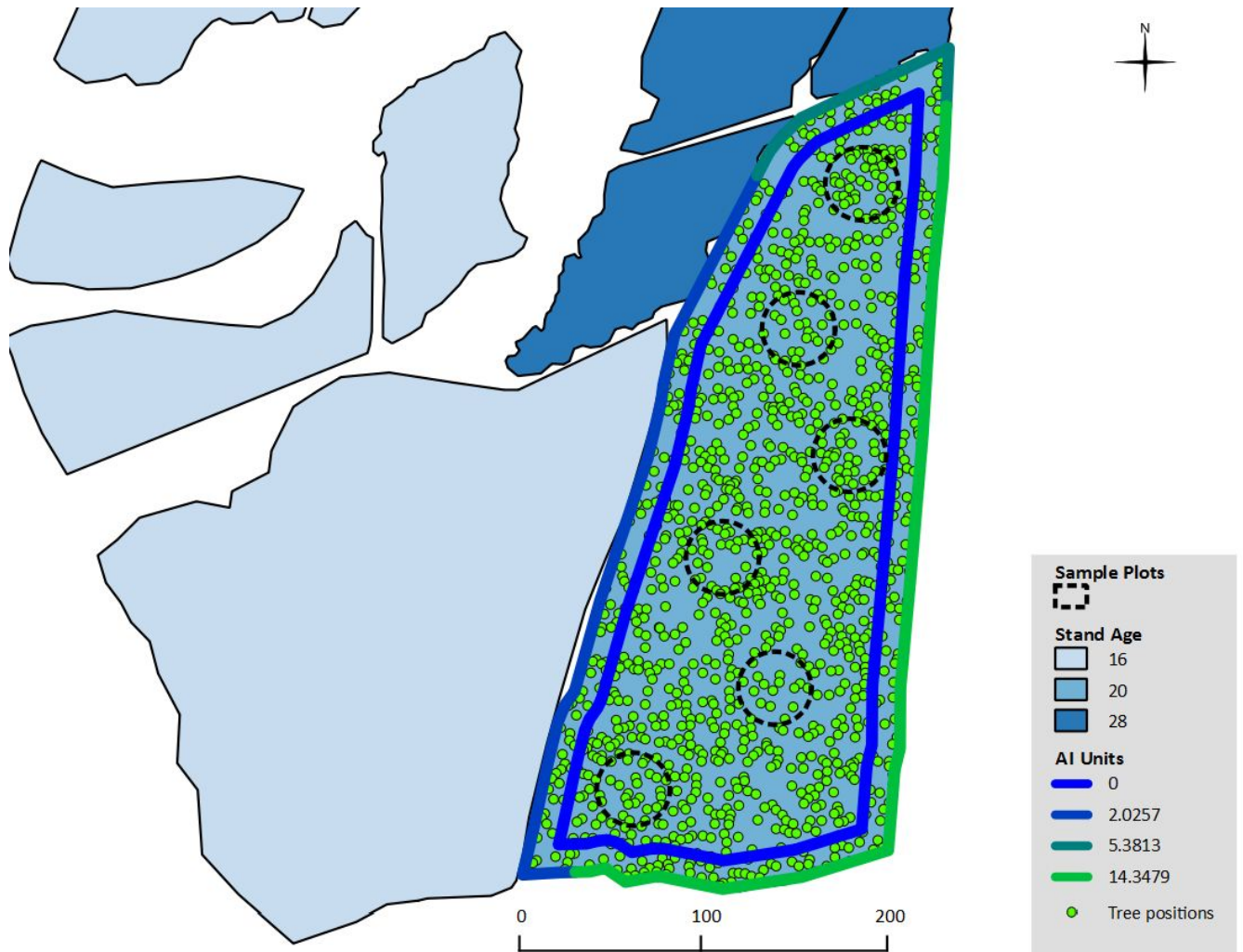


**Figure 4.13.** A representation of the separation between the inner and the edge region. The size and positions of the sample plots are also indicated by the circular dashed lines.

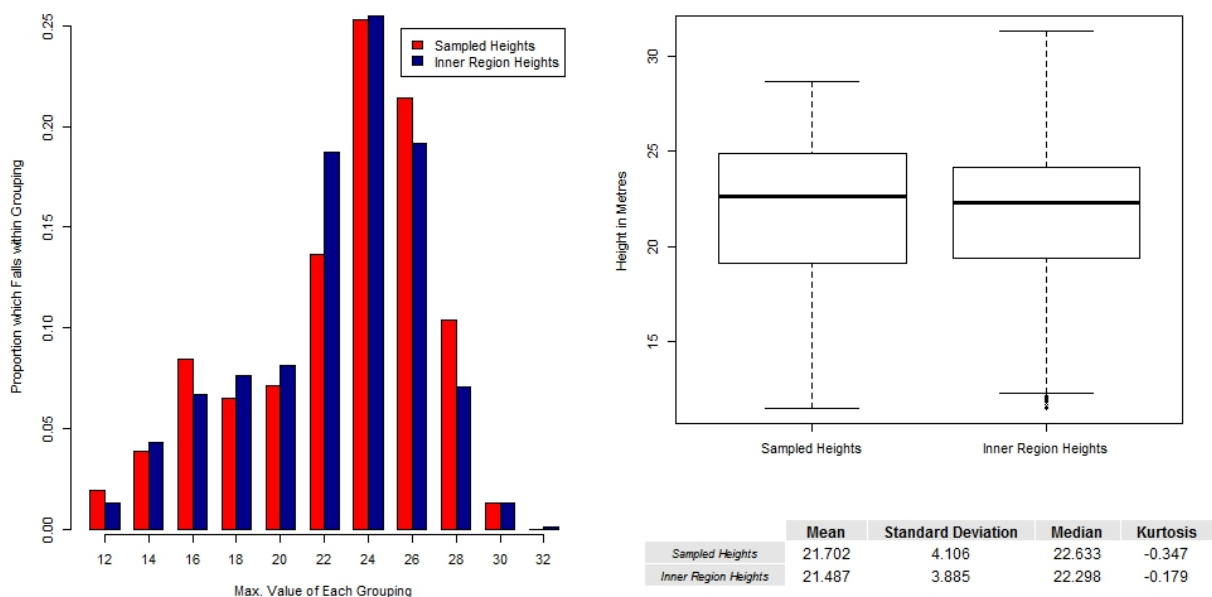


**Figure 4.14.** A comparison between the complete dataset of inner region tree data and the sampled data from trees falling within the sample plot areas. The red bars also represent the spread of data which will be used in simulation in order to generate random values for each tree in order to simulate natural stand variance.

#### 4.6 Interpolation of AI into the stand

Interpolation of the AI from the edges into the stand to the simulated tree positions was carried out (Figure 4.16) using inverse distance weighting as discussed in Section 3.7. The distribution of AI values does not correspond well when comparing the outputs for stand E3b and stand G36, showing that the stands have very different edge effect situations, which was to be expected (Figure 4.15).

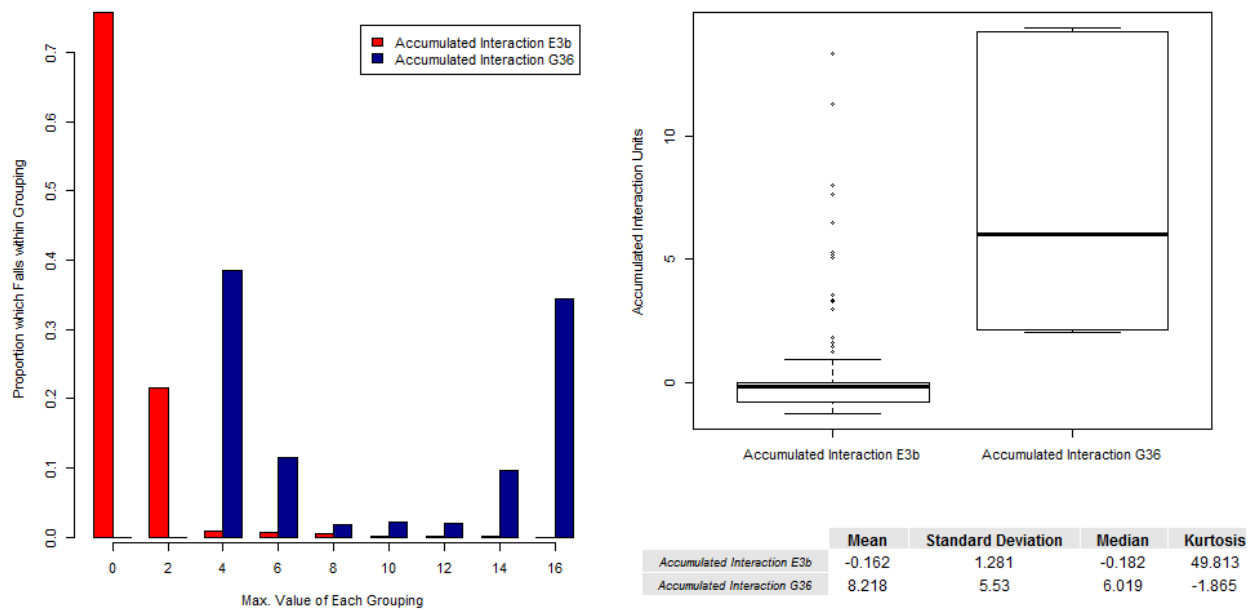


**Figure 4.15.** A visual comparison between the distribution of the AI values for stand E3b (the model calibration dataset) and stand G36 (the simulation stand). The spread of AI values of stand G36 is wider and more positive than that of stand E3b.

#### 4.7 Calculation of local tree density

Local density for each point was calculated as described in Section 3.8. The resultant local density per tree position is spatially represented in Figure 4.17.

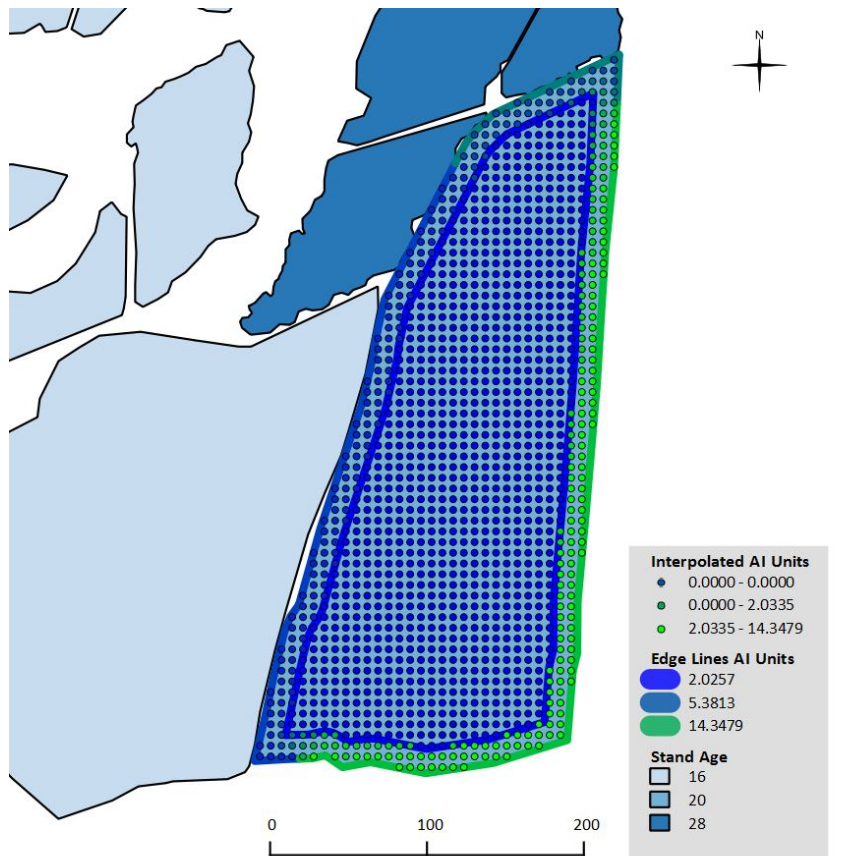


**Figure 4.16.** A figure demonstrating virtual tree positions with the points indicating interpolated AI values in graduated colouring from 0 to 14.3.

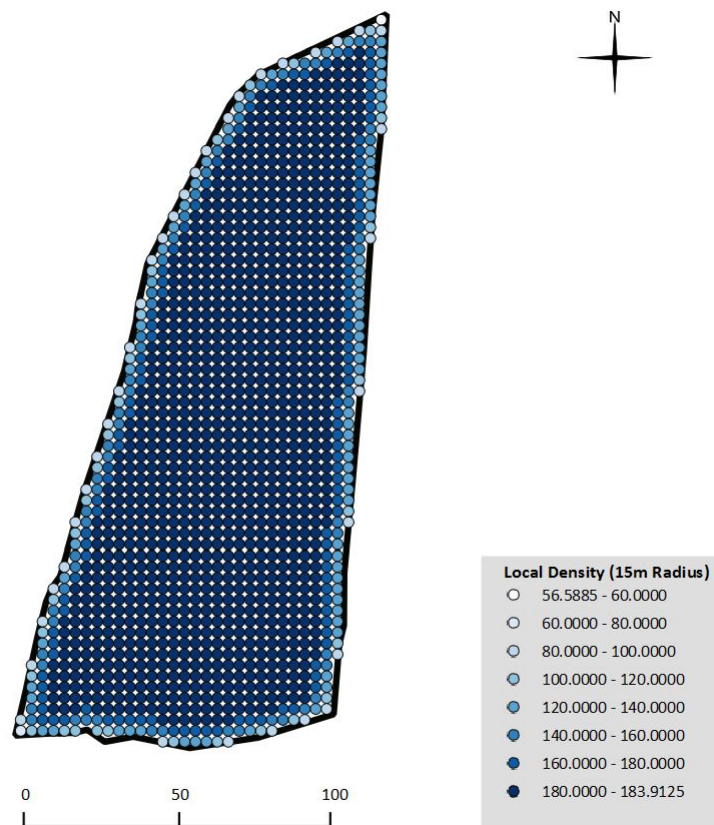


**Figure 4.17.** The local density calculation of tree positions in stand G36, taking a 15m radius into account for each tree.

#### 4.8 Prediction of stand variables

Using the data as prepared to this stage, the tree variables height, diameter and volume were predicted. Simulation of stand G36 was carried out based on the interpolated AI values, the calculated local densities and the models generated and presented for stand E3b in Chapter 3. Height, DBH and volume respectively, were calculated for each point. In order for the output to fit the stand conditions of G36, the calculated outputs were shifted by the difference between the mean at the inner region of the two stands, where the inner region means for stand G36 were extracted from the sample plot data and the inner region means for stand E3b were extracted from the complete dataset of inner trees.

In subsequent sections of this chapter, primarily results for the simulation of volume are shown. The results for height and DBH can be found in Appendix A. Volume was selected as the evaluation variable here because it combines both DBH and height in its calculation and is the main target variable in forest planning.

The result of the simulated output for volume is shown in Figure 4.18, where the predicted volumes of the stand edges are compared to the volumes as calculated from data extracted from the CHM, also only for the edges. The distribution of the predicted volumes is based on the variance explained by the edge effect only. Hence the values are fairly tightly grouped just above the mean, tailing off to the right in a similar fashion as the measured edges. It is, however clear, that the natural variance is not yet included in this output and that its inclusion is necessary in order to create a more realistic prediction.

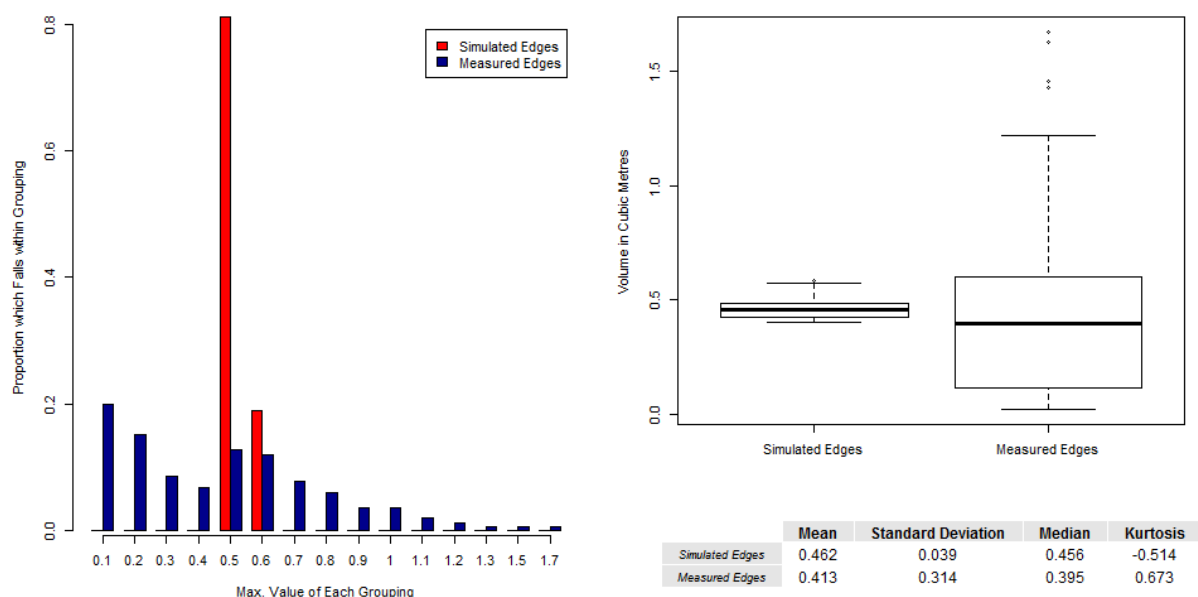


**Figure 4.18.** A comparison between the volume predicted for the edge region of stand G36 without simulation of the natural variance shown by the red bars, and the distribution of the volumes as calculated from data extracted from the CHM (blue bars).

#### 4.9 Generating random values based on natural stand variance

Once the stand had been modelled based on AI and local density, it was necessary to include the natural stand variance attributable to causes other than edge effect. In order to obtain a good

prediction of stand output, it is necessary to combine the variance attributable to the edge effect with the natural stand variance. Natural stand variance is represented by the distribution of a given tree variable for the trees in the inner region of the stand. In this case these data were collected by simulating a sample inventory in the inner region of the stand, as demonstrated in Section 4.5. These distributions were generated for all three tree variables individually. An example of the height distribution is shown in the red bars of Figure 4.14. Each point in the simulated stand was then allocated a random value for height, DBH and volume respectively, based on random numbers generated from those distributions in parameterised stochastic process. These values were combined with the modelled values as explained in Section 4.10.

In order to mimic a distribution of an unknown type, a random number generator was built in *R* based on the *sample* function (Ripley 1987; Becker et al. 1988) in the *base* package (*R* Core Team 2013) in conjunction with the *hist* histogram function in the *graphics* package (*R* Core Team 2013). In order to generate a random number within the given distribution, the total number of required random values is input with a list of all unique values for the given tree variable. A random number is then generated based on the probability of that number being present in the distribution. In this way it was possible to produce any given quantity of random values, closely mimicking any given distribution. An example of the comparison between the generated random number distribution of the heights and the heights extracted from the CHM of G36 is shown in Figure 4.19 below.

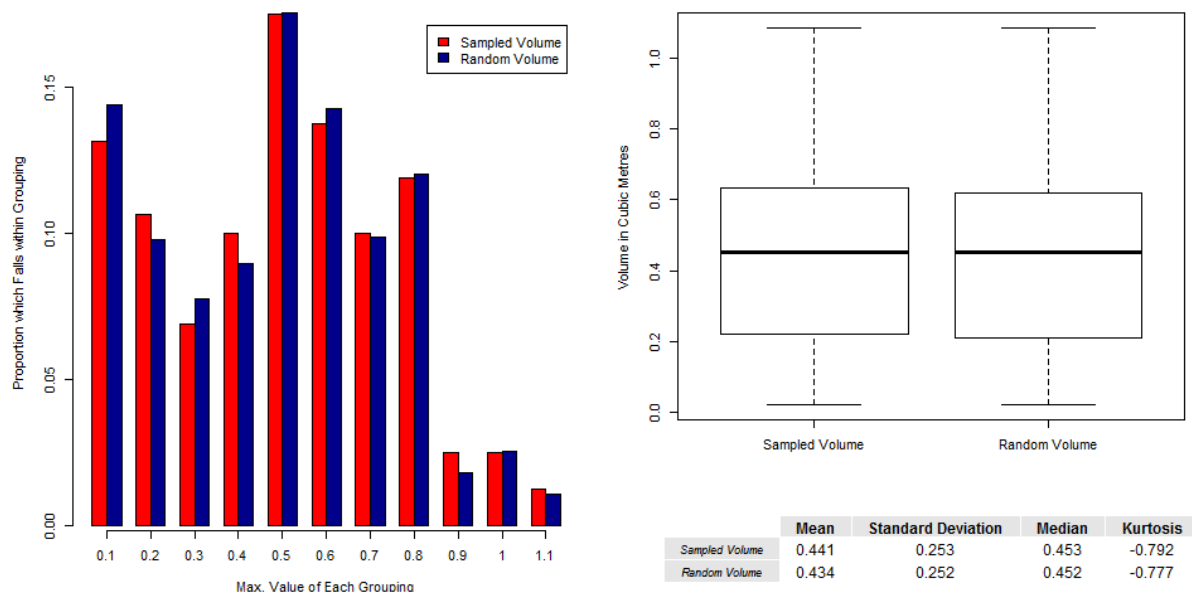


**Figure 4.19.** A comparison between the random values generated for volume of the complete stand G36 (blue bars) and the distribution of the volumes as extracted from the sample plots (red bars). The random values were generated based on the distribution of the sample plot volumes.

#### 4.10 Combining distributions to predict expected stand output

Two values were assigned to each point representing a tree. These were the predicted value attributable to the edge model as well as a random value representing the natural variance simulated by the generation of random values. These two values needed to be combined for each point so that each point would have a single value representing the predicted edge effect combined with the natural variance derived from the inner plot. In other words, trees at edges which are predicted to be

larger, would be on average larger than trees within the rest of the stand, but would still, as a whole, follow a distribution similar to that of the rest of the stand. The same would apply for regions with smaller trees and average trees (Figure 4.22).

As explained before, the distribution representing the natural stand variance was extracted from inner tree values, therefore the mean of the natural stand variance distribution is the mean of the inner stand for that given tree variable. In order to combine the two simulated values, it was necessary to consider the predicted value for any given point as the new mean of the distribution representing the natural stand variance, thus shifting the distribution to centre on the predicted value as the new mean. The distance of the shift is the amount by which the random value generated for that point must be adjusted.

The calculation of this operation is shown in Equation 8, where the random value is shifted by the difference between the mean of the inner stand and the predicted, modelled value for that point. This means that when a point has a predicted value greater than the mean of the natural stand variance, it shifts the distribution up, and the random value generated for that point must be shifted by that same amount in order to produce the final, combined simulated value for that point. An adjustment of this nature means that if one were to extract a large enough sample of points with the same original predicted tree variable (before the combination with the random value), and inspect the distribution of the final, combined, simulated value for these trees, the distribution should not be significantly different from the distribution of the natural stand variance.

$$v_n = (v_m - \bar{x}_i) + Y \quad (\text{Equation 8})$$

Where

$v_n$  = Combined simulated value, taking into account natural variance and predicted edge effect

$v_m$  = Tree variable as predicted by edge models

$\bar{x}_i$  = Inner stand mean for the given tree variable

$Y$  = Random number generated based on distribution of inner stand for the given tree variable

The resulting simulated output for the edge region is shown in Figure 4.20, while the distribution of the complete stand output for volume is shown in Figure 4.21. A spatial representation of the simulated stand is shown in Figure 4.22.



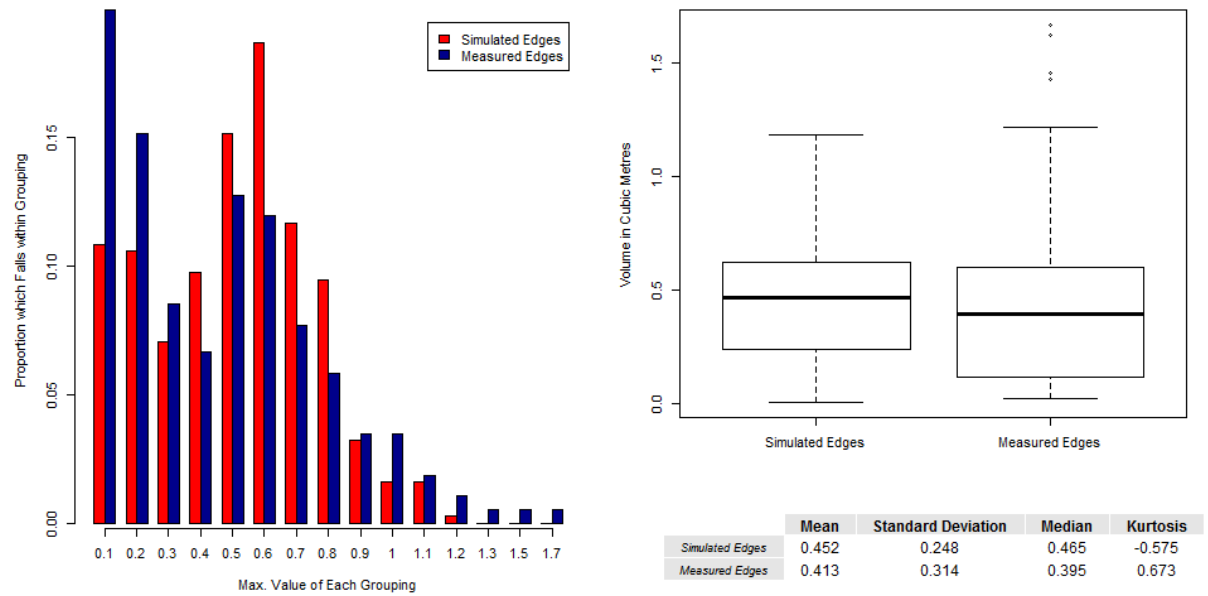


**Figure 4.20.** A comparison between the distributions of the predicted edge tree volumes (red bars) and the edge tree volumes as calculated from data extracted from the CHM for the complete stand (blue bars).

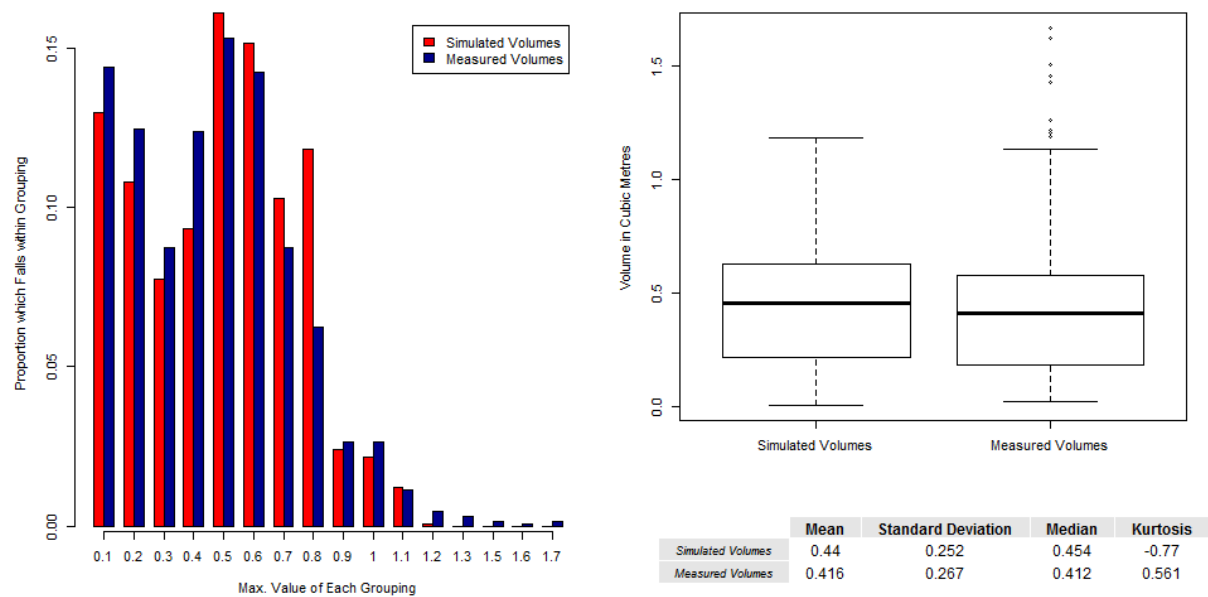


**Figure 4.21.** A comparison between the distributions of the predicted volumes for all the trees within the complete stand (red bars) and the stand volumes as calculated from data extracted from the CHM for the complete stand (blue bars).

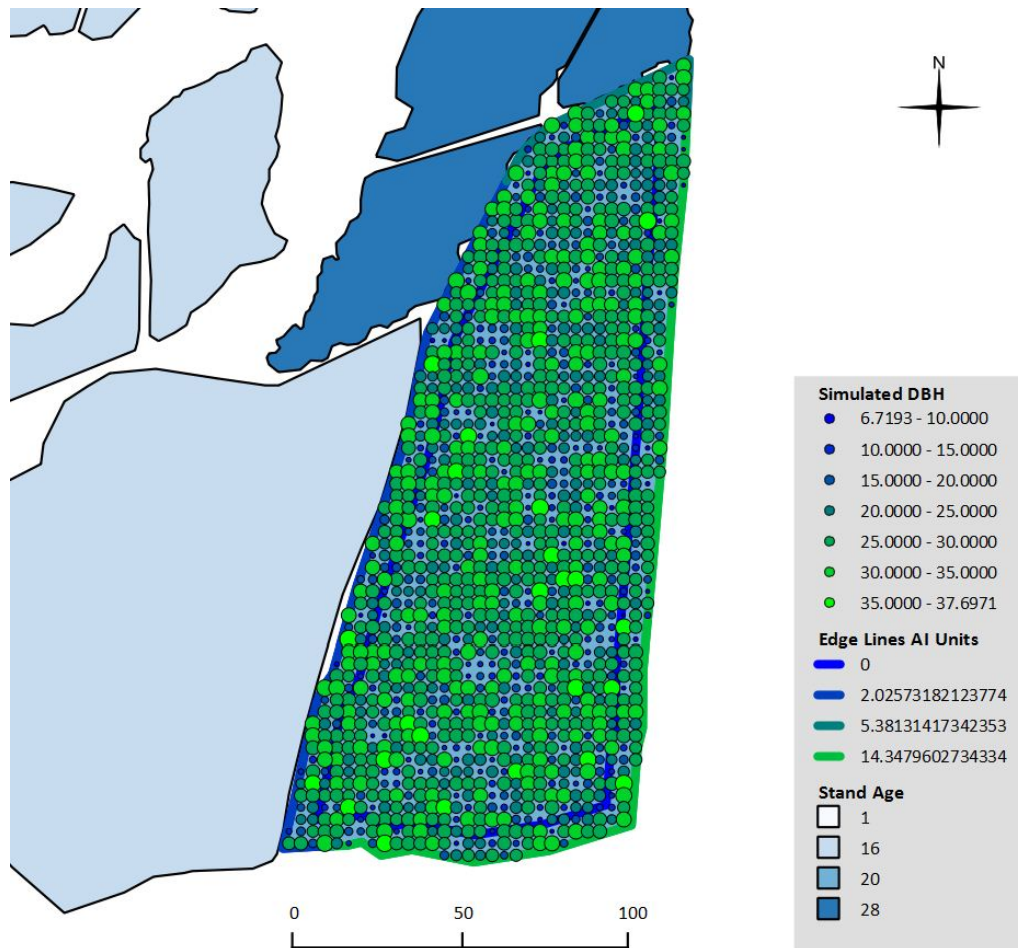


**Figure 4.22.** A spatial representation of the simulated stand G36. The colour and size graduated circles represent the simulated DBH per point where blue is a smaller and green a higher DBH as well as DBH increasing with increasing circle size.

#### 4.11 Comparing the edge region with the inner region

The edge effect for stand G36 is most clear in the results when comparing the heights for the edge region with the inner region outputs as shown in Figure 4.23, where the distribution for the edge trees is shifted to the right in the bar graph and upwards in the boxplot. This is the expected result as this stand has a large proportion of competition free edge, which should result in relatively larger trees for the edge region in general. Also, the AI values are all positive for stand G36, indicating dominance over neighbouring stands in general throughout the lifetime of the stand.

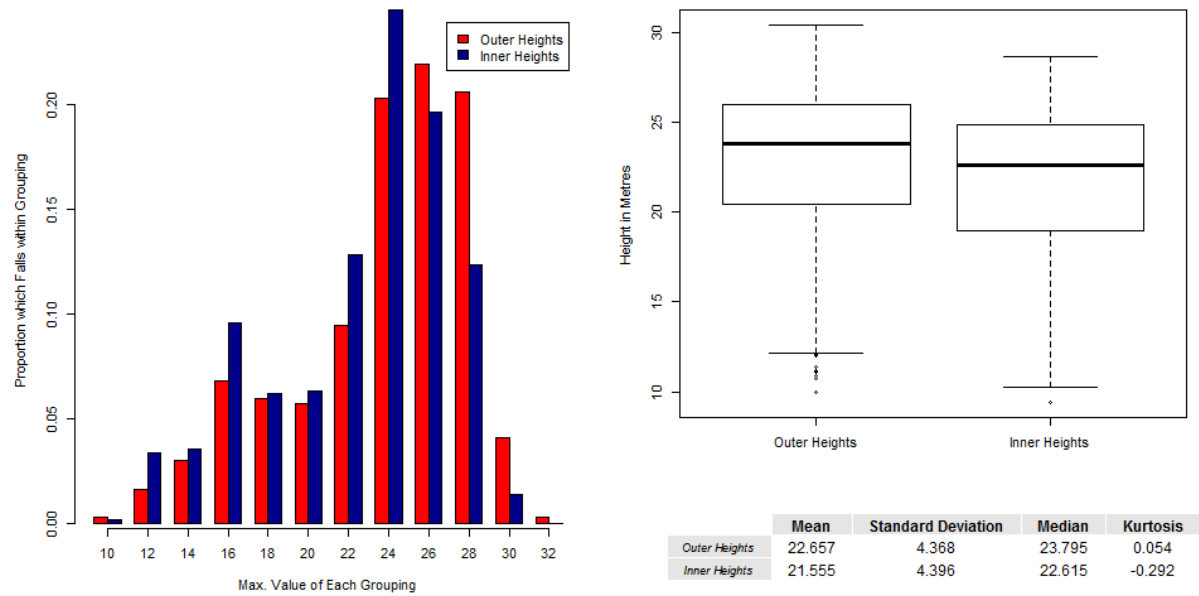


**Figure 4.23.** A comparison between the simulated heights for the outer region of the stand (red bars), with the inner region of the stand (blue bars).

## Chapter 5. Discussion and conclusions

This discussion chapter seeks to evaluate the efficacy of the spatial edge effect modelling and simulation methodology as presented in Chapters 3 and 4 by reconciling the outcomes presented in those chapters with the objectives of the framework as laid out in Chapter 1. The way in which each objective was achieved and the positive and negative aspects of each proposed solution will be discussed. Those aspects for which further research work is recommended are emphasized. Two other topics are also shortly discussed, namely the quantification of stand regularity as proposed by an evenness index and the feasibility of using the *R* framework for spatial data analysis and manipulation. It concludes with a discussion on whether the overall aim of the study was achieved and the proposed course to follow for the continuance of this work.

The objectives to be discussed are the following:

1. Providing a methodology for quantifying interaction at stand edges between trees of a given stand and trees of a neighbouring stand over the lifetime of the stand.
2. Transferring the edge interaction value from the edges to all the trees within the stand in a coherent way.
3. Identifying the spatial extent of the edge effect into the stand.
4. Providing a methodology for taking into account spaces between stands.
5. Modelling the expected variance caused by the edge and thus explaining the relationship between the edge interaction and tree variables, taking the spaces between compartments into account.
6. Simulating the edge effect and combining it with the natural stand variance in order to predict stand output by taking the edge influence into account.

### 5.1 Quantifying edge interaction

The first objective was to provide a methodology by which competition at the edge of a stand could be explained in an objective, quantitative way. Two measures of edge interaction were introduced namely Neighbour Interaction (NI) and Accumulated Interaction (AI) based on stand height as compared to neighbouring stand height. NI is an instantaneous, snapshot quantification of edge interaction at a given time, quantified on a scale ranging from -1 to 1, representing total suppression to total dominance on the scale respectively. AI is the time weighted, accumulated NI over the lifetime of the stand, combining the time for which the edge was suppressed with the time for which it was dominant, as the edge dynamic changes. An edge therefore accumulates AI units, which reflect the degree to which it was suppressed or dominant throughout the rotation. NI and AI proved to be two measures which can be used to quantify edge interaction. This first objective was therefore successfully achieved in the introduction of these measures.

#### 5.1.1 Permanent sample plot data

The two measures of edge interaction can, however, be further improved in future work, where they are calculated using permanent sample plot (PSP) data, which is more specific to the given situation, instead of a more generic growth and yield table. Another possible improvement would be to

monitor the development of edges over time in a similar fashion to PSP data in order to produce yield tables for edge trees, specifically throughout the rotation. This monitoring could be carried out for edges at different levels of interaction. Maintaining such a sample plot network would require high inputs in terms of time and costs. It is therefore suggested that remote sensing be used, where, for example, annually repeated flights could be carried out along the specified edges and tree data extracted from those datasets. These data could then be used when calculating NI and AI in order to provide a better quantification of edge interaction by measuring the development of the edge trees over time instead of the stand mean.

#### **5.1.2 Including aspect in edge interaction calculation**

The inclusion of aspect in spatial edge effect modelling was briefly investigated in Section 3.10. A proposed method was the calculation of the bearing for the edge lines and the interpolation of these values into the stand interior in order to link trees with edge aspect. Further investigation of the inclusion of these data in the AI models should be carried out where the bearing provides an additional variable in the model or simply in order to identify the spatial extent of the edge effect as a function of the aspect of the edge, as discussed in Section 5.3.1. However, further data beyond the available dataset for this study would be required.

### **5.2 Transferring edge interaction into the stand**

A straightforward inverse distance weighting (IDW) approach was applied in order to interpolate the AI values of the edges to the tree positions within the stand. The reasoning was that all edges have an effect on tree growth but the further away the edge, the less the impact it has at that point while proximate edges have a greater impact. IDW proved a satisfactory interpolation in that it was a simple, self-explanatory, smooth interpolation that achieved its purpose of transferring the edge interaction from the edges into the stand, tending towards zero as the positions of the tree moved towards the inner region of the stand and tending towards the edge value as the position approached that given edge. The objective regarding the transference of edge interaction into the stand in a coherent, quantitative way was therefore successfully achieved.

### **5.3 Identifying the spatial extent of the edge effect**

Quantifying the extent by which the edge effect reaches into the stand is a procedure which can be carried out in a number of ways. The method presented and used in this study is a segmented regression which identifies the breakpoint between linear piecewise models for a dataset. This breakpoint was identified for the complete dataset of DBHs for a terrestrially measured stand as a function of distance from the edge. It was accepted that the breakpoint was the point at which the edge effect on the variables of interest stopped and the inner region of the stand, unaffected by edge effect, began. This proved to be a clear way of identifying the extent of the edge effect in an objective and quantitative manner, and the calculated distance of 15m corresponds well with previous studies.

### 5.3.1 Including aspect in edge effect extent calculation

In this study, only one distance was used for identifying the extent of the edge for all sides of the stand, however, it is clear from previous studies (Cancino 2005) that aspect plays a role in the extent of the edge effect. In future work it would be beneficial to group the data into separate classes by bearing (as calculated in Section 3.10) and then carry out breakpoint analysis in the same way as described in Section 3.5) for each class. The result would be a varying edge zone from which to extract data or in which to carry out simulation, an example of which is demonstrated in Figure 5.1 below. Some smoothing might be required in order to form a coherent spatial edge extent model.

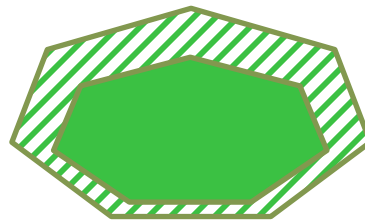


**Figure 5.1.** A simplistic, exaggerated representation of a stand with an edge effect of varying extent, depending on the cardinal direction of the edge. The solid region represents the inner region of the stand, beyond the extent of the edge effect, while the striped region represents the area affected by the edge.

Another consideration for future work would be to take this variation in extents into account for the different tree variables, where the effect of edge on DBH might not be the same as the extent of the edge effect on height, for example. Further work on modelling these differing extents is suggested but larger datasets would be required. These data could all be collected remotely in order to have a large enough dataset to be representative of the reality.

### 5.4 A methodology for taking spaces between stands into account.

In Section 3.8, the need to include some measure of space between neighbouring stands was discussed. A proposed local density function was introduced and designed in R, which calculated the stems per hectare in the local neighbourhood of each tree, defined by a circle with a radius of 15m (the spatial extent of the edge effect). A clear negative correlation was found between the local density and DBH. Such a density function ensures that spaces between stands, e.g. roads or logging trails are taken into account and are quantified in edge effect modelling. This index will then also take into account trees in the interior region of irregular stands, which have above average growing space. Trees which have a similar local density should display similar growth even though they are not necessarily on the edge, thus this measure provides additional benefit when modelling from irregular stand data.

When calculating local density in this study, it was assumed that the space between neighbouring stands was at least 15m and thus no trees from neighbouring stands were taken into account. However, in future studies, neighbouring stands within a 15m radius from the edge need to be considered when calculating local density.

Variation in the spatial extent of the edge effect within a stand needs to be considered when calculating the local density. The radius of the circle within which local density is calculated should be no less than the greatest extent of edge effect within a stand.



A local density measure as proposed should also make allowance for gaps within stands which are not edges in the sense of compartment boundaries but which undergo an edge effect. It is proposed that in future work, the variation in local density also be included in a stand simulation, where this variation is mimicked in the same way as that in which the natural variance of the stand is mimicked, providing a range of inner region tree densities instead of a single, uniform density. Mimicking the local density could be done by generating a simulated stand tree layout which is not structured according to a regular grid but which is structured in such a way that the spatial layout of the simulated stand produces a distribution of local densities which closely matches the expected local density. The use of Canopy Density Models derived from LiDAR data could be considered as an alternative to the local density calculation for the purpose of quantifying gaps between stands and within stands.

## 5.5 Modelling the edge effect

From the terrestrially measured dataset (stand E3b), three models were generated explaining the interaction between AI and individual tree DBH, AI and tree height and AI and tree volume

Although the data presented some general trends, a good fit was not obtained for any of these variables because of the large variance in the tree variable data. The general trend for DBH and volume was slightly negative with increasing AI, which was not expected. An increase in AI indicated an increase in dominance, which implies improved production. The general trend for height was positive, thus confirming the hypothesis that a higher AI indicates improved growth. However, these trends are merely preliminary because the dataset was obtained from E3b only and was concentrated in the negative values with a large amount of variance in the data not attributable to the edge effect. An explanation is also that the roads which surrounded the compartment obviously masked the competitive AI based effect for DBH and volume, which is quadratically dependent on DBH. The resulting pattern of tree dimensions shows that height growth was still influenced by the neighbouring stands, while DBH was more influenced by a short distance opening caused by the road. Further data collection and model fitting will have to be done in future in order to make more conclusive assumptions regarding the relationships between AI and tree variables.

A larger spread of data would have been more desirable in the model calibration dataset. The comparison between the AI values of stand E3b, which was used to calibrate the models, and the AI values of stand G36, which was simulated, is shown in. In future, with additional data collection, the spread of data will improve and the models will improve in accuracy.

### 5.5.1 Taking stand age into account

The methodology applied in this study should in future be carried out across a range of age classes in order to be able to simulate the complete range of ages in order to verify this influence of age in the relationship between AI and tree growth.

While trees are still young and there is not yet any competition for resources because the trees have not developed enough to have a spatial interaction with neighbouring trees, accumulated interaction will not yet have any effect on tree growth. However, as trees get older and larger, spatial interaction between trees and neighbouring edges will increase and thus effect of AI on tree growth is expected to increase. Therefore, it is expected that the relationship between AI and the tree variables is age

dependent. From the combination of such models a three dimensional relationship surface could be produced, which would contain the AI and age as x and y axes and the tree parameter on the z axis. An example of the possible surface for the height *Pinus radiata* on a site index of  $SI_{20}=25$  is demonstrated in Figure 5.2. This example assumes that at a younger age, the edge effect has little influence on the growth of the trees but as the growth progresses, the influence of the edge on the growth of the tree changes to varying degrees.

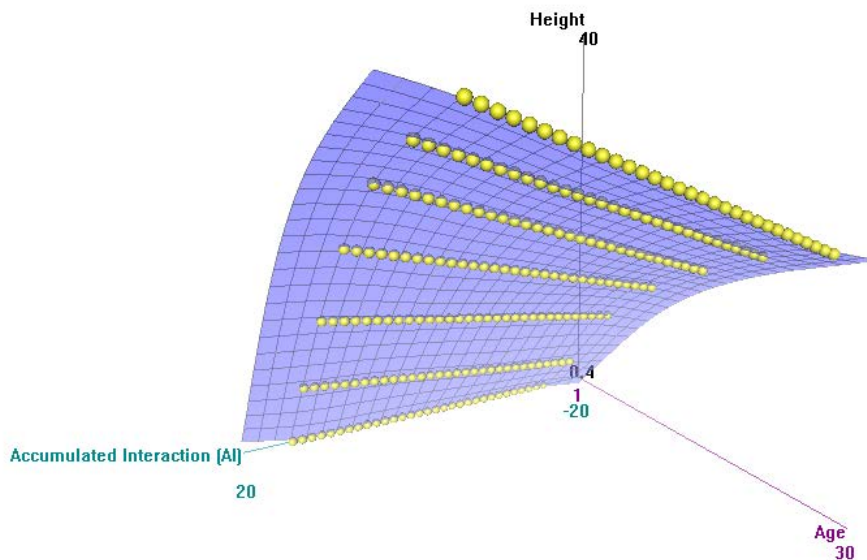


**Figure 5.2.** A visualisation of the effect that age could possibly have on the relationship between AI and height for a *Pinus radiata* stand on a site index of  $SI_{20}=25$ .

In order to further the work on the edge effect model framework, it would be necessary to study the relationship between AI and edge tree development over the complete rotation and build a model where age is also a parameter describing the tree variable. Data could be collected for this modelling process in much the same way as the PSPs proposed in Section 5.1.1, where different edge interactions are measured, being monitored throughout the rotation length.

## 5.6 Simulating the edge effect and natural stand variance

Simulation of the edge effect for a stand (G36), which had been remotely sensed for data collection was carried out. The investigation and implementation of a number of techniques in order to extract data, adjust the models to fit stand conditions, generate random values and combine random variables with predicted variables was necessary. In terms of the remotely sensed dataset, it was clear that there were various errors in the dataset in terms of homogenous elevation throughout a homogenous stand and a ground level at zero.

### 5.6.1 Using local maxima to extract tree positions

A moving window, extracting local maxima within a weighted grid roughly representing a circle proved the simplest solution for identifying treetops within a CHM using the *R* framework and

provided satisfactory results. However, some questions remain regarding the size of the moving window, the amount of understory to be removed and the matching of tree positions with ground truthing data. Although the initial expectation for this study was to be able to pair terrestrially measured tree data with remotely sensed tree data in order to answer these questions in a more satisfactory way, this was not found to be possible with the data available. These questions could possibly be answered or optimised with a better quality CHM in future work where data from trees measured terrestrially could be matched with data from trees as extracted from a CHM. However, the data and methods as extracted proved sufficient in order to demonstrate the methodology as desired.

### 5.6.2 Correcting CHM data

In order to extract reasonably realistic data from the CHM, it was however necessary to make two adjustments to the original dataset. As a result of some error in the DEM, the lowest point in the CHM was below zero, which is unrealistic if the lowest point is ground level and the treetops are the height above ground. The elevation of the CHM as a whole was raised in order for the data to be realistic. It was presumed that the lowest point in the CHM did indeed represent the ground.

Also, as a result of imprecision in the DEM, certain regions of the CHM were disproportionately lower than other regions, causing a skewed distribution of tree heights and an exaggerated removal of understory in the some areas of the DSM with almost no understory removal in others. Correction was made by applying a square moving window of one hectare over the stand, adjusting the centre pixel per iteration, by the difference between the stand mean and the neighbourhood mean. This process resulted in a much improved, more homogenous stand CHM. The question does remain whether one hectare is a large enough window to keep local tree interactions intact while adjusting the neighbourhood. It is assumed that plantation forests are homogenous in this way and that edge effect extends only about 15m. A square window of one hectare should therefore retain the effect of the edge but adjust the neighbourhood to a more realistic stand level. A verification of this method could be carried out once an improved dataset for the same area becomes available; however, the data as extracted provided sufficient information for the demonstration of the methodology.

During this study LiDAR data were not available but it is recommended that in future studies LiDAR data be used as this would improve the accuracy of datasets and less error should be present in the dataset.

### 5.6.3 Adjusting the models to different stand conditions

Edge effect models, explaining the relationship between AI and a given tree variable, for example height, were fitted using terrestrially measured data from a stand of a given age and height. Two questions are still not clearly answered in this regard. What effect does age have on this relationship? How can the models be applied to a stand where the average tree height differs from that of the model calibration dataset?

The effect of age is discussed in Section 5.5.1. However, when applying these models to a different stand of roughly the same age but with a different mean height for simulation, it would be necessary to adjust the outputs from the predictions to match the reality of the stand. For the purposes of this study, the outputs were simply shifted up or down to match the extracted value for that parameter

at the stand inner region. This adjustment would have to be investigated in future work where some kind of scaling might be required in order shift the model proportionately throughout the stand, or not. However, a larger dataset will be required in order to further develop this adjustment methodology.

#### 5.6.4 Generating natural variance distributions

An important aspect in providing a realistic simulation of a stand output at a finer, tree level, is the need to be able to predict the unknown, natural variance of the stand. In this study, the effect of neighbour interaction was singled out from the total stand variance to be modelled purely as a function of neighbour interaction. All other variance in the stand had to be simulated by a parameterised stochastic process based on the variance in that region of the stand which was beyond the reach of the edge effect. When extracting the distribution of the data from that inner region it was found that the data did not clearly have any standard normal distribution trend. A novel technique based on random number generation per diameter class was therefore developed in *R*. With that technique any given distribution of any shape could be mimicked. This random number generator solved the question of mimicking the natural stand variance because a random variable could be assigned to each point representing a tree and the resultant distribution of all the points combined would closely match the sampled inner region distribution. By re-introduction of the natural variance, plausible tree variable distributions were simulated based on empirical data as e.g. originating from stand enumerations of the inner region of the stand.

#### 5.6.5 Combining variances

Once a random value had been assigned to a tree in the parameterised stochastic process, it had to be combined with the predicted value from the edge effect modelling process. Combining the two values was done by shifting the generated random value for that point by the difference between the inner stand mean (the natural variance distribution mean) and the predicted value for that point. The natural variance distribution thus remained intact but that distribution was adjusted up or down for that given tree by the change resulting from the edge effect. Two values describing different variances for a single point were thus successfully combined in such a way as to take them both into account without prejudicing the integrity of the distribution.

### 5.7 Quantifying evenness

An attempt was made to quantify the regularity, or evenness, of tree layout in order to use this value as an additional explanatory spatial variable when modelling DBH as a function of height. The proposed evenness index is the coefficient of variation of all the distances between each tree and its neighbours, as calculated by means of Delaunay triangulation. Although no significant improvement was achieved when including the evenness index in the model, it is still suggested that continued verification be carried out on this index with datasets containing less variance in the tree variables.

## 5.8 Using the *R* framework for spatial data analysis

The capacity of *R* to manage spatial data was widely explored in the development of the framework. It was found that the capabilities of *R* meet this challenge well with the wide variety of functions already developed in the various spatial data packages. Where a built-in function does not meet the need, a user-defined function can generally be developed to solve the specific problem. The manipulation of spatial data in *R* does, however, occasionally require some unorthodox thinking in order to come to a solution that would appear simple at first view.

## 5.9 Taking relief into account

Within this study, the effect of the relief of the terrain was not included in the methodology. It Considering how that slope and the shape of a watershed has an effect on the dynamics of water flow and build-up, relief is a consideration for future application of this work. A stand growing on a slope might manifest superior growth on the lower areas of the slope where water accumulates than on the upper areas where water could be more restricting to such favourable growth. Relief would also affect the edge dynamic in terms of light, where shading is more pronounced in some slope-edge combinations than in others. The demonstrated effect of aspect might be interacting with relief shading effects. With the availability of more data, especially large datasets obtained by means of remote sensing, the effect of relief could be included in the edge effect modelling process.

## 5.10 Achieving the overall aim of the study and continuing this work

The primary aim of the study was to provide a methodology for quantifying the variance in stand output attributable to the interaction between a plantation forest stand and its neighbour. In order to achieve this, a quantification methodology was presented and successfully verified in a simulation process. Many methodological steps have been successfully proposed to reach this aim, providing feasible means for the achieving of the objectives as laid out in the beginning of the study. The presented methodological framework includes:

1. A methodology for quantifying interaction at stand edges between trees of a given stand and trees of a neighbouring stand over the lifetime of the stand was proposed and successfully validated.
2. A logical and clear method was proposed and applied in order to transfer the edge interaction value from the edges to all the trees within the stand in a coherent way.
3. Breakpoint regression was proposed as a novel way of identifying the spatial extent of the edge effect into the stand and this was successfully applied.
4. In order to provide a methodology for taking into account spaces between stands and irregular spacing, a local density algorithm was successfully developed and tested.
5. The relationship between the edge interaction and tree variables, taking the spaces between compartments into account, was explained by modelling the expected variance caused by the edge.
6. This edge effect was then simulated on an independent stand and the natural variance was reintroduced by combining it with a random value generated during a parameterised stochastic process variance in order to predict stand output by taking the edge influence into account.

The algorithms for these processes, as well as an evenness index were developed and implemented in *R*. With this implementation, a framework was created that forms the foundation for a combined application of GIS and spatial statistics in the context of spatial plantation modelling.

In order to advance this study of the spatial modelling of edge effects, to parameterise the models and optimise the NI and AI values, it is suggested that a network of edge plots be set up in a similar way to PSPs, with various levels of interaction taken into account by varying the age differences between the various plots and monitoring these plots over the length of at least one rotation. Remote sensing of these regions would be the more viable option, especially the use of aerial LiDAR where possible. It is also suggested that the distance between edges be maintained as constant as possible for the various plots. With these data available, it should be possible to incorporate the implementation of spatial edge modelling into standard growth and yield modelling in conjunction with a standardised inner region inventory method. However, this study showed the importance of spatial mapping to solve questions around stand heterogeneity and edge effects.

Incorporating this approach into growth and yield modelling could provide the input for position dependent individual tree models in order to provide more realistic initial stand information. The inputs for the system would be a standardised form of enumeration data from the inner region of stands in conjunction with the spatial layout of the stands in shapefile format. The output would be spatialised individual tree data and stand distributions that provide realistic information for bottom up planning, from the tree, its dimensions and spatial position, to the stand and then the plantation as a whole, at all temporal planning levels.



## References

- Ackerman, S., Ackerman, P. & Seifert, T., 2013. Effects of irregular stand structure on tree growth. *Southern Forests (In Press)*.
- Adler, D. & Murdoch, D., 2013. rgl: 3D visualization device system (OpenGL). Available at: <http://cran.r-project.org/package=rgl>.
- Aguirre, O., Hui, G., Gadow, K. Von & Jiménez, J., 2003. An analysis of spatial forest structure using neighbourhood-based variables. *Forest Ecology and Management*, 183(1-3), pp.137–145.
- Andrews, G.S., 1936. Tree heights from air photographs by simple parallax measurements. *Forestry Chronicles*, 32, pp.444–450.
- Anon, 2013. Oxford English Dictionary Online. *Oxford English Dictionary*. Available at: <http://www.oed.com/view/Entry/189940?redirectedFrom=stereopsis#eid> [Accessed September 9, 2013].
- Bartier, P.M. & Keller, C.P., 1996. Multivariate interpolation to incorporate thematic surface data using inverse distance weighting (IDW). *Computers & Geosciences*, 22(7), pp.795–799.
- Becker, R.A., Chambers, J.M. & Wilks, A.R., 1988. *The New S Language*, Pacific Grove, Ca.: Wadsworth & Brooks.
- Berg, P., 1973. Silviculture of *Pinus radiata* stand edge trees at Woodhill Forest. *New Zealand Journal of Forestry*, 18(1), pp.115–123.
- Betts, M.G., Forbes, G.J. & Diamond, A.W., 2007. Thresholds in songbird occurrence in relation to landscape structure. *Conservation biology : the journal of the Society for Conservation Biology*, 21(4), pp.1046–58.
- Cadenasso, M.L., Pickett, S.T.A., Weathers, K.C. & Jones, C.G., 2003. A Framework for a Theory of Ecological Boundaries. *BioScience*, 53(8), pp.750–758.
- Cadenasso, M.L., Traynor, M.M. & Pickett, S.T., 1997. Functional location of forest edges: gradients of multiple physical factors. *Canadian Journal of Forest Research*, 27(5), pp.774–782.
- Campbell, J.B. & Wynne, R.H., 2011. *Introduction to Remote Sensing*, New York: The Guilford Press.
- Cancino, J., 2005. Modelling the edge effect in even-aged Monterey pine (*Pinus radiata* D. Don) stands. *Forest Ecology and Management*, 210(1-3), pp.159–172.
- Cape Pine, 2013. Cape Pine - Forests. Available at: <http://www.capepine.co.za/forests/> [Accessed July 12, 2013].
- Delaunay, B., 1934. Sur la sphère vide. *Otdelenie Matematicheskikh i Estestvennykh Nauk*, (7), pp.793–800.
- Diggle, P.J., 2003. *Statistical Analysis of Spatial Point Patterns* 2nd ed., London: Arnold.

- Dignan, P. & Bren, L., 2003. Modelling light penetration edge effects for stream buffer design in mountain ash forest in southeastern Australia. *Forest Ecology and Management*, 179(1-3), pp.95–106.
- Donovan, T.M., Jones, P.W., Elizabeth, A.M. & Frank, T.R., 1997. Variations in Local Scale Edge Effects: Mechanisms and Landscape Context. *Ecological Society of America*, 78(7), pp.2064–2075.
- Dryden, I.L., Faghihi, M.R. & Taylor, C.C., 1997. Procrustes Shape Analysis of Planar Point Subsets. *Journal of the Royal Statistical Society: Series B (Statistical Methodology)*, 59(2), pp.353–374.
- Dryden, I.L., Taylor, C.C. & Faghihi, M.R., 1999. Size Analysis of Nearly Regular Delaunay Triangulations. *Methodology and Computing in Applied Probability*, 1, pp.97–117.
- Ducey, M.J., Gove, J.H. & Valentine, H.T., 2004. A Walkthrough Solution to the Boundary Overlap Problem. , 50(2186), pp.427–435.
- Evans, P.J.. & Clark, F.C., 1954. Distance to Nearest Neighbor as a Measure of Spatial Relationships in Populations. *Ecology*, 35(4), pp.445–453.
- Ewers, R.M. & Didham, R.K., 2006. Continuous response functions for quantifying the strength of edge effects. *Journal of Applied Ecology*, 43(3), pp.527–536.
- Gadow, K., Zhang, C.Y., Wehenkel, C., Pommerening, A., Corral-rivas, J., Korol, M., Myklush, S., Hui, G.Y., Kiviste, A. & Zhao, X.H., 2012. *Continuous Cover Forestry* T. Pukkala & K. Gadow, eds., Dordrecht: Springer Netherlands.
- Golser, M. & Hasenauer, H., 1997. Predicting juvenile tree height growth in uneven-aged mixed species stands in Austria. , 97, pp.133–146.
- Gong, P., Greg S. Biging, Lee, S.M., Mei, X., Sheng, Y., Pu, R., Xu, B., Schwarzr, K.-P. & Mostafa, M., 1999. Photo Ecometrics for Forest Inventory. *Geographic Information Sciences*, 5(1), pp.9–14.
- Gregoire, T.G., 2012. Boundary Overlap Bibliography. , 49(January). Available at: <http://environment.yale.edu/content/documents/00001653/Boundary-Overlap.pdf?1380030906>.
- Hansen, A.J., Lee, P. & Horvath, E., 1993. Do Edge Effects Influence Tree Growth Rates in Douglas-fir Plantations ? Abstract. *Northwest Science*, 67(2), pp.112–116.
- Harper, K.A., Macdonald, S.E., Burton, P.J., Chen, J., Brososke, K.D., Saunders, S.C., Euskirchen, E.S., Roberts, D., Jaiteh, M.S. & Esseen, P.-A., 2005. Edge influence on forest structure and composition in fragmented landscapes. *Conservation Biology*, 19(3), pp.768–782.
- Hijmans, R.J. & Etten, J. Van, 2013. raster: Geographic data analysis and modeling. Available at: <http://cran.r-project.org/package=raster>.
- Howard, M., 2012. Plantation Inventory. In B. Bredenkamp & S. Upfold, eds. *South African Forestry Handbook*. Southern African Institute for Forestry, pp. 211–217.
- Huang, S., Price, D. & Titus, S., 2000. Development of ecoregion-based height–diameter models for white spruce in boreal forests. *Forest Ecology and Management*, 129, pp.125–141.

- Huggard, D. & Vyse, A., 2002. Edge effects in high-elevation forests at Sicamous Creek. Extension Note 62. Ministry of Forests, Forest Science Program, British Columbia.
- Hylander, K., 2005. Aspect modifies the magnitude of edge effects on bryophyte growth in boreal forests. *Journal of Applied Ecology*, 42(3), pp.518–525.
- Jacobs, C., Keltner, J., Vant-Hull, B. & Elderkin, R.H., 1986. Contour interpolation of random data. *Mathematical Modelling*, 7(4), pp.577–583.
- Joseph, V.R. & Kang, L., 2011. Regression-Based Inverse Distance Weighting With Applications to Computer Experiments. *Technometrics*, 53(3), pp.254–265.
- Kätsch, C. & Kunneke, A., 2006. Forest inventory in the digital remote sensing age. *The Southern African Forestry Journal*, 206(1), pp.43–49.
- Korpela, I., Anttila, P. & Pitkänen, J., 2006. The performance of a local maxima method for detecting individual tree tops in aerial photographs. *International Journal of Remote Sensing*, (September 2013), pp.37–41.
- Kotze, H., Kassier, H.W., Fletcher, Y. & Morley, T., 2012. Growth Modelling and Yield Tables. In B. V Bredenkamp & S. Upfold, eds. *South African Forestry Handbook*. Southern African Institute for Forestry, pp. 175–209.
- Van Laar, A., 1978. Edge Effects in *Pinus radiata*. *South African Forestry Journal*, (104), pp.35–37.
- Lu, G.Y. & Wong, D.W., 2008. An adaptive inverse-distance weighting spatial interpolation technique. *Computers & Geosciences*, 34(9), pp.1044–1055.
- Malcolm, J.R., 1994. Edge Effects in Central Amazonian Forest Fragments. *Ecological Society of America*, 75(8), pp.2438–2445.
- Miller, D.R., Quine, C.P. & Hadley, W., 2000. An investigation of the potential of digital photogrammetry to provide measurements of forest characteristics and abiotic damage. *Forest Ecology and Management*, 135(1-3), pp.279–288.
- Minko, G. & Hepworth, G., 1990. Growth effects of large gaps in *Pinus radiata* plantations. *New Zealand Journal of Forestry Science*, 20(1), pp.22–28.
- Muggeo, V., 2008. Segmented: an R package to fit regression models with broken-line relationships. *R news*. Available at: [http://ftp1.us.debian.org/pub/cran/doc/Rnews/Rnews\\_2008-1.pdf#page=20](http://ftp1.us.debian.org/pub/cran/doc/Rnews/Rnews_2008-1.pdf#page=20) [Accessed September 4, 2013].
- Nanos, N., Calama, R., Montero, G. & Gil, L., 2004. Geostatistical prediction of height/diameter models. *Forest Ecology and Management*, 195(1-2), pp.221–235.
- Olson, C.M. & Helms, J.A., 1996. Forest Growth and Stand Structure at Blodgett Forest Research Station 1933-95. *Sierra Nevada Ecosystem Project: Final report to Congress*, III, pp.682–732.
- Pitkänen, J., 2001. Individual tree detection in digital aerial images by combining locally adaptive binarization and local maxima methods. *Canadian Journal of Forest Research*, 31, pp.832–844.
- Pommerening, A., 2002. Approaches to quantifying forest structures. *Forestry*, 75(3), pp.305–324.

- Porensky, L.M., 2011. When edges meet: interacting edge effects in an African savanna. *Journal of Ecology*, 99(4), pp.923–934.
- Pryke, J.S. & Samways, M.J., 2012. Ecological networks act as extensions of protected areas for arthropod biodiversity conservation. *Journal of Applied Ecology*, pp.591–600.
- QGIS Development Team, 2013. QGIS Geographic Information System. Available at: <http://qgis.osgeo.org>.
- R Core Team, 2013. R: A Language and Environment for Statistical Computing. Available at: <http://www.r-project.org>.
- Ripley, B.D., 1987. *Stochastic Simulation*, New York: John Wiley & Sons.
- Roberts, J., Tesfamichael, S., Gebreslasie, M., van Aardt, J. & Ahmed, F., 2007. Forest structural assessment using remote sensing technologies: an overview of the current state of the art. *Southern Hemisphere Forestry Journal*, 69(3), pp.183–203.
- Sandoval, S. & Cancino, J., 2008. Modeling the edge effect in even-aged Monterrey pine (*Pinus radiata* D. Don) stands incorporating a competition index. *Forest Ecology and Management*, 256(1-2), pp.78–87.
- Schmidt, M., Kiviste, A. & Gadow, K., 2010. A spatially explicit height–diameter model for Scots pine in Estonia. *European Journal of Forest Research*, 130(2), pp.303–315.
- Seifert, T., Kunneke, A., Ackerman, P., Baptista, C. & Ham, C., 2010. Country report : the design and use of forest Decision Support Systems in South Africa. *European Forest and Communication System*, pp.1–12.
- Shepard, D., 1968. A two-dimensional interpolation function for irregularly-spaced data. *Proceedings of the 1968 23rd ACM National Conference*, pp.517–524.
- St-Onge, B., Jumelet, J., Cobello, M. & Véga, C., 2004. Measuring individual tree height using a combination of stereophotogrammetry and lidar. *Canadian Journal of Forest Research*, 34, pp.2122–2130.
- St-Onge, B., Vega, C., Fournier, R. a. & Hu, Y., 2008. Mapping canopy height using a combination of digital stereo-photogrammetry and lidar. *International Journal of Remote Sensing*, 29(11), pp.3343–3364.
- Tuller, S., 1973. Effects of vertical vegetation surfaces on the adjacent microclimate: the role of aspect. *Agricultural Meteorology*, 12, pp.407–424.
- Turner, R., 2013. deldir: Delaunay Triangulation and Dirichlet (Voronoi) Tessellation. Available at: <http://cran.r-project.org/package=deldir>.
- Ulm, K., 1991. A statistical method for assessing a threshold in epidemiological studies. *Statistics in Medicine*, 10(3), pp.341–349.
- Wickham, H., 2011. The Split-Apply-Combine Strategy for Data Analysis. *Journal of Statistical Software*, 40(1), pp.1–29.

- Wolf, P. & DeWitt, B., 2000. *Elements of Photogrammetry with Applications in GIS*, United States of America: McGraw-Hill.
- Zenner, E. & Hibbs, D., 2000. A new method for modeling the heterogeneity of forest structure. *Forest Ecology and Management*, 129, pp.75–87.
- Zhang, S., Burkhardt, H.E. & Amateis, R.L., 1997. The Influence of Thinning on Tree Height and Diameter Relationships in Loblolly Pine Plantations. *Southern Journal of Applied Forestry*, 21(4), pp.199–205.

Appendix A. Additional results

5.11 DBH simulation results

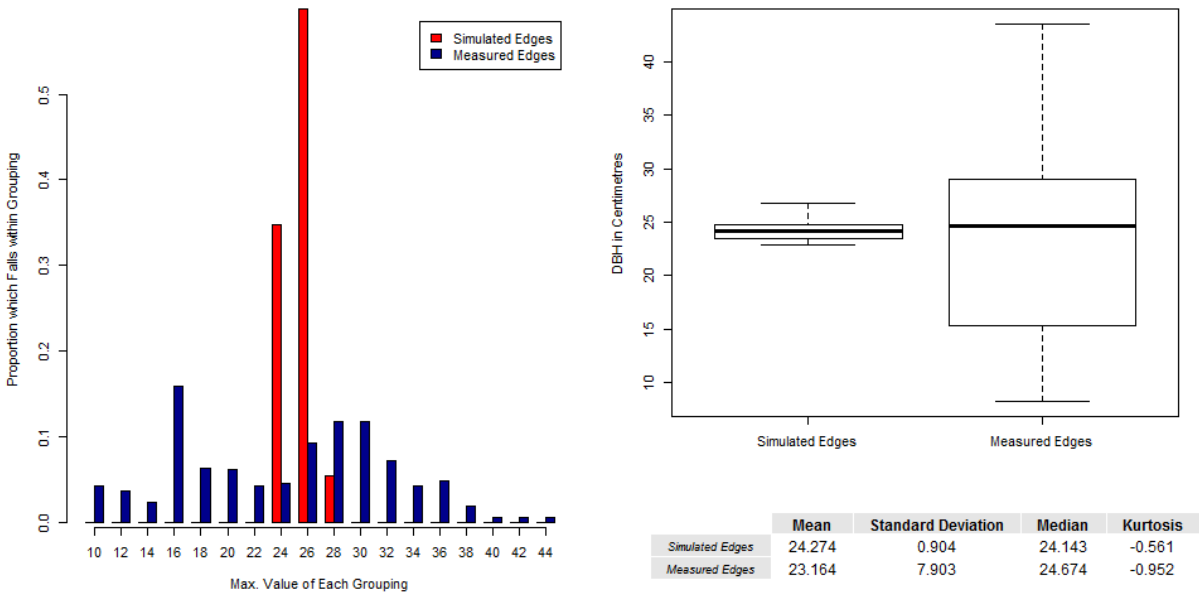


Figure A.1. A comparison between the DBH predicted for the edge region of stand G36 (red bars) and the distribution of the volumes as calculated from data extracted from the CHM (blue bars).

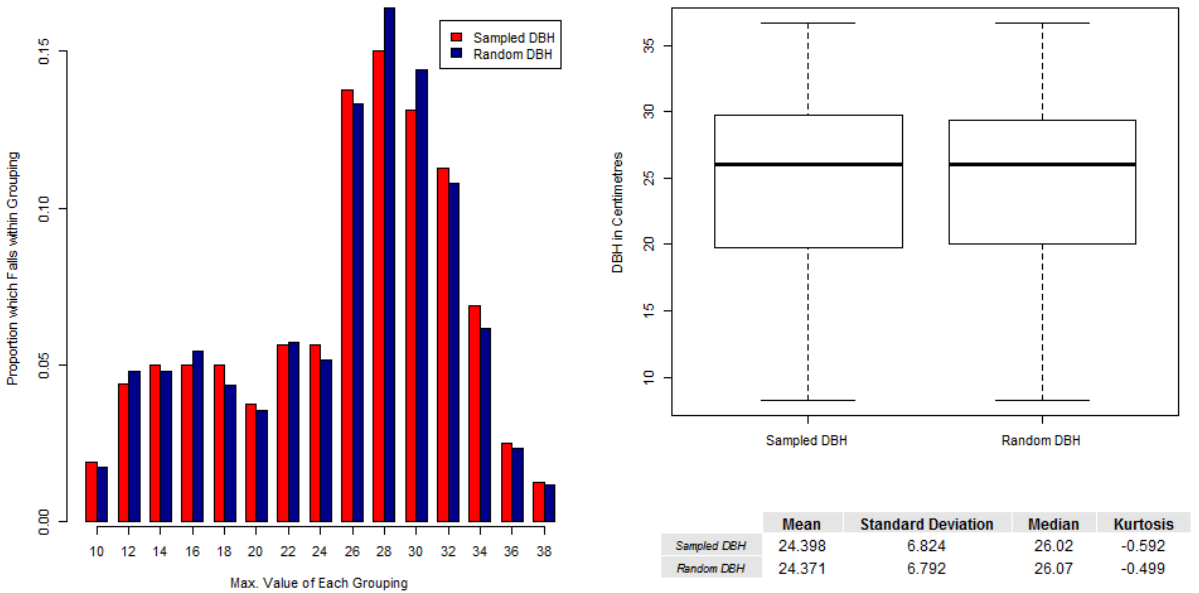
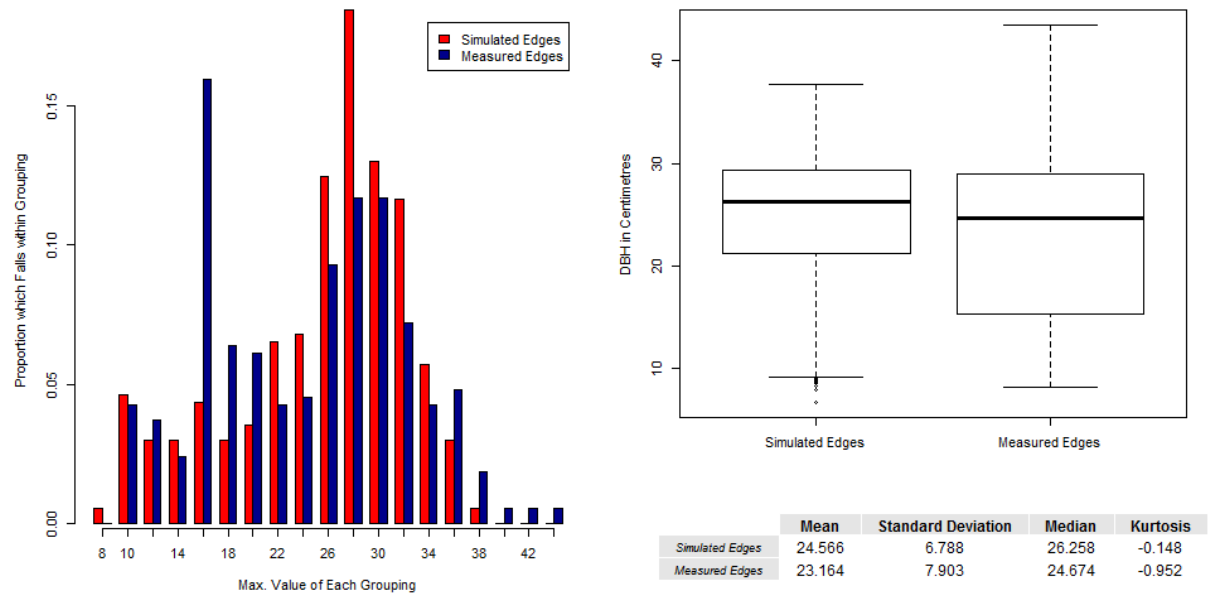
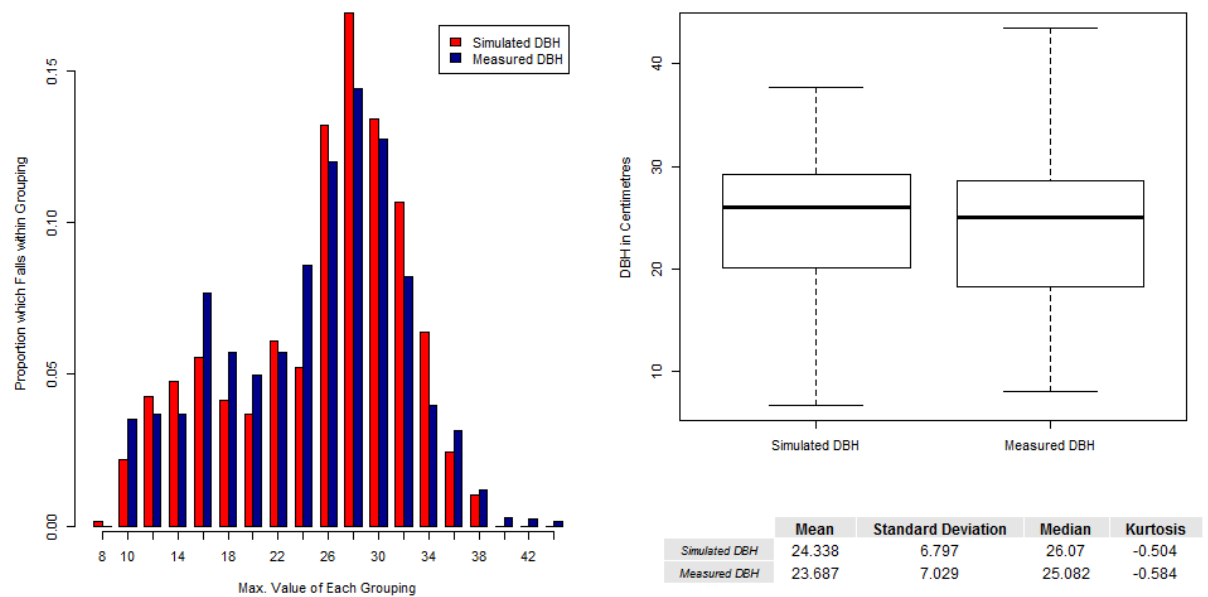


Figure A.2. A comparison between the random values generated for DBH of the complete stand G36 (blue bars) and the distribution of the DBHs as extracted from the sample plots (red bars). The random values were generated based on the distribution of the sample plot DBHs.





**Figure A.3.** A comparison between the distributions of the predicted edge DBHs (red bars) and the edge tree DBHs as calculated from data extracted from the CHM (blue bars).



**Figure A.4.** A comparison between the distributions of the predicted DBHs for the complete stand (red bars) and the stand DBHs as calculated from data extracted from the CHM (blue bars).

## 5.12 Height simulation results

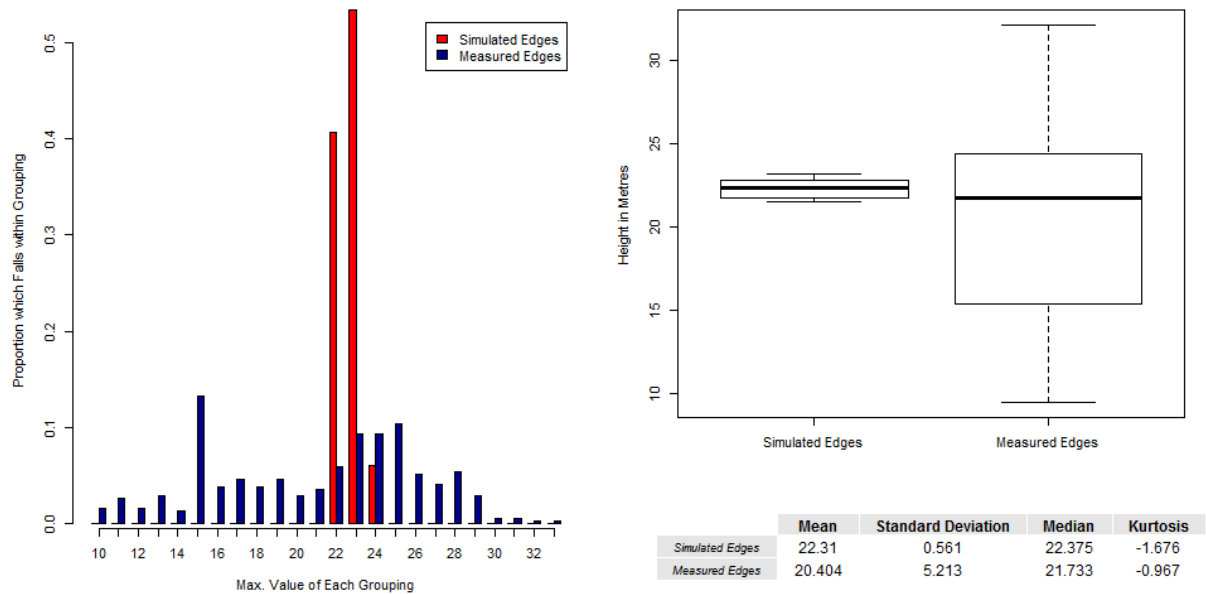


**Figure A.5.** A comparison between the height predicted for the edge region of stand G36 (red bars) and the distribution of the heights as calculated from data extracted from the CHM (blue bars).

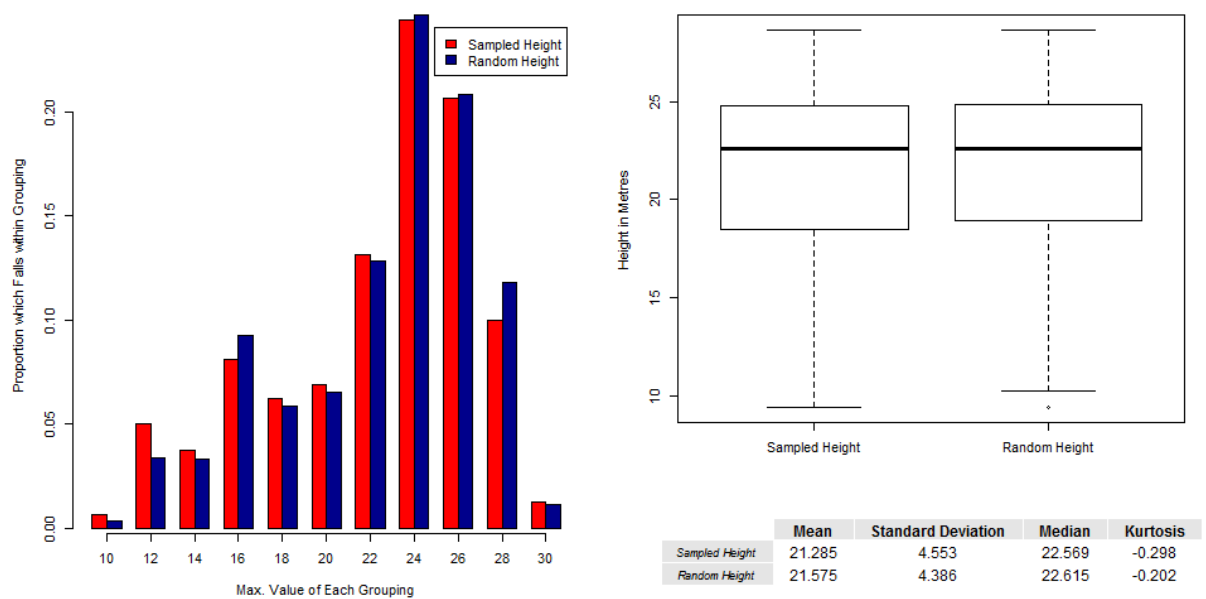


**Figure A.6.** A comparison between the random values generated for height of the complete stand G36 (blue bars), and the the distribution of the heights as extracted from the sample plots (red bars). The random values were generated based on the distribution of the sample plot DBHs.

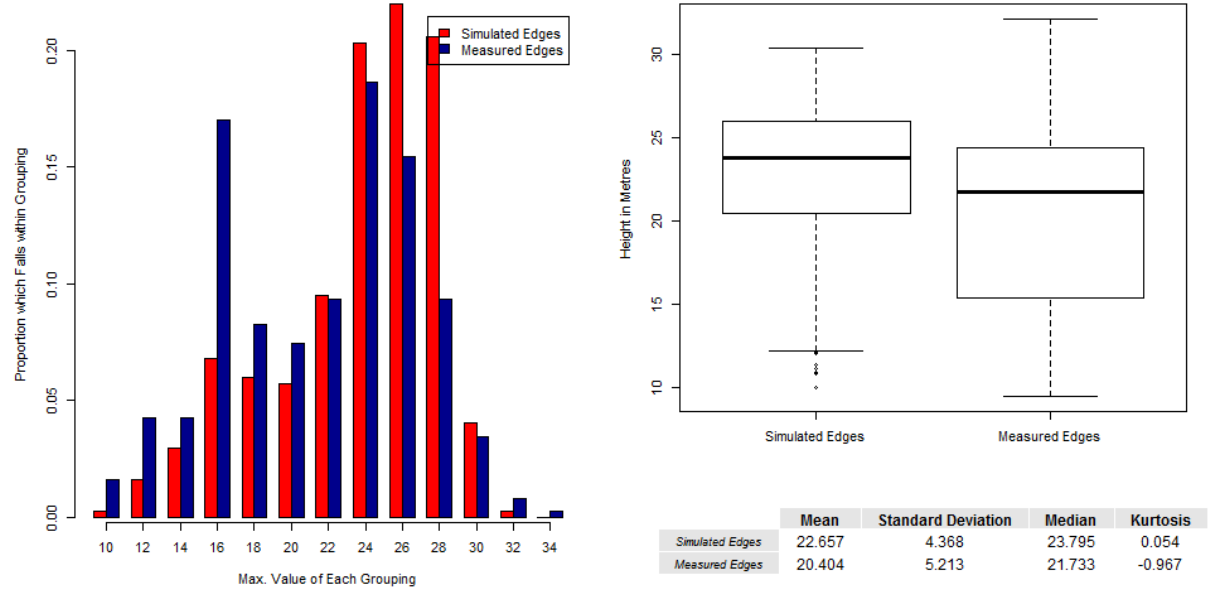


**Figure A.7.** A comparison between the distributions of the predicted edge heights (red bars) and the edge tree heights as calculated from data extracted from the CHM (blue bars).

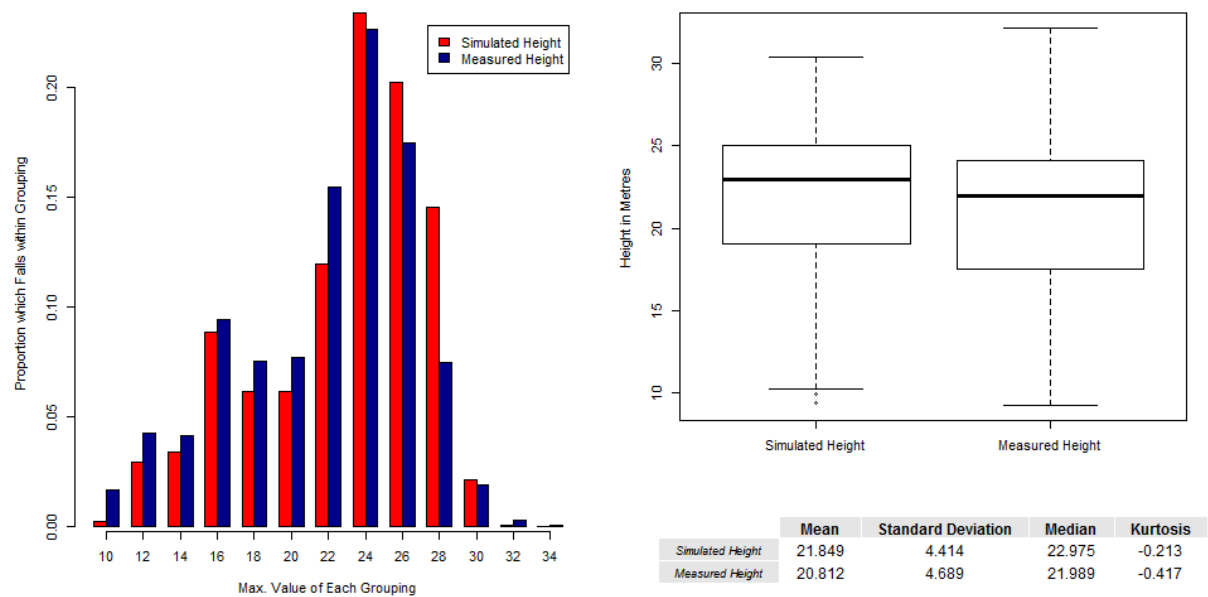


**Figure A.8.** A comparison between the distributions of the predicted heights for the complete stand (red bars) and the stand heights as calculated from data extracted from the CHM (blue bars).